NASA/CR-2005-213767

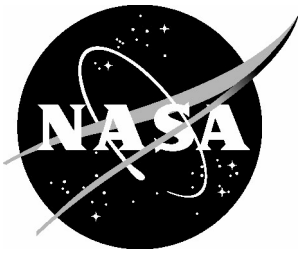

Airframe Noise Studies – Review and Future Direction

Robert G. Rackl and Gregory Miller
Boeing Commercial Airplanes, Seattle, Washington

Yueping Guo and Kingo Yamamoto
Boeing Phantom Works, Long Beach, California

June 2005

The NASA STI Program Office . . . in Profile

Since its founding, NASA has been dedicated to the advancement of aeronautics and space science. The NASA Scientific and Technical Information (STI) Program Office plays a key part in helping NASA maintain this important role.

The NASA STI Program Office is operated by Langley Research Center, the lead center for NASA's scientific and technical information. The NASA STI Program Office provides access to the NASA STI Database, the largest collection of aeronautical and space science STI in the world. The Program Office is also NASA's institutional mechanism for disseminating the results of its research and development activities. These results are published by NASA in the NASA STI Report Series, which includes the following report types:

- TECHNICAL PUBLICATION. Reports of completed research or a major significant phase of research that present the results of NASA programs and include extensive data or theoretical analysis. Includes compilations of significant scientific and technical data and information deemed to be of continuing reference value. NASA counterpart of peer-reviewed formal professional papers, but having less stringent limitations on manuscript length and extent of graphic presentations.

- TECHNICAL MEMORANDUM. Scientific and technical findings that are preliminary or of specialized interest, e.g., quick release reports, working papers, and bibliographies that contain minimal annotation. Does not contain extensive analysis.

- CONTRACTOR REPORT. Scientific and technical findings by NASA-sponsored contractors and grantees.

- CONFERENCE PUBLICATION. Collected papers from scientific and technical conferences, symposia, seminars, or other meetings sponsored or co-sponsored by NASA.

- SPECIAL PUBLICATION. Scientific, technical, or historical information from NASA programs, projects, and missions, often concerned with subjects having substantial public interest.

- TECHNICAL TRANSLATION. English-language translations of foreign scientific and technical material pertinent to NASA's mission.

Specialized services that complement the STI Program Office's diverse offerings include creating custom thesauri, building customized databases, organizing and publishing research results ... even providing videos.

For more information about the NASA STI Program Office, see the following:

- Access the NASA STI Program Home Page at ***http://www.sti.nasa.gov***

- E-mail your question via the Internet to help@sti.nasa.gov

- Fax your question to the NASA STI Help Desk at (301) 621-0134

- Phone the NASA STI Help Desk at (301) 621-0390

- Write to:
  NASA STI Help Desk
  NASA Center for AeroSpace Information
  7121 Standard Drive
  Hanover, MD 21076-1320

NASA/CR-2005-213767

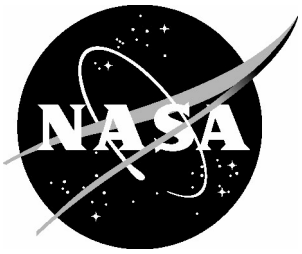

Airframe Noise Studies – Review and Future Direction

Robert G. Rackl and Gregory Miller
Boeing Commercial Airplanes, Seattle, Washington

Yueping Guo and Kingo Yamamoto
Boeing Phantom Works, Long Beach, California

National Aeronautics and
Space Administration

Langley Research Center
Hampton, Virginia 23681-2199

Prepared for Langley Research Center
under Contract NAS1-97040

June 2005

Available from:

NASA Center for AeroSpace Information (CASI)
7121 Standard Drive
Hanover, MD 21076-1320
(301) 621-0390

National Technical Information Service (NTIS)
5285 Port Royal Road
Springfield, VA 22161-2171
(703) 605-6000

Foreword

A compact disk with computer data files is available as a supplement to this report. The last Appendix contains details of the contents of the data files. The input data files are formatted for use with the NASA Aircraft Noise Prediction Program (ANOPP).

TABLE OF CONTENTS

TABLES

FIGURES

1 Acronyms, Symbols and Abbreviations

Acronym/ Symbol	Explanation
ACD	Acoustic Data Module of ANOPP
ANOPP	Aircraft Noise Prediction Program
ARC	NASA Ames Research Center
ASCII	American Standard Code for Information Interchange
ASCOT	Advanced Concepts to Test
AST	Advanced Subsonic Technology Program
BART	Basic Aerodynamic Research Tunnel (LaRC)
b.l.	Boundary Layer
CAA	Computational Aeroacoustics
CFD	Computational Fluid Dynamics
DERA	… [has a pressurized wind tunnel]
DES	Detached Eddy Simulation (CFD method)
DNS	Direct Numerical Simulation
EET	Energy Efficient Transport
FACT	Futuristic Airframe Concepts and Technologies
FPL	Fluctuating Pressure Level
FSE	Flap Side Edge
FW-H	Ffowcs Williams and Hawkings (equation)
LADA	Large Aperture Directional Array
LaRC	NASA Langley Research Center
LQ	Large Quad (Boeing 747-400)
LSAF	Low Speed Aeroacoustics Facility (Boeing Seattle)
LTPT	Low Turbulence Pressure Tunnel
M	Mach number
MT	Medium Twin (Boeing 767-300)
NAF	National Acoustics Facility (NASA Ames 40x80 tunnel)
QFF	Quiet Flow Facility (LaRC)
PF	Pressure Fluctuation(s)
PNL	Perceived Noise Level
PWT	Ames 12’ tunnel?
PSP	Pressure Sensitive Paint

PML	Perfectly Matched Layer
RANS	Reynolds Averaged Navier Stokes
Re	Reynolds Number
SADA	Small Aperture Directional Array
SPF	Surface Pressure Fluctuations
ST	Small Twin (Boeing 737-300)
TET	Trailing edge thickness (of slat)

2 Statement of Work

NASA CONTRACT **NAS1-97040, Task Assignment No. 12**

STATEMENT OF WORK

AIRFRAME NOISE STUDIES

1.0 TECHNICAL OBJECTIVE — The primary objective of this task shall be to identify and prioritize the airframe noise reduction technologies needed to accomplished the NASA Pillar goals (baselined to accomplishment of the current program).

2.0 CONTRACTOR'S TASK REQUIREMENTS — The Contractor shall perform the following requirements under this task assignment:

2.1 Apply data and prediction tools from the Advanced Subsonic Technology (AST) program to assess the current status of noise reduction technologies relative to NASA pillar goals for large commercial jet aircraft.

2.2 Apply noise prediction tools and airframe noise codes to identify and to evaluate new noise reduction concepts.

- For the NASA Aircraft Noise Prediction Program (ANOPP) input, provide one third octave spectra (Small Twin, Medium Twin or Large Quad) for each noise source affected by the noise reduction concept.
- The spectra shall cover the frequency range from 50 to 10K Hertz and shall include propagation effects—atmospheric absorption, spherical spreading and ground reflections.
- For the aircraft being evaluated, the spectra shall correspond to the same received times, acoustic angles and propagation distances specified in NASA CR-198298 "Definition of the 1992 Technology Aircraft Noise Levels and the Methodology for Assessing Airplane Noise Impact of Component Noise Reduction Concepts".
- The data shall be provided in both hardcopy and electronic formats.

2.3 Deliver a report of the results of these studies by December 31, 2000. This report should also serve as an industry input for future NASA airframe noise reduction research program planning.

This statement of work was amended as follows:

- In the first bullet of paragraph 2.2, "Small Twin, Medium Twin, or Large Quad" was changed to "Small Twin, Medium Twin, **and** Large Quad".
- The report deadline was moved to end of February 2001.

3 Introduction

The 'Pillar Goals' mentioned in the Statement of Work for this task were articulated dramatically by NASA Administrator Daniel Goldin in March 1997. We quote from a NASA brochure published at that time entitled *'Aeronautics & Space Transportation: Three Pillars for Success'*; under the heading *'Pillar One: Global Civil Aviation'* we find (emphasis added):

> Aircraft noise is the other area where future environmental regulations will challenge us to provide advanced technology concepts and innovations. Previous NASA noise-reduction research is now embodied in new aircraft entering the fleet, and in modifications to existing aircraft. Can we go further and create aircraft that are so quiet that the predominant noise at airports comes from cars and buses? NASA research directed at engine configurations, lighter materials, and **lower airframe noise** will provide the answers.
>
> *Enabling Technology Goal:* Reduce the perceived noise levels of future aircraft by a factor of two from today's subsonic aircraft within 10 years, and by a factor of four within 20 years. *
>
> * A factor of 2 reduction in perceived noise is about 10 EPNdB and 4 is about 20 EPNdB.

Also, NASA Office of Aeronautics presentation material from January 1997 envisions that noise could be reduced by 20 EPNdB through:

- Higher bypass ratio will lower fan pressure ratio and tip speeds
- Airplane and engine efficiency to reduce engine size and flow
- Active noise control in inlet and nozzles

While this is not an exhaustive list of required research endeavors, it points out that reductions in propulsion noise will make airframe noise a more significant contributor to the overall noise. Airframe noise reduction must be addressed vigorously in order to avoid for it to become the 'long pole in the noise emission tent' especially during approach to landing when the engine operates at a much lower power setting than during takeoff.

3.1 Scope

This report concerns itself with 'pure' airframe community noise only, which consists of all noise sources not connected to propulsion or auxiliary power generation, nor actuation of control surfaces or high lift device movements. Specifically, excluded are the interaction of engine exhaust flows with high lift devices, and included are noise from flows over wings and fuselage, with control surfaces, high lift devices, and landing gear.

As per the Statement of Work, this study covers three representative aircraft: the Small Twin ("ST") represented by the Boeing 737-300, the Medium Twin ("MT") represented by the Boeing 767-300, and the Large Quad ("LQ"), represented by the Boeing 747-400.

3.2 Report Organization

The guiding ideas are to present the progress of the Advanced Subsonic Technology (AST) program in the area of airframe noise in several steps (see also Figure 1):

- History
- Progress in prediction technologies
  - Use latest methods available at Boeing at the time of this writing to establish a new predicted baseline set of noise levels. Compare with 1992 Technology baseline noise data.
- Progress in noise reduction options and treatments

- Demonstrate the effect of various treatments by applying predicted and/or measured noise reductions to the newly predicted baseline. For the most part, only successful treatments are included here numerically; those that were tried but did not have desired effects may just be mentioned.

- Conclude the report with recommendations for future airframe noise research activities.

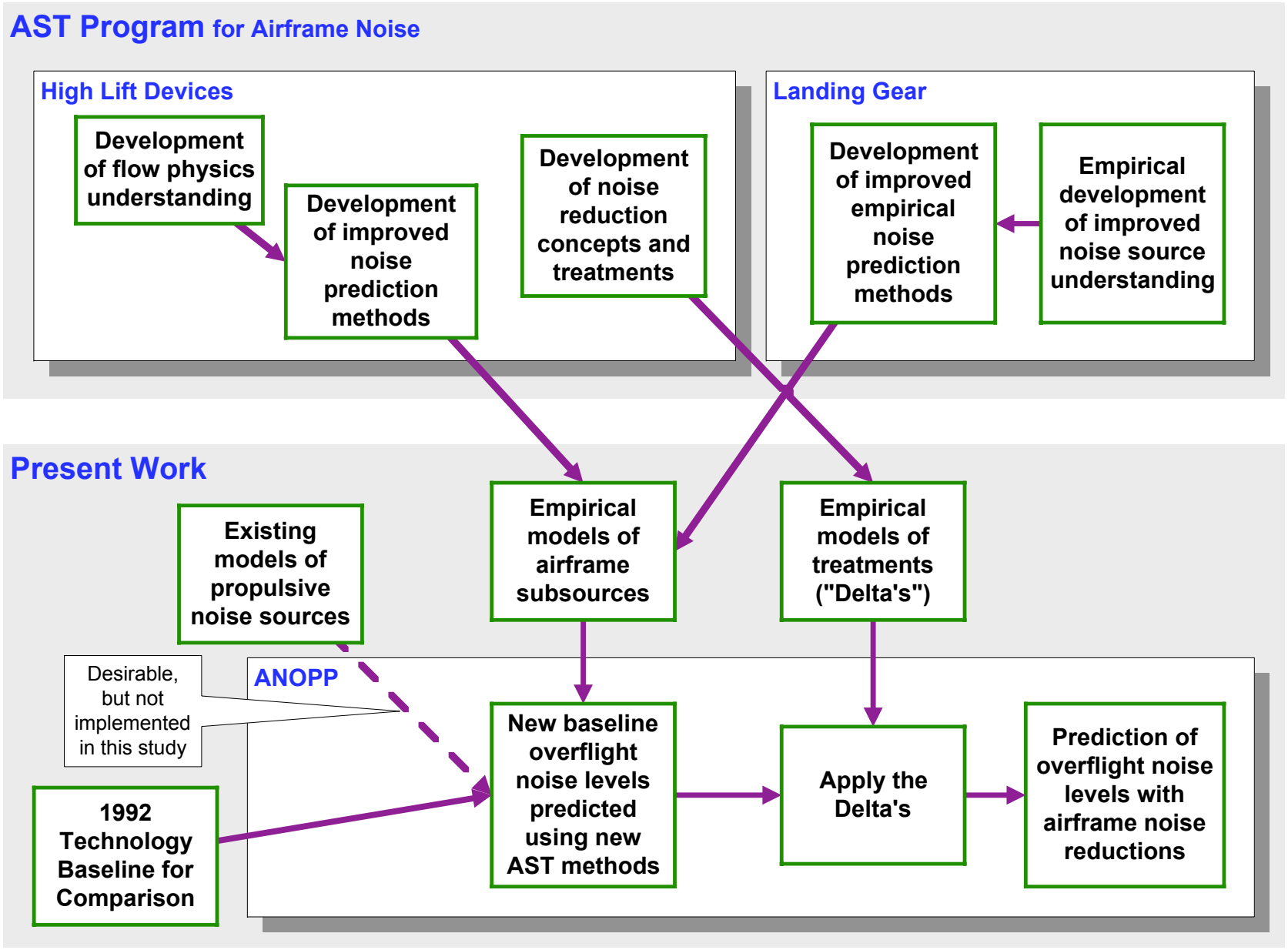

Figure 1 Data flow in the present work

4 Brief History

Before the NASA AST program, airframe noise prediction was largely based on a combination of empiricism and a very rudimentary understanding of the high lift system noise. The approach can be typified by the Fink method and that implemented in ANOPP (e.g. Ref. 1 and Ref. 5). In a nutshell, those methods basically correlate airframe noise to the gross geometry parameters of the high lift system, such as wing span and chord. In the development of those methods, trailing edge noise theory was used to provide a theoretical foundation, providing scaling laws such as the fifth power law on flow Mach number and the half angle far field directivity resulting from the trailing edge diffraction. The trailing edge noise theory was used because for many years, the wing trailing edge was considered as a major source for airframe noise. As is commonly known now, airframe noise dominantly comes from three competing sources, namely, the flap side edges, the slat flows and the landing gears. Thus, the prediction methods based on the trailing edge theory completely missed the physical sources of airframe noise. For prediction, those methods usually give reasonably accurate results (e.g. Ref. 10). This is because they were heavily calibrated with test data, both in amplitudes and in spectra, which leads to reasonable predictions even though the physics of airframe noise generation are not included in the theory.

In recognizing this lack of physics in airframe noise prediction, the NASA AST program tasked Boeing to develop a more accurate method with the objective of incorporating some physical principles in the prediction methodology. This was believed to be important, especially in predicting the effects of noise reduction treatment and in incorporating noise assessment into aerodynamic designs of future aircraft. By using the database available at that time, a component prediction method was developed, which is reported in Ref. 30**.** That task was a significant step forward in airframe noise prediction. It has three major important contributions that differ from other previous methods. They are

the use of an elliptic mirror for the noise measurements;

the development of component-based prediction;

the correlation between noise and flow quantities.

The noise database that was used to develop the prediction codes was derived from measurements by an elliptic mirror, which can be considered as a precursor of the phased microphone array technology widely used in recent years. The data differ from conventional free field microphone measurements in that not only the total noise in the far field, but also the source distributions on the aircraft can be derived from the measurements. This provided a useful tool in identifying the dominant sources on the high lift system, which confirmed the dominance of the flap side edges and the leading edge slats. The second aspect of that task is that the noise prediction is component-based. This was made possible by the use of the elliptic mirror, which can map the source distribution on the high lift system. By integrating the source distribution in different regions, noise from individual components can be derived (such as flaps and slats). The third aspect of that task is that for the first time, airframe noise was related to aerodynamic parameters in the near field flow. This is in contrast to previous methods that only use gross geometry parameters. The decision to include aerodynamic parameters in the prediction was made based on the belief that the real physical sources are the flows, and thus, should be parameterized by flow quantities.

In developing that method, analytical studies were also used to guide the choice of flow quantities to be correlated to noise. A good example is the flap side edge noise. In modeling flap noise, it was learned that the flap side edge vortex plays an important role in the noise generation process (e.g. Ref. 4, Ref. 6, Ref. 12, Ref. 17, Ref. 23, Ref. 24, Ref. 27, Ref. 35, Ref. 36, Ref. 37, Ref. 40, Ref. 42, Ref. 43, Ref. 44, Ref. 46, Ref. 56). In particular, the vortex strength and location critically control the way by which near field vortical energy is scattered into sound. Thus, a correlation was derived between the flap side edge noise and the side edge vortex strength. It should be noted that the un-

derstanding of the noise source mechanisms such as the flap side edge vortex also helped in developing noise reduction treatments. There have been many flap side edge treatments studied in recent years, including side edge fences, porous surfaces, micro tabs, and serration. All these can be regarded as devices designed to favorably modify the vortical flow in the flap side edge region, and thereby achieving noise reduction.

As summarized in Ref. 30, the component method provides a very useful tool for airframe noise prediction, and comparisons with full-scale flight test data showed very satisfactory results. However, because of the limitation of the database available at that time, the results of that task also left room for improvements, which was recognized almost immediately after its completion. As a result, the NASA AST Program initiated a follow-on task reported in Ref. 64. It basically followed the methodology of the original task, but made significant improvements including the use of a much larger and more accurate database, larger because the continuous efforts under the NASA AST Program had tested more aircraft configurations, and more accurate because of the development of the phased microphone array technology. This improved database also contained some information on the far field directivity. Also, in view of the success in relating noise to flow quantities, the aerodynamic parameters were systematically re-computed in the follow-on task. The choices of the aerodynamic parameters were also re-examined in order to model the noise source process more accurately. Another important improvement was that an empirical model for landing gear noise prediction was developed and incorporated in the codes.

With these improvements, Ref. 64 endeavored to include in the airframe noise prediction tool seven components, namely landing gear, leading edge slat, outboard flap edge, inboard flap edge, trailing edge, high-speed aileron, and residual noise floor. The task was tight on budget and needed to focus on the more important sources. Two components, trailing edge and residual noise floor, turned out to be very weak as per the phased array data; for them, no prediction formulas were developed.

These noise components are predicted on a spectral basis, taking geometry as well as aerodynamic parameters as input. The total noise is then derived by adding the component contributions from which, together with a directivity for the total noise, noise metrics such as PNLT and EPNL are computed. This is basically the approach we take for the work documented in this report.

5 Airframe Noise Prediction

Predictions are made, and noise reduction concepts are evaluated, for three generic aircraft: the small twin, the medium twin, and the large quad, where ‘twin’ means ‘two engines’, and ‘quad’ means ‘four engines’. We selected the following representatives in each category:

ST	Small Twin	Boeing 737-300
MT	Medium Twin	Boeing 767-300
LQ	Large Quad	Boeing 747-400

Figure2 shows a 747-400 in approach/landing configuration with flaps and leading edge devices deployed, and landing gear down.

Figure 2 Photograph of underside of Boeing 747-400 in landing configuration.

5.1 Prediction Process Summary

Figure 3 shows an example of an empirical prediction scheme used in this work; that sample is for flap side edge noise. A number of aerodynamic parameters are required which are generated using a relatively simple potential flow lifting surface code. The prediction results in tables describing acoustic radiation from a source at a 1-foot distance as a function of directivity angles, and as a function of Mach number. This prediction was adjusted using Boeing proprietary approach certification data for the three aircraft. The 1-foot sphere tables were then recast into the format required by ANOPP.

All baseline predictions in this report use the methods developed in Ref. 64. These methods are all empirical. Although great progress has been made during the AST program in the area of CFD modeling, physics-based prediction methods have not yet matured sufficiently to be used routinely.

$$OASPL(90°) = 92.1 + 53.0\text{Log}(M) + 20.15\text{Log}(\text{Sin}\,\delta) + 0.5\text{Log}(C_l) + 17.8\text{Log}(\xi \cdot t) + 0.11\text{Log}(V_y) + 0.12\text{Log}(\Gamma)$$

$$SPL(f, 90°) - OASPL(90°) = a_6 \cdot X^6 + a_5 \cdot X^5 + a_4 \cdot X^4 + a_3 \cdot X^3 + a_2 \cdot X^2 + a_1 \cdot X + a_o$$
$$X = \text{Log}(f \cdot \xi \cdot t / V)$$

a_0	a_1	a_2	a_3	a_4	a_5	a_6
-13.1814	10.0319	-9.4077	-6.6166	4.0970	1.4162	-1.0740

M = Flight Mach number, C_l = Lift coefficient for inboard flap (1st flap element),
δ = Flap deflection angle, t = Inboard flap edge chord (1st element), V_y = Spanwise flow velocity,
Γ = Circulation, V = Flight velocity, f = One-third-octave center frequency,
ξ = length scale factor

Note: Arguments of logarithmic function are non-dimensionalized by reference values.

Figure 3 Sample prediction equations from Ref. 64

5.2 Aerodynamic Data

The airframe noise prediction methods for flaps and slats require aerodynamic data that varies with flow speed and configuration (angle of attack, flap deflection, slat extension). These data were generated using Boeing-internal program A449 that is a vortex lattice code that models lifting surfaces using networks of vortex panels, and a body using an axi-symmetric body-theory approximation. The code differs from a strict vortex-lattice formulation in that the chordwise variation of vortex panel strength is piecewise linear, rather than discrete on each panel. The planform, camber, and twist of a lifting surface are defined by the panel network geometry, but thickness is not modeled. Dihedral and incidence can be specified for the entire lifting surface. A complete description of the theory and use of A449 can be found in Ref. 2. In the present study, separate lifting surfaces were used to define the wing and individual flap elements, while the effect of leading edge slats was simulated by extending the leading edge of the wing forward and drooping it to match the planform and camber of the slat on the wing. Trailing vorticity is automatically continued directly downstream from the trailing edges of lifting surfaces. The body length and diameter matched the airplane geometry, but the slender body-theory formulation enforced axi-symmetry, thus masking the (small) effects of a low nose + high cockpit windows at the front, gear fairings, and the up-swept aft body. The vortex-lattice wire-frame model for the LQ is shown in Figure 4.

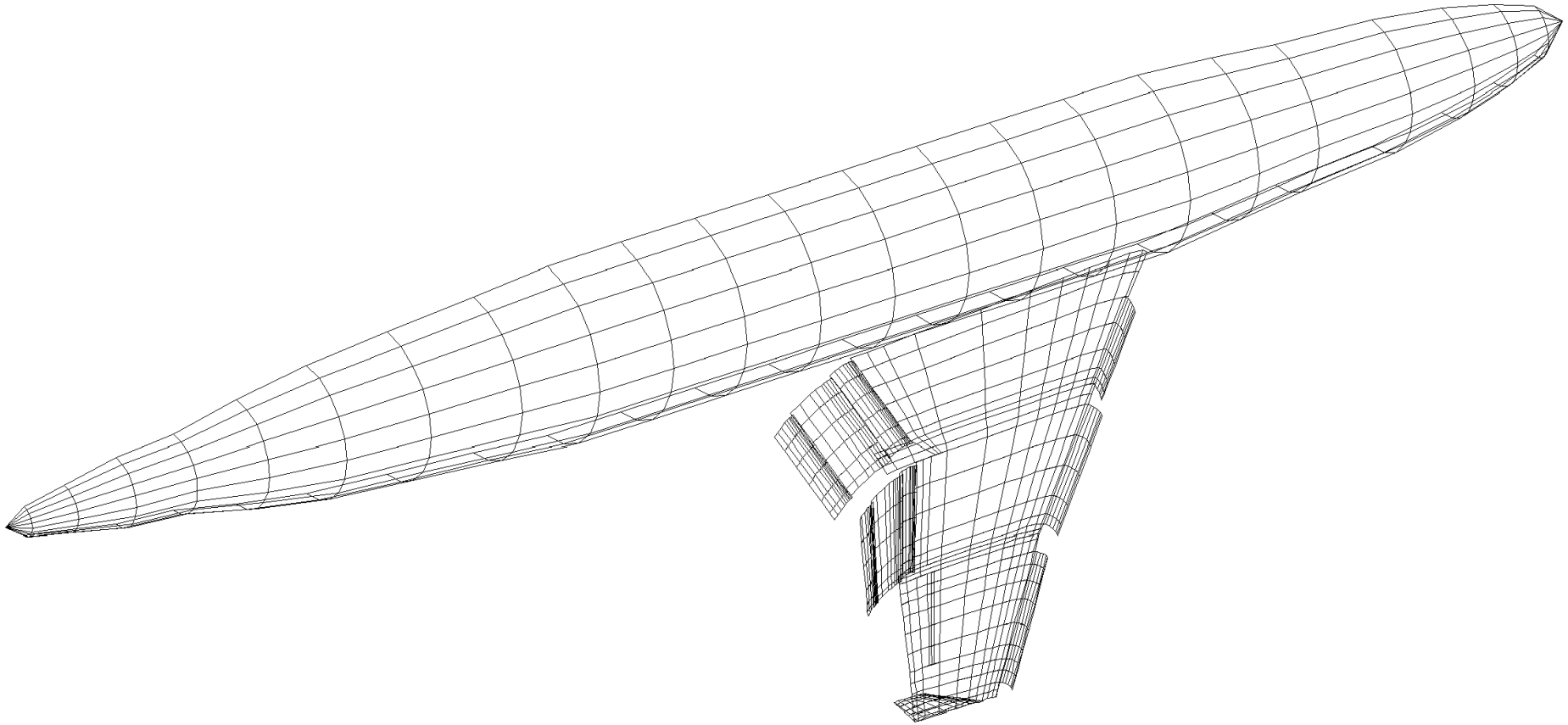

Figure 4 Large Quad Wireframe Model Used in Vortex Lattice Method for Aerodynamic Calculations

5.3 Noise Prediction Models

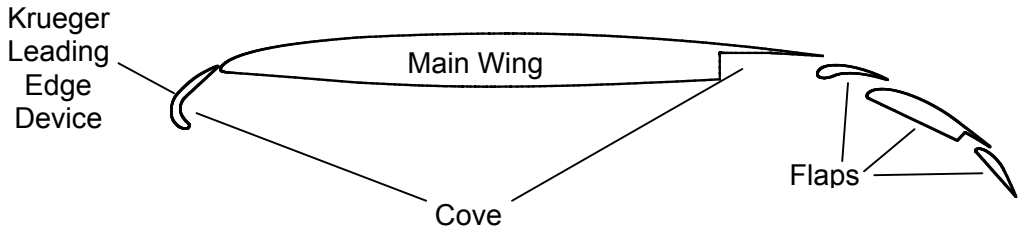

Figure 5 Wing Cross-section of Boeing 747-400 at Mid-Span, high lift devices deployed, flaps set at 30.

5.3.1 Flaps

In the past few years under the NASA AST Program, flap side edge noise has been studied by various methods, ranging from analytical to numerical to experimental. This is reflected in the large number of papers and reports, as quoted in the reference section in this report. Keeping in mind that it is not the objective of this report to comprehensively review all the methods, we briefly summarize in this section a few relevant approaches.

In Ref. 46 and Ref. 56, a semi-analytical/semi-empirical model for noise generation by flow separation in the flap side edge region is reported. The model is based on the concept that complex flow features such as shear layer instabilities cause flow separation in the flap side edge region where unsteady vorticity fluctuations generate noise predictable from the classical theory of vortex sound. These vorticity fluctuations are modeled by unsteady nonlinear motions of vortex clusters, representing thin shear layers in real flows, and by dynamic vortex shedding from the sharp corners, modeling vorticity production by flow separation. The model calculates the near field flow fluctuations, including unsteady pressures on the flap surfaces, which are then used to compute the far field radiation. The near field flow is calculated in a two-dimensional approximation, with the model representing a stream-wise strip of the real flap surface. In the formulation, surface pressure spectra from the two-dimensional calculation are related to far field noise through the use of a frozen convection assumption. The model is basically inviscid so that vortex merge is not accounted for, which may or may not be important for flap noise of real aircraft. To validate the prediction model, both the unsteady surface pressures on the flap and the far field predictions were compared with available test data, as reported in Ref. 55. The comparisons show very good agreement, not only in the dominant trends, such as frequency characteristics, flow Mach number dependence and far field directivity, but also in the absolute amplitudes of the noise levels. The model is coupled to the aerodynamic properties of the high lift system because the inputs that it requires include aerodynamic parameters such as the static chord-wise loading distribution on the flap. This can be readily derived from conventional aerodynamic design computations, which makes the model a potential candidate suitable for engineering applications. For instance, it can be developed into a tool for assessing the acoustic impact of changes in aircraft high lift system design.

For empirical prediction, an aeroacoustic model test was conducted to investigate the mechanisms of sound generation on high-lift wing configurations, as reported in Ref. 71. That report presents an analysis of flap side-edge noise, which is often the most dominant source. A model of a main element wing section with a half-span flap was tested at low speeds of up to a Mach number of 0.17, corresponding to a wing chord Reynolds number of approximately 1.7 million. Results are presented for flat (or blunt), flanged, and round flap-edge geometries, with and without boundary-layer tripping, deployed at both moderate and high flap angles. The acoustic database is obtained from a Small Aperture Directional Array (SADA) of microphones, which was constructed to electronically

steer to different regions of the model and to obtain farfield noise spectra and directivity from these regions. The basic flap-edge aerodynamics is established by static surface pressure data, as well as by Computational Fluid Dynamics (CFD) calculations and simplified edge flow analyses. Distributions of unsteady pressure sensors over the flap allow the noise source regions to be defined and quantified via cross-spectral diagnostics using the SADA output. It is found that shear layer instability and related pressure scatter is the primary noise mechanism. For the flat flap edge, two noise prediction methods based on unsteady surface pressure measurements are evaluated and compared to measured noise. One is a new causality spectral approach. The other is a new application of an edge-noise scatter prediction method. The good comparisons for both approaches suggest that the prediction models capture much of the physics. Areas of disagreement appear to reveal when the assumed edge noise mechanism does not fully define the noise production. For the different edge conditions, extensive spectra and directivity are presented. Significantly, for each edge configuration, the spectra for different flow speeds, flap angles, and surface roughness were successfully scaled by utilizing aerodynamic performance and boundary layer scaling methods developed therein.

There has also been quite noticeable progress in numerical modeling of flap side edge noise in the past few years. This approach usually starts with CFD calculations of the flow field in the flap side edge region. The flow calculations are then used as input in the acoustic computation, using the Lighthill acoustic analogy, the Ffowcs Williams/Hawkings equation, or some variations of the two (e.g. Ref. 12, Ref. 35, Ref. 36, Ref. 37, Ref. 40, Ref. 41, Ref. 42, Ref. 49, Ref. 50). These numerical studies have provided details of the flow field, and hence, helped the understanding of the noise generation mechanisms. The noise prediction from this approach, however, has only seen limited success. This is largely because of the heavy computation load, which prevents application to realistic aircraft configurations, prevents extensive validation with real aircraft test data. In our view, this approach will probably remain a research tool in the foreseeable future.

5.3.2 Leading Edge Devices

In comparison with flap noise prediction, fewer efforts have been made in the area of prediction of noise from leading edge devices. One method developed under the NASA AST Program is the one documented in Ref. 70. It is based on a discrete vortex model. It models noise generation by vortical flow fluctuations in the slat cove region and the interactions between the vortical flow and the slat trailing edge. The model simulates flow separation at the slat cusp and trailing edges by vortex shedding in the form of discrete, multiple point vortices. The near field flow is solved by implementing the vortex shedding model in an unsteady panel method, in which the effects of the high lift system are accounted for by time-dependent source panels on the body surfaces. Time domain solutions for the near field flow are derived by the fourth order Runge-Kutta method, which shows the development of the slat cove vortical flow from the vorticity shed at the slat cusp. The flow reaches an oscillatory equilibrium at which flow fluctuations are induced by the balance between the vorticity convected away by the mean flow and that shed by flow separation. The convected vorticity passes through the gap between the slat trailing edge and the main wing, causing vortex/edge interaction. Thus, the model captures the noise generation mechanisms of both the unsteady fluctuations of the highly vortical flow in the slat cove and the scattering of vortical energy into acoustic energy by the slat trailing edge. The noise prediction is done by the Ffowcs Williams/Hawkings equation. It is shown that the noise from these two mechanisms has broadband spectral characteristics, covering about two decades in frequency. The noise spectrum has a negative slope, with the fall-off approximately following the inverse square of frequency. Because the sources are high frequency in nature and are non-compact, the overall sound pressure level is shown to scale on the flow Mach number according to a power law with the power index approximately equal to 2.5. This is in sharp contrast to the fifth or sixth power law for low Mach number, low frequency noise. It is shown that the cove flow fluctuations mainly cause pressure fluctuations on the surface of the forward portion of the main wing, which radiates to the fly-over direction normal to the wing chord. The vor-

tex/trailing edge interaction is shown to mostly induce fluctuations on the slat, causing radiation in the direction normal to the slat chord. Predictions from the model are validated by experimental data in terms of the spectral characteristics, the far field directivity and the Mach number scaling, which all show good agreements. Functional dependencies on the angle of attack, the slat deployment angle and the slat gap are also derived and validated by experimental data. It is shown that the most promising noise reduction comes from decreasing the slat gap. By reducing the slat gap by one percent of the stowed wing chord, it is shown that 5 dB noise reduction can be achieved in the peak radiation angle, consistent with test data. Noise variation with the angle of attack and/or the slat deployment angle is shown to depend on how well the incoming steady flow aligns with the tangent of the slat surface near the cusp where vortex shedding occurs.

Though not aimed at developing prediction tools, there have been numerical studies concerning slat flows. For example, Ref. 54 and Ref. 55 studied the detailed viscous shedding from the slat trailing edge. In an attempt to interpret a high frequency hump observed in the integrated spectra of phased microphone array measurements for slat noise, Ref. 55 proposed a trailing edge vortex shedding mechanism. The mechanism considers the finiteness of the slat trailing edge and the local viscous boundary layer separation. They reported CFD results that seem to predict the frequencies of the observed data. To explain the same experimental results, Ref. 54 proposed a feedback mechanism between the vortex shedding from the sharp trailing edge and the reflected acoustic wave from the main wing. They also reported CFD results that predict the frequencies well, though the two proposed mechanisms from the two groups of authors are quite different. In view of these, together with some uncertainties involved in converting phased microphone array measurements into spectral quantities, it seems to be appropriate to keep an open mind regarding the true source of that hump in the integrated spectra. For practical applications, the tonal component of the slat noise is unlikely to survive for real airplanes, because it is relatively easy to suppress by noise reduction treatment such as trailing edge serration. Also, the phenomenon is highly configuration dependent.

5.3.3 Landing Gear

If there have been fewer efforts on slat noise modeling than flap noise modeling, attempts to model and predict landing gear noise are even fewer. This is largely because of the complex geometry of the typical landing gear assembly and the complex flow associated with the geometry. Clearly, flow modeling for realistic landing gear assemblies is out of reach for practical purposes, which essentially rules out detailed precise prediction of the noise field. In the foreseeable future, landing gear noise prediction will probably heavily depend on empiricism and/or approximations. This is what has led to the task of statistical modeling of landing gear noise, under the NASA AST Program. The task is on-going and will be reported in Ref. 73. In essence, we make use of statistic descriptions of the flow properties, such as its ensemble-averaged cross and auto spectra, to avoid detailed deterministic computation of the near field flow. The statistical information of the flow is then used to calculate the far field noise with the help of asymptotic expansions in the limits of high and low frequencies. The entire frequency domain of practical interest is covered by empirically matching the two asymptotic results and the total noise is predicted by statistical energy addition of the noise contributions from individual components of the landing gear assembly.

The level of effort of empirical modeling and prediction of landing gear noise has also been low, largely because of a lack of quality test data, though the efforts have speeded up recently. Test data obtained before the NASA AST Program were mostly for simplified gear geometries, consisting of only the main components while omitting the details such as the small bolts, nuts, tubes, hoses, and wires. In recent years, it has been recognized that those small details are responsible for the mid and high frequency landing gear noise, which are the most important frequency domains for aircraft noise certification. Thus, wind tunnel model fidelity is the most crucial issue in landing gear noise testing, and empirical modeling must be based on quality data with high fidelity. The first attempt of this kind is the B737 landing gear test, reported in Ref. 59. The data from this test were

used to develop an empirical prediction code, which is reported in Ref. 64 and is the method used in this report. It should be pointed out that this empirical method is based entirely on one test and clearly needs to be expanded with other test data.

5.4 Baseline Noise Data

As mentioned in Section 5.1, the baseline noise characteristics of all three representative aircraft were obtained using the methods in Ref. 64. The data were cast into the format required to build ANOPP libraries to be used by ANOPP's ACD (Acoustic Data) module.

5.4.1 Presentation Format

ANOPP's Acoustic Data Module requires acoustic data in this general form: $SPL(f,\theta,\phi;\Pi,M)$, where:

SPL – Sound Pressure Level
f = frequency
θ = polar directivity angle (measured in a plane containing the aircraft longitudinal axis, 0 is forward)
ϕ = azimuthal directivity angle (measured in a plane perpendicular to that axis, 0 is down)
Π = power setting
M = Mach number

The method of providing such data to ANOPP is by creating a *'Member'* on a *'data unit'*; using the UPDATE control statement. See the ANOPP user's manual, Ref. 1. The following is a sample data structure (data are taken from the Large Quad inboard flap side edge noise tables for approach flaps (detent 30), file `inboard.tbi`; a line-by-line discussion follows this table):

Table 1 Baseline Noise Data Presentation Format

Line #	**ANOPP Input Lines**
L 1	`$  AIRFRAME NOISE PREDICTION: B747-400 M = 0.249 and 0.259`
L 2	`$  LOSSLESS 1-FT ARC SPECTRA`
L 3	`$  FLAPS 30`
L 4	`$   INBOARD FLAP SIDE EDGE NOISE`
L 5	`$`
L 6	`UPDATE NEWU=IBFLP3 SOURCE=* $`
L 7	`  -ADDR OLDM=* NEWM=SPL FORMAT=0 $`
L 8	`   1.00  $ SOURCE RADIUS`
L 9	`   24   17    1    1    2  $ NFREQ, NTHETA, NPHI, NPOWER, NMACH`
L 10	`   0.  0.249  0.1 $ PHI, MACH, POWER`
L 11	`              10.00  20.00  30.00  40.00  50.00  60.00  70.00  80.00  90.00 100.00`
L 12	`            110.00 120.00 130.00 140.00 150.00 160.00 170.00 $`
L 13	`         50. 122.70 122.70 123.50 124.20 124.70 125.00 125.10 125.00 124.70 124.30`
L 14	`            123.60 122.80 121.80 120.60 119.20 117.70 115.90 $`
L 15	`         63. 123.10 123.10 124.00 124.70 125.20 125.50 125.70 125.60 125.40 125.00`
L 16	`            124.40 123.60 122.60 121.50 120.10 118.60 116.80 $`
L 17	`         80. 123.20 123.20 124.20 124.90 125.40 125.80 126.00 126.00 125.80 125.40`
L 18	`            124.80 124.00 123.10 121.90 120.60 119.10 117.40 $`
L 19	`        100. 123.20 123.20 124.10 124.80 125.40 125.80 126.00 126.00 125.80 125.40`
L 20	`            124.80 124.10 123.10 122.00 120.70 119.20 117.50 $`
L 21	`        125. 122.90 122.90 123.80 124.60 125.10 125.50 125.70 125.70 125.50 125.10`
L 22	`            124.60 123.80 122.90 121.80 120.50 119.00 117.30 $`
L 23	`        160. 122.30 122.30 123.30 124.00 124.50 124.90 125.10 125.10 124.90 124.50`
L 24	`            123.90 123.20 122.20 121.10 119.80 118.30 116.60 $`
L 25	`        200. 121.60 121.60 122.50 123.30 123.80 124.10 124.30 124.30 124.00 123.60`
L 26	`            123.10 122.30 121.30 120.20 118.90 117.40 115.70 $`
L 27	`        250. 120.80 120.80 121.60 122.30 122.80 123.10 123.30 123.20 123.00 122.50`
L 28	`            121.90 121.10 120.20 119.00 117.70 116.10 114.40 $`
L 29	`        315. 119.70 119.70 120.60 121.20 121.60 121.90 122.00 121.90 121.60 121.10`

L 30	120.50 119.70 118.70 117.50 116.10 114.60 112.90 $
L 31	400. 118.60 118.60 119.40 119.90 120.30 120.50 120.60 120.40 120.10 119.60
L 32	118.90 118.00 117.00 115.80 114.40 112.80 111.10 $
L 33	500. 117.70 117.70 118.40 119.00 119.30 119.40 119.40 119.20 118.80 118.30
L 34	117.50 116.60 115.50 114.30 112.80 111.20 109.50 $
L 35	630. 117.70 117.70 118.30 118.80 119.10 119.10 119.10 118.80 118.30 117.70
L 36	116.90 115.90 114.80 113.50 112.00 110.30 108.50 $
L 37	800. 119.20 119.20 119.70 120.10 120.30 120.30 120.10 119.80 119.30 118.60
L 38	117.70 116.60 115.40 114.00 112.40 110.70 108.80 $
L 39	1000. 121.30 121.30 121.80 122.20 122.30 122.20 122.00 121.50 120.90 120.10
L 40	119.20 118.00 116.70 115.20 113.60 111.70 109.80 $
L 41	1250. 123.50 123.50 123.90 124.20 124.20 124.10 123.70 123.20 122.50 121.60
L 42	120.60 119.30 117.90 116.30 114.60 112.70 110.60 $
L 43	1650. 125.30 125.30 125.70 125.80 125.80 125.50 125.10 124.40 123.60 122.60
L 44	121.50 120.10 118.60 116.90 115.10 113.00 110.90 $
L 45	2000. 125.90 125.90 126.10 126.20 126.10 125.80 125.30 124.60 123.70 122.60
L 46	121.40 120.00 118.40 116.60 114.70 112.60 110.40 $
L 47	2500. 125.60 125.60 125.80 125.80 125.60 125.30 124.70 123.90 123.00 121.80
L 48	120.50 119.00 117.40 115.60 113.60 111.40 109.10 $
L 49	3150. 124.50 124.50 124.60 124.50 124.30 123.80 123.20 122.30 121.30 120.10
L 50	118.80 117.20 115.50 113.70 111.70 109.50 107.20 $
L 51	4000. 122.40 122.40 122.50 122.40 122.00 121.50 120.80 120.00 118.90 117.70
L 52	116.30 114.70 113.00 111.10 109.10 106.90 104.50 $
L 53	5000. 120.00 120.00 120.00 119.80 119.50 118.90 118.20 117.30 116.20 115.00
L 54	113.60 112.00 110.30 108.40 106.30 104.20 101.90 $
L 55	6300. 117.40 117.40 117.40 117.20 116.80 116.20 115.50 114.60 113.50 112.30
L 56	110.80 109.30 107.60 105.70 103.70 101.50 99.20 $
L 57	8000. 115.50 115.50 115.50 115.30 114.90 114.30 113.60 112.70 111.60 110.40
L 58	109.00 107.40 105.70 103.90 101.90 99.80 97.50 $
L 59	10000. 115.30 115.30 115.30 115.10 114.80 114.20 113.50 112.60 111.50 110.30
L 60	108.90 107.40 105.70 103.80 101.80 99.70 97.50 $
L 61	0. 0.259 0.1 $ PHI, MACH, POWER
L 62	10.00 20.00 30.00 40.00 50.00 60.00 70.00 80.00 90.00 100.00
L 63	110.00 120.00 130.00 140.00 150.00 160.00 170.00 $
L 64	50. 124.60 124.60 125.40 126.10 126.60 126.90 127.00 126.90 126.70 126.20
L 65	125.60 124.70 123.70 122.50 121.10 119.50 117.70 $
L 66	63. 125.00 125.00 125.90 126.70 127.20 127.50 127.70 127.60 127.40 127.00
L 67	126.40 125.60 124.60 123.40 122.00 120.50 118.70 $
L 68	80. 125.30 125.30 126.20 126.90 127.50 127.90 128.00 128.00 127.80 127.40
L 69	126.80 126.10 125.10 123.90 122.60 121.00 119.30 $
L 70	100. 125.20 125.20 126.20 126.90 127.50 127.90 128.10 128.10 127.90 127.50
L 71	126.90 126.20 125.20 124.10 122.70 121.20 119.50 $
L 72	125. 125.00 125.00 125.90 126.70 127.30 127.70 127.90 127.90 127.70 127.30
L 73	126.70 126.00 125.00 123.90 122.50 121.00 119.30 $
L 74	160. 124.50 124.50 125.40 126.20 126.80 127.10 127.30 127.30 127.10 126.70
L 75	126.10 125.40 124.40 123.30 121.90 120.40 118.70 $
L 76	200. 123.90 123.90 124.80 125.50 126.00 126.40 126.60 126.50 126.30 125.90
L 77	125.30 124.50 123.60 122.40 121.00 119.50 117.80 $
L 78	250. 123.00 123.00 123.90 124.60 125.10 125.40 125.60 125.50 125.30 124.80
L 79	124.20 123.40 122.40 121.20 119.90 118.30 116.60 $
L 80	315. 122.00 122.00 122.90 123.50 124.00 124.20 124.30 124.20 123.90 123.50
L 81	122.80 122.00 120.90 119.70 118.40 116.80 115.00 $
L 82	400. 120.90 120.90 121.70 122.20 122.60 122.90 122.90 122.70 122.40 121.90
L 83	121.20 120.30 119.20 118.00 116.60 115.00 113.20 $
L 84	500. 120.00 120.00 120.70 121.20 121.50 121.70 121.60 121.40 121.00 120.50
L 85	119.70 118.80 117.70 116.40 115.00 113.30 111.50 $
L 86	630. 119.70 119.70 120.30 120.70 121.00 121.10 121.00 120.70 120.30 119.60
L 87	118.80 117.80 116.70 115.30 113.80 112.20 110.30 $
L 88	800. 120.80 120.80 121.30 121.70 121.90 121.90 121.70 121.40 120.80 120.10
L 89	119.20 118.20 116.90 115.50 113.90 112.20 110.30 $
L 90	1000. 122.80 122.80 123.30 123.60 123.70 123.70 123.40 123.00 122.40 121.60

L 91	120.60 119.40 118.10 116.60 114.90 113.10 111.10 $
L 92	1250. 125.00 125.00 125.40 125.70 125.70 125.60 125.20 124.70 124.00 123.10
L 93	122.00 120.80 119.30 117.70 116.00 114.00 111.90 $
L 94	1650. 127.00 127.00 127.30 127.50 127.40 127.20 126.70 126.10 125.30 124.30
L 95	123.10 121.70 120.20 118.50 116.60 114.50 112.30 $
L 96	2000. 127.70 127.70 127.90 128.00 127.90 127.60 127.10 126.40 125.50 124.40
L 97	123.10 121.70 120.10 118.30 116.40 114.20 112.00 $
L 98	2500. 127.60 127.60 127.80 127.80 127.60 127.20 126.60 125.90 124.90 123.70
L 99	122.40 120.90 119.20 117.40 115.40 113.20 110.90 $
L 100	3150. 126.60 126.60 126.70 126.70 126.40 125.90 125.30 124.40 123.40 122.20
L 101	120.80 119.30 117.50 115.60 113.60 111.40 109.00 $
L 102	4000. 124.70 124.70 124.80 124.60 124.30 123.80 123.10 122.20 121.10 119.90
L 103	118.50 116.90 115.10 113.20 111.10 108.90 106.50 $
L 104	5000. 122.40 122.40 122.40 122.20 121.80 121.30 120.50 119.60 118.50 117.30
L 105	115.80 114.20 112.50 110.50 108.50 106.20 103.90 $
L 106	6300. 119.80 119.80 119.80 119.60 119.20 118.60 117.90 116.90 115.80 114.60
L 107	113.10 111.50 109.80 107.90 105.80 103.60 101.30 $
L 108	8000. 117.80 117.80 117.80 117.60 117.20 116.60 115.90 114.90 113.80 112.60
L 109	111.20 109.60 107.80 106.00 103.90 101.70 99.40 $
L 110	10000. 117.40 117.40 117.40 117.20 116.90 116.30 115.50 114.60 113.50 112.30
L 111	110.90 109.30 107.60 105.70 103.70 101.50 99.20 $
L 112	END* $

Discussion:

Table 2 Line-by-line Explanation of Table 1

Line #	Comment
L 1 to L 5	Lines starting with $-signs are comments and explanatory notes
L 6	The UPDATE command will operate on new data unit IBFLP3 and read its contents from the subsequent lines.
L 7	The –ADDR directive adds records from the input stream (OLDM=*) to a new data member called SPL. FORMAT=0 means that the input format is 'undefined' where a data item's data type is determined from its appearance: numbers containing just digits are integers, those containing a decimal point are real single precision.
L 8	The radius of the reference sphere on which the subsequent noise levels are applicable. The units depend on whether the ANOPP input deck uses SI (meters) or English units (feet). Here, English units are used.
L 9	The number of points for each of the independent variables: 24 frequencies, 17 polar directivity angles, 1 azimuthal directivity angle, 1 power setting, and 2 Mach numbers.
L 10	Lines L 10 through L 60 are repeated below for two Mach numbers. Azimuthal directivity angle PHI and power setting POWER stay the same at 0.0 and 0.10, respectively. The Mach number for the first block is 0.249.
L 11 & L 12	The 17 values of polar directivity angle. Note that the $-sign only occurs at the end of L 12 to conclude the set.
L 13 & L 14	The first values are the frequency in Hertz, followed by 17 third-octave band sound pressure levels for the 17 polar angles.
L 15 - L 60	Repeat of L 13 and L 14 for 23 more frequencies.
L 61	starts the second set for Mach 0.259
L 112	Required terminator

The SPL values themselves are arrived at according to these considerations:

- They assume that the source is a point in a free field.
- They are applicable on a sphere of radius r_a. It is chosen here as 1 foot.

- They are calculated by applying corrections for spherical spreading and atmospheric absorption; at 1 foot the data are ‘loss-less’.
- They include all scaling effects, shear layer corrections, and frequency shifts due to source motion.
- Ground reflection is added by ANOPP when using these data in making predictions.

Configuration effects cannot be built directly into data tables as described above. Of course, gear up, gear down is handled in ANOPP by absence or presence of the noise source. Different flap deflection angles need to be handled by providing separate data tables for each angle.

5.4.2 Data Proper

The data tables are contained in computer files that are provided on a compact disk that accompanies this report. The structure and contents of the disk are described in the appendix. Baseline noise level data are contained in files with the extension `'tbi'`, mnemonic for 'to be included' in library make files.

The individual data files were combined into ANOPP libraries. You can find the ANOPP input files for library creation in the 1_Baseline directory under each airplane: `STAF2K_makeLIB.inp`, `MTAF2K_makeLIB.inp`, and `LQAF2K_makeLIB.inp`. Running those as ANOPP jobs results in library files `LQAF2K.WRK`, `MTAF2K.WRK`, `STAF2K.WRK`. The first two letters of the file names designate the airplane; “AF” stands for ‘air frame’, and “2K” stand for ‘year 2000’.

5.4.3 Overflight Noise Levels

Using the above described data, airframe-noise-only overflight EPNLs and time histories of PNLT were predicted for all three aircraft, and for the three FAR 36 noise certification points 'sideline', 'cutback', and 'approach'. They are all marked 'baseline' since no airframe noise reduction concepts have been applied. In the following figures, the thus predicted total airframe noise data are compared to the 1992 data (often 'Y92' in the figures) published in Ref. 16. Also shown are the airframe noise components that contribute to the newly predicted airframe noise, often marked Y2K (year 2000) or not marked at all. In the following discussion, EPNL differences are given in terms of the current prediction less the 1992 value.

Table 3 summarizes that data and provides pointers to directories on the compact disk containing files that were used to generate the figures. Files ending in `.inp` are ANOPP input files, those ending in `.dat` are ANOPP output files, those ending in `.plt` are TecPlot ASCII data files, and those ending in `.lay` are TecPlot layout files. The ANOPP runs were carried out on NASA Langley's computer `iasos2.larc.nasa.gov` using ANOPP executable program version `anopp_dbg_L15.exe`.

The differences between current predictions and the Year 1992 baseline are small for the cutback and approach conditions (of the order of 1 dB). For sideline, they are somewhat larger.

Table 3 Overflight Prediction Comparisons

			Y2K EPNL	Y92 EPNL	ΔEPNL	Compact Disk Path
Figure 6	LQ	Sideline	86.37	88.62	-2.25	4_OverFlightSim\1_Baseline\3_LargeQuad\1_Takeoff\lqtko.*
		Cutback	90.35	90.95	-0.60	
Figure 7		Approach	99.22	98.13	1.09	4_OverFlightSim\1_Baseline\3_LargeQuad\2_Approach\lqapp.*
Figure 8	MT	Sideline	79.84	82.22	-2.38	4_OverFlightSim\1_Baseline\2_MediumTwin\1_Takeoff\mttko.*
		Cutback	79.75	80.33	-0.58	
Figure 9		Approach	92.71	93.06	-0.35	4_OverFlightSim\1_Baseline\2_MediumTwin\2_Approach\mtapp.*
Figure 10	ST	Sideline	77.53	81.08	-3.55	4_OverFlightSim\1_Baseline\1_SmallTwin\1_Takeoff\sttko.*
		Cutback	76.02	77.03	-1.01	
Figure 11		Approach	91.79	91.52	0.27	4_OverFlightSim\1_Baseline\1_SmallTwin\2_Approach\stapp.*

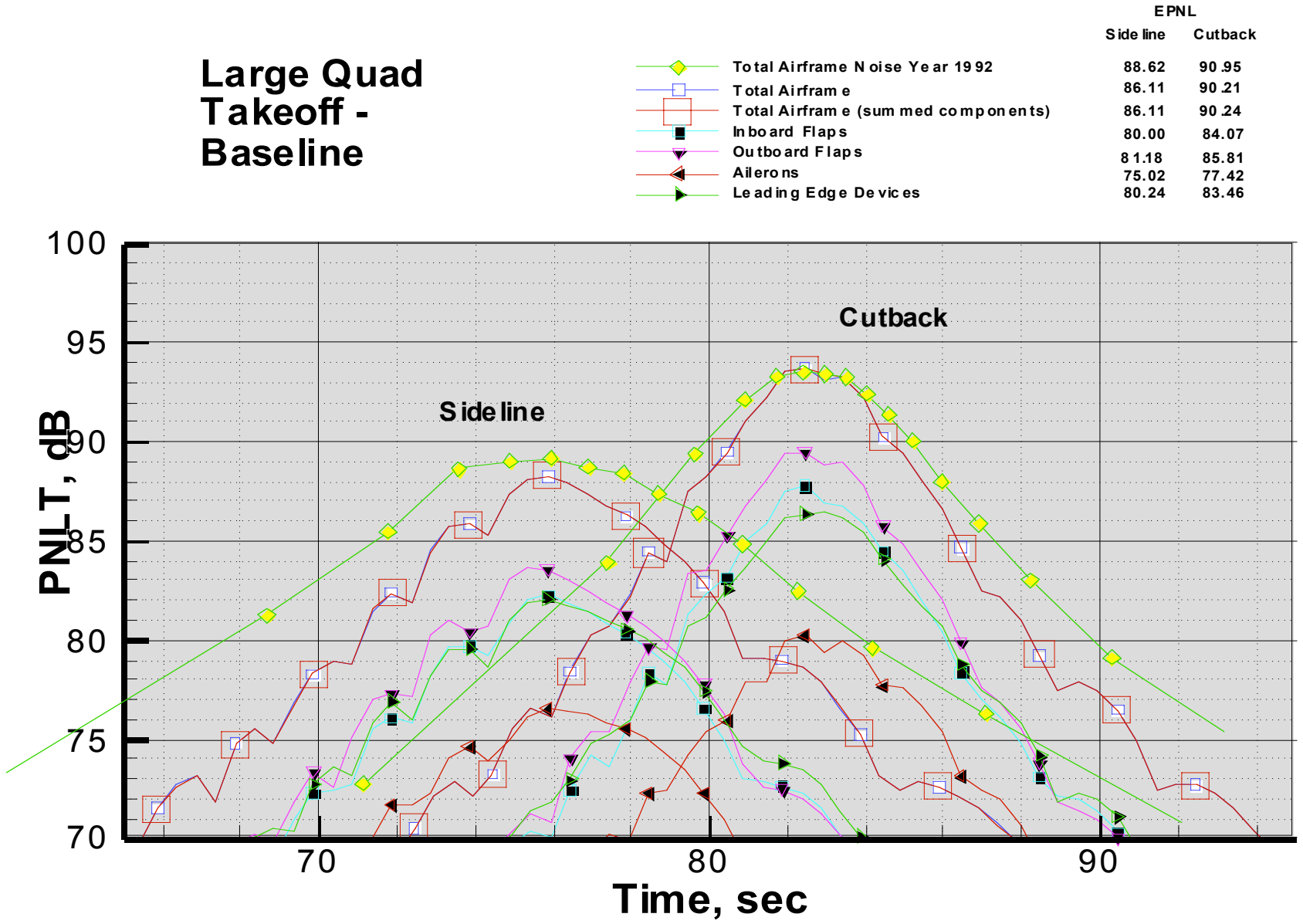

Figure 6 PNLT vs. time for Large Quad, Sideline and Cutback - Baseline

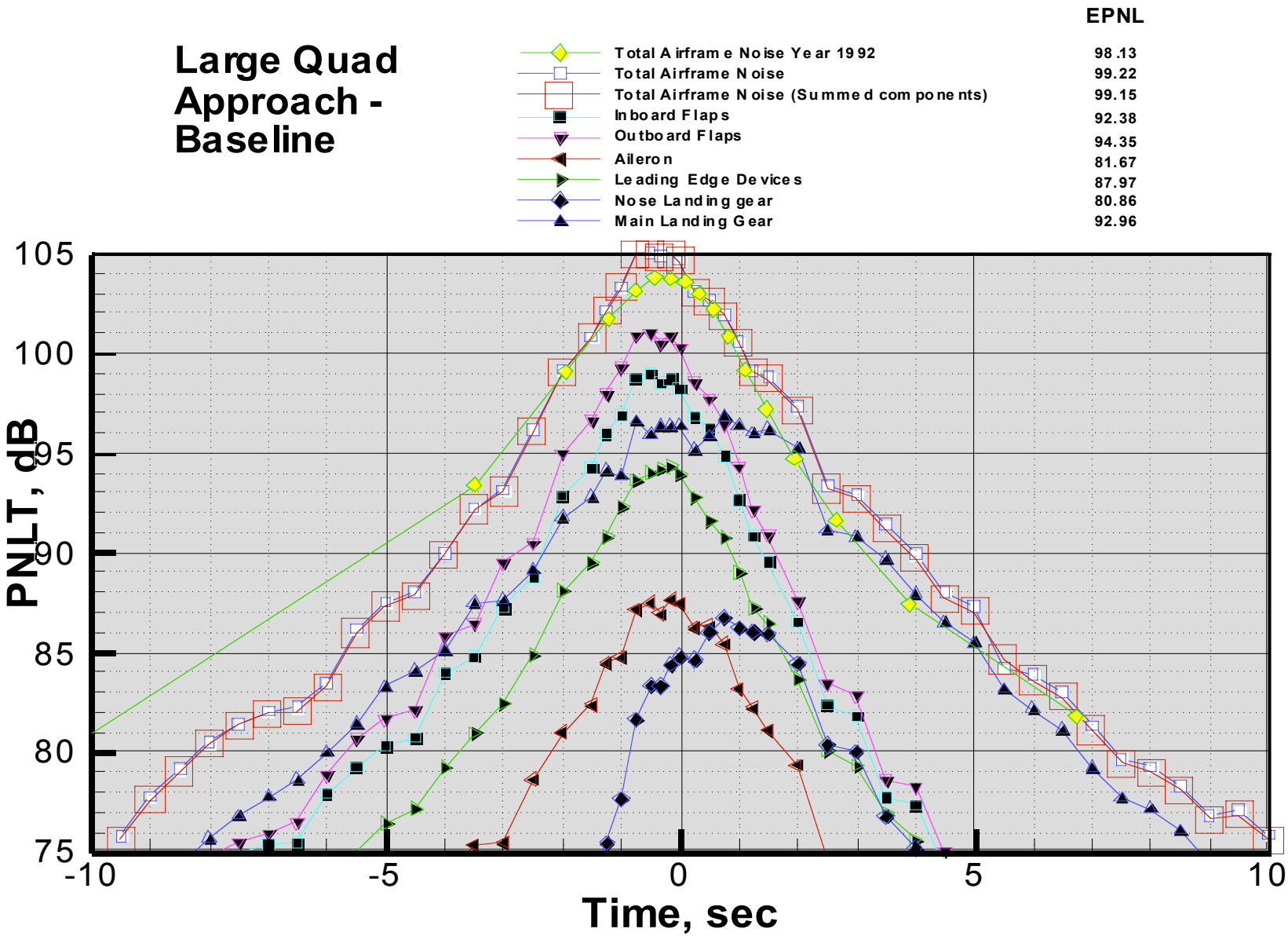

Figure 7 PNLT vs. Time for Large Quad Approach - Baseline

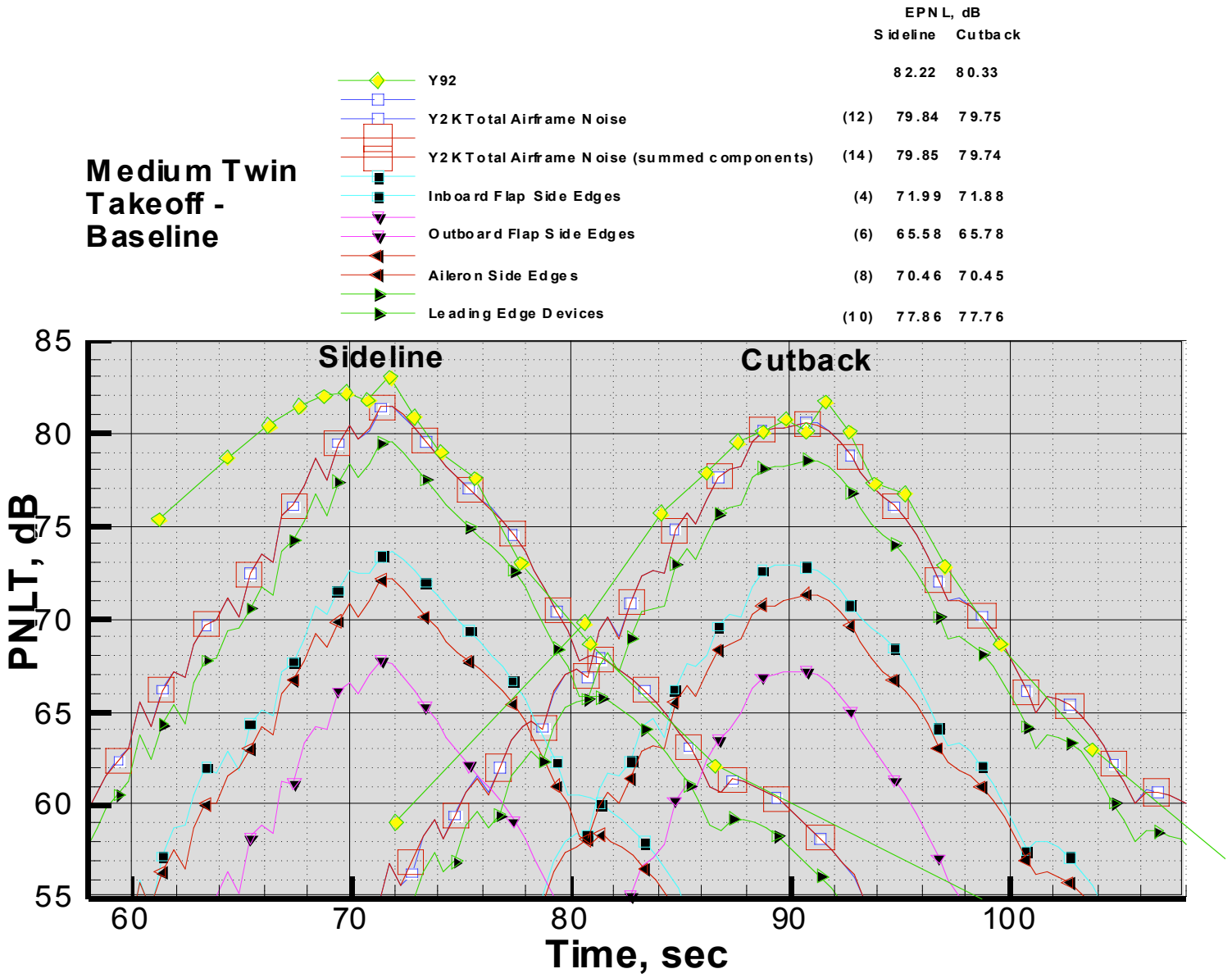

Figure 8 PNLT vs. Time for Medium Twin Takeoff - Baseline

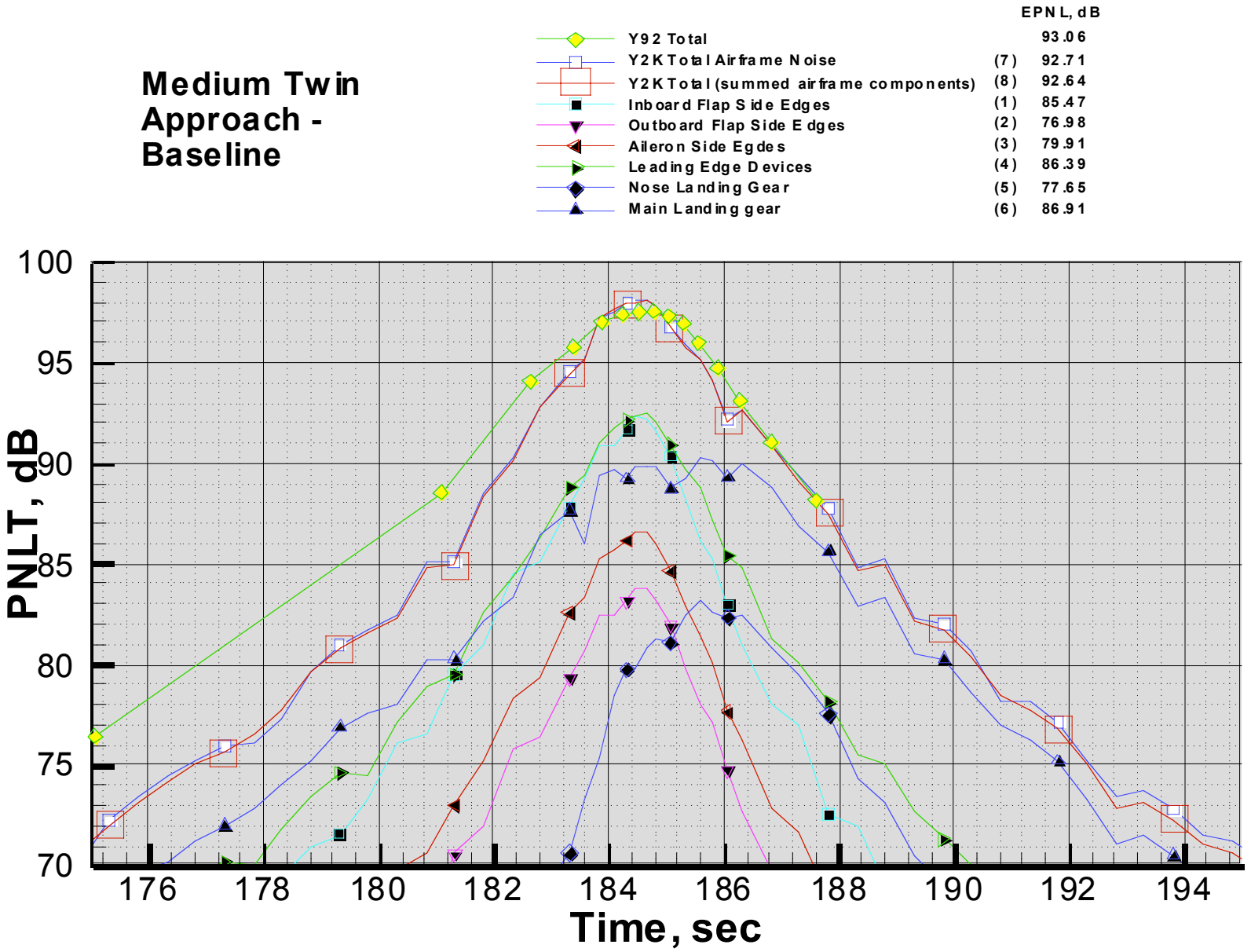

Figure 9 PNLT vs. Time for Medium Twin Approach - Baseline

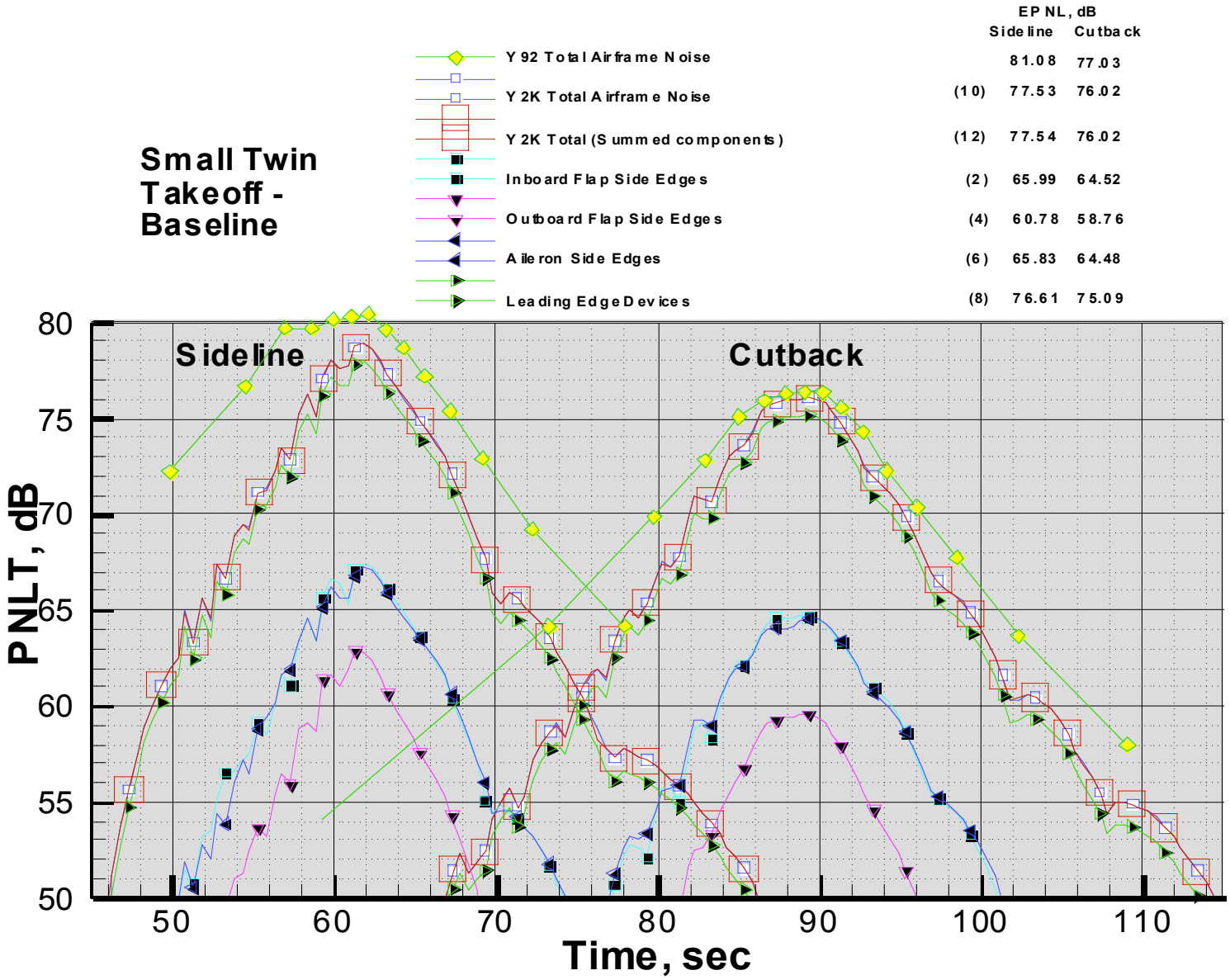

Figure 10 PNLT vs. Time for Small Twin Takeoff - Baseline

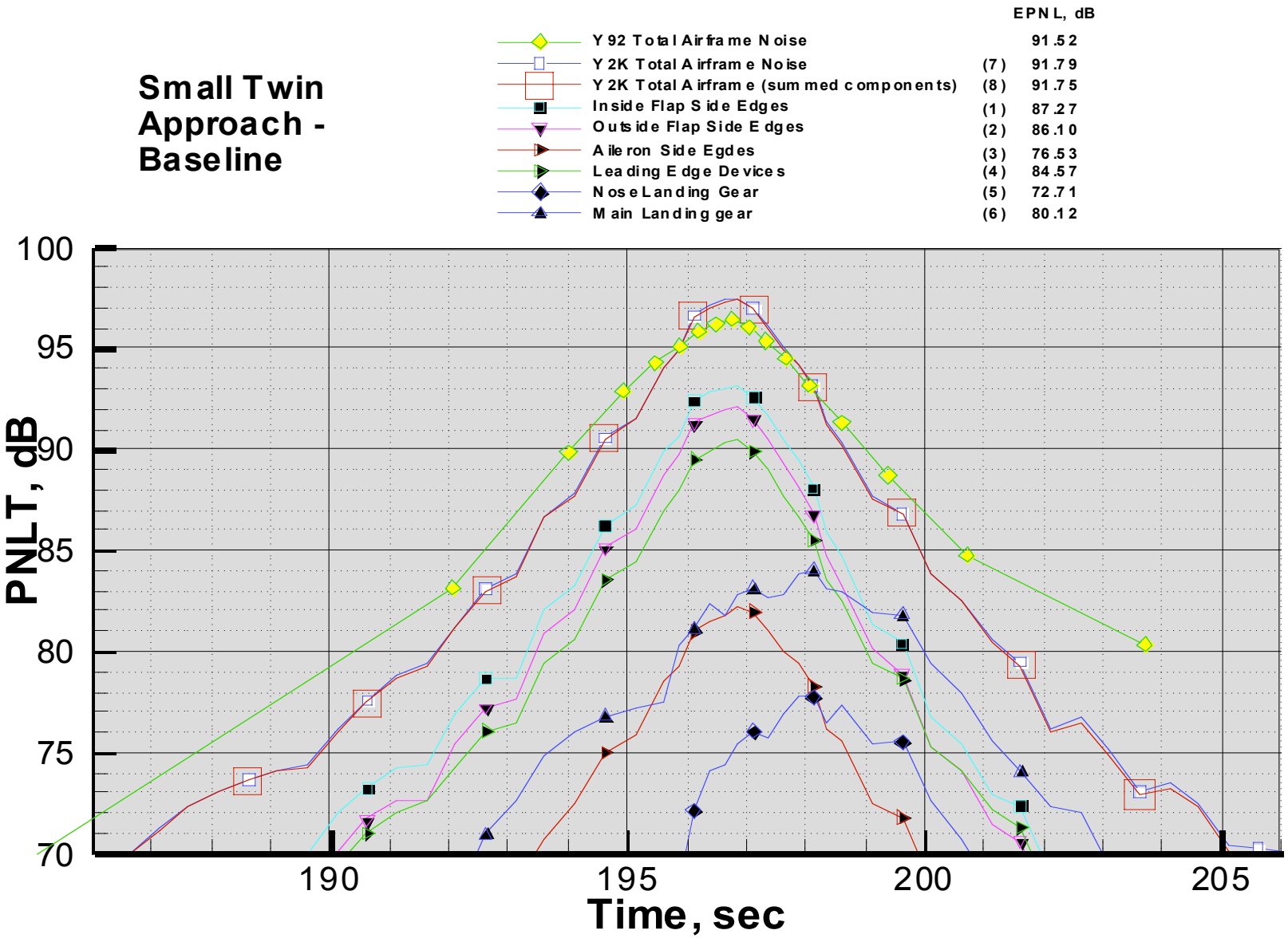

Figure 11 PNLT vs Time for Small Twin Approach - Baseline

6 Noise Reduction Concepts Evaluation

This evaluation uses the latest modeling methods and experimental data available in the AST literature and at the Boeing Company.

6.1 Scaling from Model Scale to Full Scale

Most of the available data on various treatment options was obtained at model scale. In order to apply it to full-scale airplanes it needs to be scaled. Since we are dealing only with "deltas" due to treatment, one may assume that the same decibel delta's can be used to adjust absolute levels albeit at scaled frequencies. Guo in Ref. 31 argues that a Reynolds number dependent frequency scaling law should be used; assuming fully turbulent boundary layer flows the scaling law turns out be

$$f_{\text{FULL}} = \left(\frac{L_{\text{MODEL}}}{L_{\text{FULL}}} \right)^{0.8} f_{\text{MODEL}} \qquad \text{Eq. 1}$$

where f denotes frequency, and L denotes a characteristic length.

Ref. 61 compares in its Fig. 14 (reproduced here in Figure 12) DC-10 flight airframe noise data with data from a 4.7% wind tunnel model. The comparison is at full-scale frequencies. The model data was corrected in amplitude according to Reynolds number effects discovered in that study (dashed curve). Frequencies were scaled linearly using the constant Strouhal number assumption as documented for example in Ref. 7 and Ref. 22, which leads to

$$f_{\text{FULL}} = \frac{L_{\text{MODEL}}}{L_{\text{FULL}}} f_{\text{MODEL}} \qquad \text{Eq. 2}$$

Quoting from Ref. 61: *The 40x80 prediction matches the flight data within 5 dB up to 1 KHz; above 1 KHz the departure grows to almost 10 dB at 4 KHz.* If the model data had been frequency scaled according to Eq. 1 then the frequencies would have come out by a factor of $(0.047)^{0.8-1} = 1.84$ higher. The dashed curve would become the double-line curve in Figure 12 and the agreement would be a lot better at higher frequencies that are the ones important in EPNL calculations. This provides some support for the use of Eq. 1 for airframe noise frequency scaling.

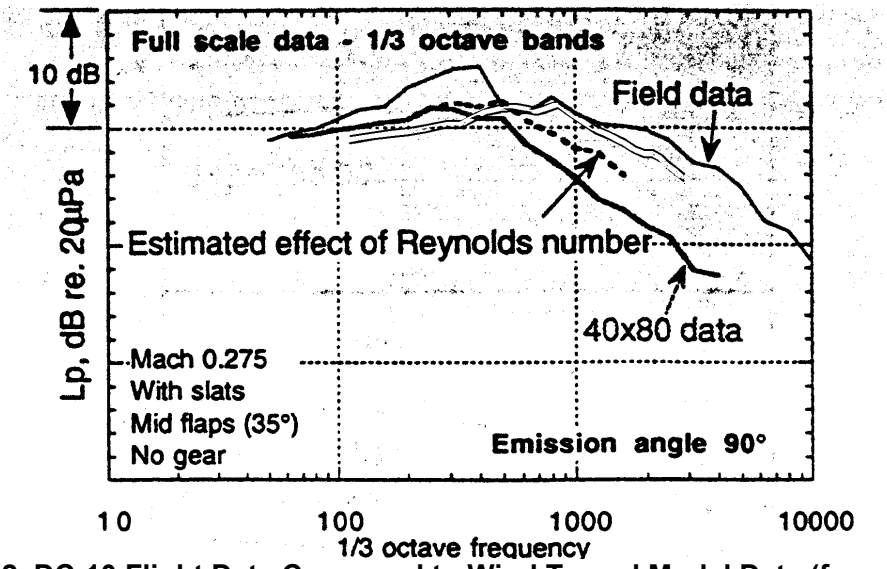

Figure 12 DC-10 Flight Data Compared to Wind Tunnel Model Data (from Ref. 61)

6.2 Flap Side Edge

6.2.1 Fence

Flap side edge fences are simple devices: flat plates attached to the side surfaces of the flaps protruding into the flow on the lower side of the flaps.

Ref. 11 carried out flap fence experiments early in the AST program; we quote: *"Two flap fence configurations were tested in this program and a relationship between the fence size and noise source frequency is indicated. The fences were vertical plates set adjacent to the outboard flap edge, from the wing trailing edge extending to the flap trailing edge. A large fence dramatically reduced the flap edge noise source. The noise reduction in the outboard flap region was as much as 9 decibels at the high one-third octave band and 3 decibels in the middle one-third octave band. A smaller fence, approximately half the height of the large fence, reduced noise levels at high frequencies but increased levels at middle frequencies."*

Ref. 21 looked into aerodynamic effects of flap side edge fences and found a significant drag reduction (20%) with a lower flap tip fence, with a marginal increase in maximum lift with minimal effects on the lift curve at lower angles of attack.

Ref. 25 investigated the effects of flap side edge fences experimentally in the NASA Ames 40x80 tunnel using a DC-10 4.7% scale model. The following is a quote from that paper's summary: *"1) addition of the flap tip fences decreases the sound levels measured from the source at the flap side edges without affecting the levels from the sources at the slats (indicating that the aerodynamic loading of the slat is not affected when the flow at the flap is fenced); 2) the flap tip fences are generally more effective in reducing the noise on the outboard edge of the outboard flap than on the inboard edge with and without slats. The outboard edge is aligned with the freestream flow, while the inboard edge is not. The flap tip fences have been shown to be most effective when the flap side is aligned with the freestream flow in testing conducted in the Ames 7x10 wind tunnel."*

The data describing the fence effect used in this report are based on these DC-10 4.7% scale model tests. The experimental data show little change of the fence effect with polar (front to back) directivity, especially around the overhead flyover position. Azimuthal directionality is typically not measured because it is of little interest to noise certification. The flap tip fence noise reduction effect is assumed to be invariant in the azimuthal direction. Noise reduction data are shown in Figure 13, Figure 14, and Figure 15. All flap side edges on the airplane are assumed to be given the same type of fence at the same time.

From Ref. 58: Flap side edge fences only affect local flow without changing the overall performance of the high lift system. Typically, side edge fences achieve a noise reduction on the order of 4 dB in the mid to high frequencies. The reduction is due to the cross flow being blocked by the fences leading to a lowering of the dominant frequencies and reduction of fluctuation amplitudes at higher frequencies. The lower frequencies are due to lower velocities and due to an increase in the side edge surface dimensions leading to increased characteristic time scales in the flow. Amplitudes at lower frequencies may actually be increased, but this is more than compensated by the higher weighting given to spectral contents at higher frequencies in human loudness evaluation (such as PNL).

As mentioned above, fence effects are derived from one set of test data. Because of the lack of other data, we have not been able to establish a correlation to airplane configurations. Thus, we are assuming that the same noise reductions apply to all airplanes, which, hopefully, can be verified in the future. This may not be too bad because it is known from aero measurements that the fence effects are only very weakly related to the overall aerodynamics, indicating that their correlation with airplane configuration may be weak.

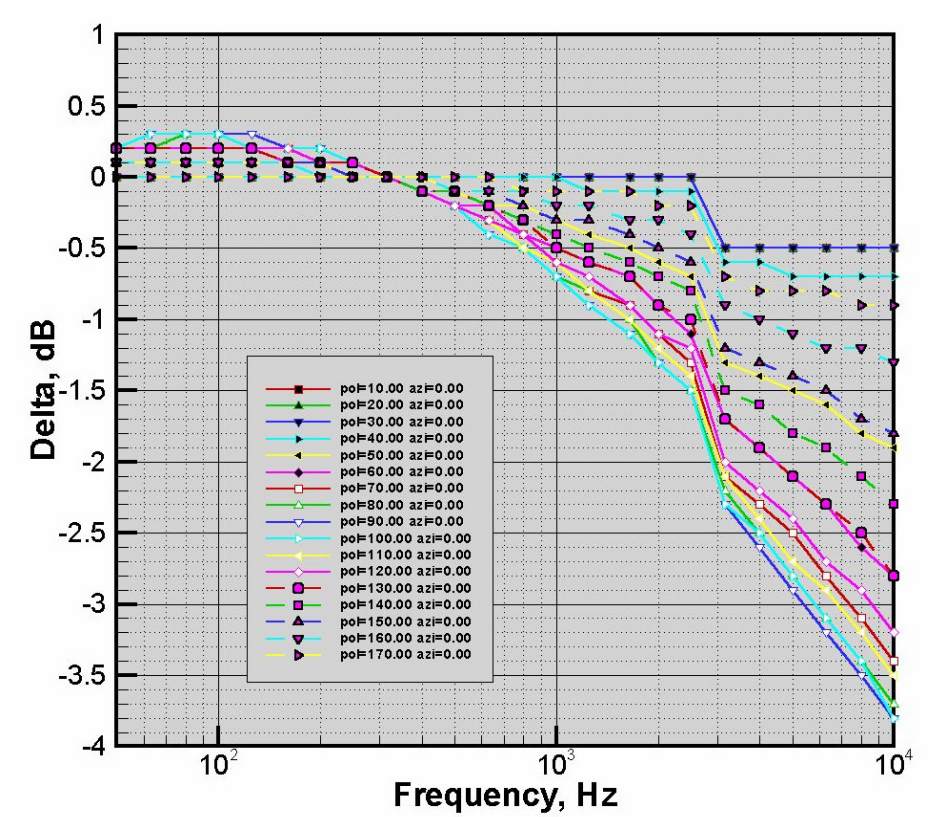

Figure 13 Delta Data for Flap Side Edge Fences, Fence Height = 1/2 Flap Side Edge Max Thickness

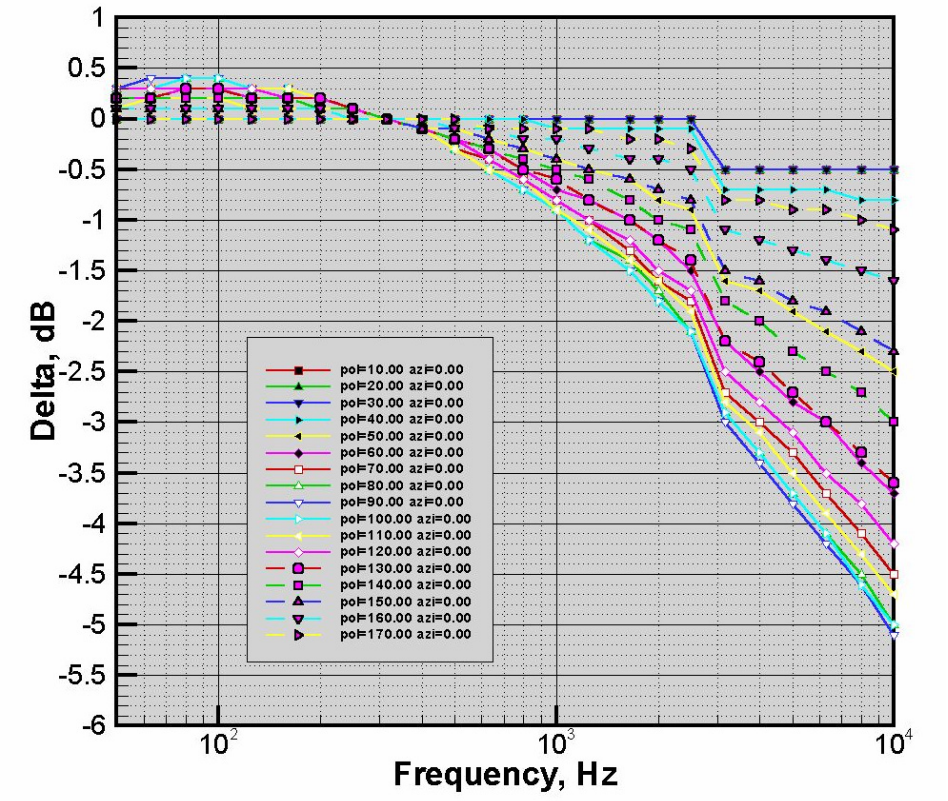

Figure 14 Delta Data for Flap Side Edge Fences, Fence Height = Flap Side Edge Max Thickness

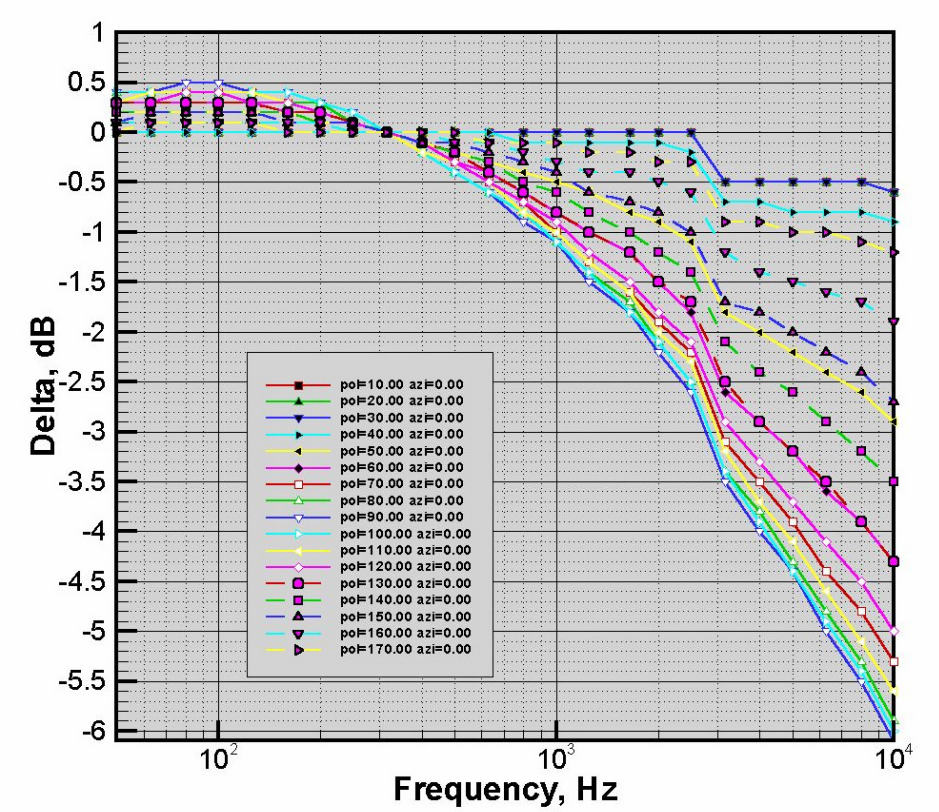

Figure 15 Delta Data for Flap Side Edge Fences, Fence Height = Twice Flap Side Edge Max Thickness

6.2.2 Side Edge Shaping

In 1997, T.F. Brooks started reporting on experiments using a phased array in NASA Langley's Quiet Flow Facility where the shape of the side edge is varied (Ref. 31). The data used here are taken from Ref. 71:

Data are available at 29° and 39° flap deflection angles. For the 747-400 (Large Quad), the 39° case was selected as more representative at the 30° flap detent than the 29° case: the main flap element's deflection angle is about 28°; however, the last of the three flap elements causes a lot of flow deflection as its angle with the main wing is 52°. The same data were also used for the Medium and Small Twins, but with different frequency scaling.

Data are available for Mach numbers of 0.07, 0.11, and 0.17. What is needed here are Mach numbers around 0.25. One might be tempted to extrapolate on an M^5 basis; however, when comparing the Ref. 71 noise reductions for different Mach numbers the trend is towards significantly smaller differences between Mach 0.17 and 0.11 than between 0.11 and 0.07. The Mach 0.17 deltas between flat and treated side edges are therefore taken to apply also around Mach 0.25.

Data are available for several side edge shapes: flat (baseline), flange, round, and round with grit (the grit's intent is to produce thickened and well developed turbulent boundary layers in the vicinity of the side edge). The one with the most promising noise reduction potential appears to be the latter; only the difference between it and the baseline flap side edge is considered here.

The data in Ref. 71 were scaled in frequency per Eq. 1 using flap chord length ratios. The model chord is 4.8 inches. The 747-400's inboard flap chord at its outboard edge, measured over all three elements, is 150 inches; for the outboard flap, the inboard edge chord is 114 inches. These values are then used for 'Large Quad' scaling:

Inboard flap: $$f_{\text{FULL}} = \left(\frac{4.8}{150}\right)^{0.8} f_{\text{MODEL}} = 0.0637 f_{\text{MODEL}},$$

Outboard flap: $$f_{\text{FULL}} = \left(\frac{4.8}{114}\right)^{0.8} f_{\text{MODEL}} = 0.0793 f_{\text{MODEL}}$$

This results in the deltas shown in Figure 16 and Figure 17 for azimuth 0 (directly under flight path). We note that the values are positive as well as negative, i.e., at many frequency/angle combinations there is an increase in noise due to side edge shaping. The data are given for 5 azimuthal angles (–28, -15, 0, 15, 28).

For the 'Small Twin' we use the 737-300's flap chords: 63 inches for the inboard flaps (does not vary with span), and 61.5 inches for the inboard edge of the outboard flap, leading to

Inboard flap: $$f_{\text{FULL}} = \left(\frac{4.8}{63}\right)^{0.8} f_{\text{MODEL}} = 0.1275 f_{\text{MODEL}},$$

Outboard flap: $$f_{\text{FULL}} = \left(\frac{4.8}{61.5}\right)^{0.8} f_{\text{MODEL}} = 0.1300 f_{\text{MODEL}}$$

For the 'Medium Twin' we use the 767-300's flap chords: 58.22 inches for the inboard flaps' outboard edge, and 56.88 inches for the inboard edge of the outboard flap, leading to

Inboard flap: $$f_{\text{FULL}} = \left(\frac{4.8}{58.22}\right)^{0.8} f_{\text{MODEL}} = 0.1362 f_{\text{MODEL}},$$

Outboard flap: $$f_{\text{FULL}} = \left(\frac{4.8}{56.88}\right)^{0.8} f_{\text{MODEL}} = 0.1384 f_{\text{MODEL}}$$

When resolving frequency into 1/3-octave bands, the noise reduction deltas for the Small and Medium Twins, both inboard and outboard flaps, are obtained by moving the Large Quad outboard flap side edge data up in frequency by two 1/3-octave bands.

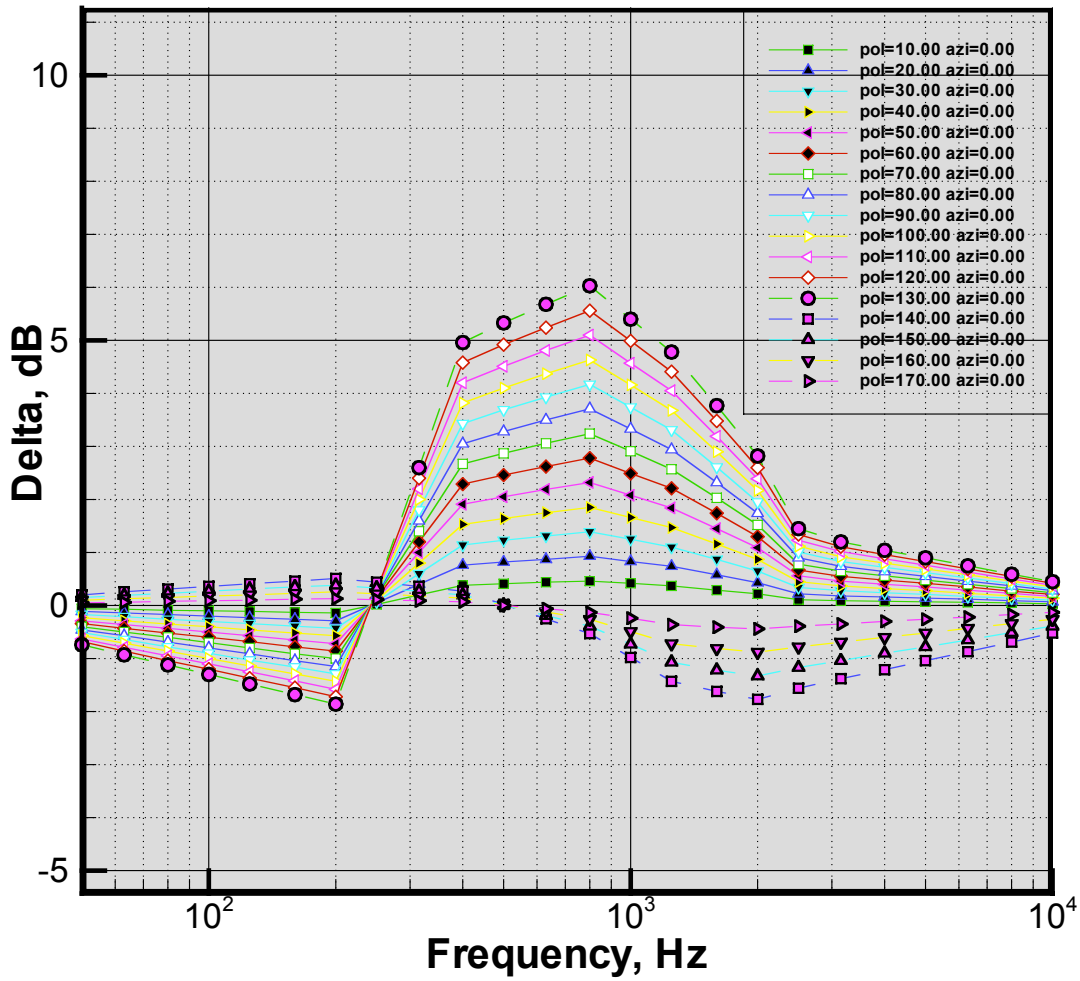

Figure 16 Delta Data for Inboard Flap Side Edge Shaping (Round with Grit), Azimuth 0°

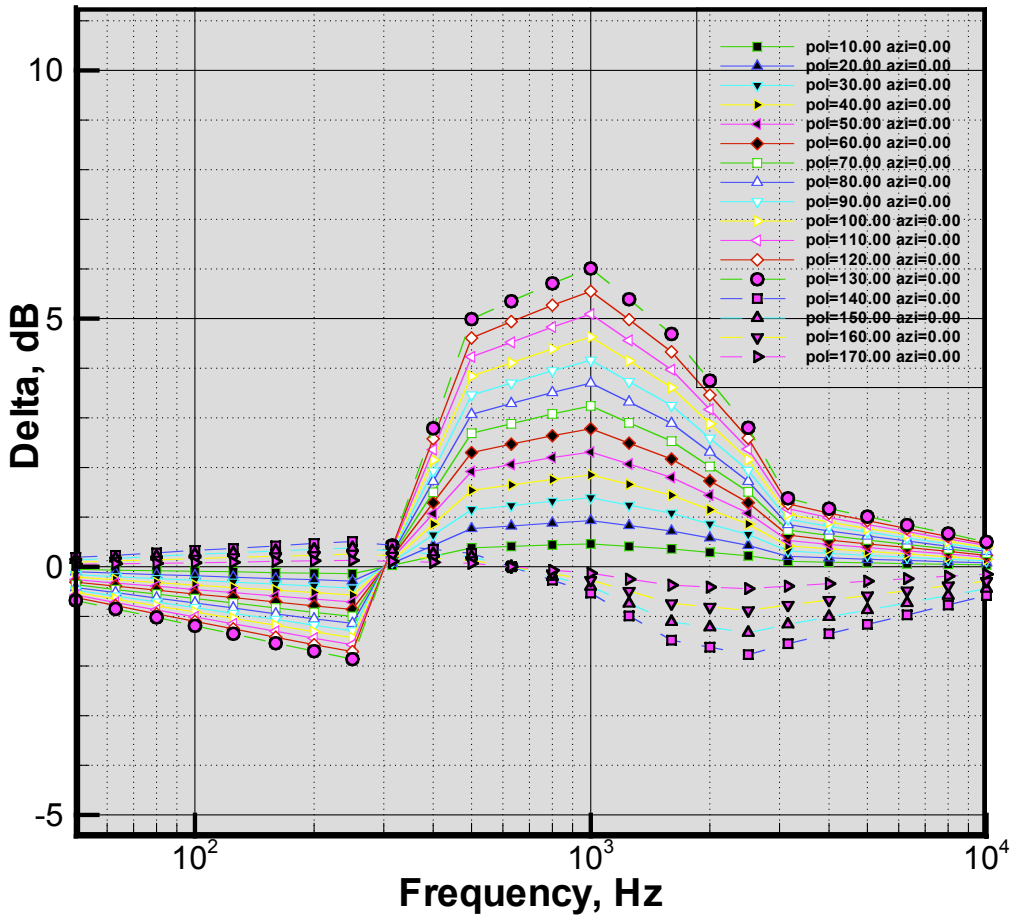

Figure 17 Delta Data for Outboard Flap Side Edge Shaping (Round with Grit), Azimuth 0°

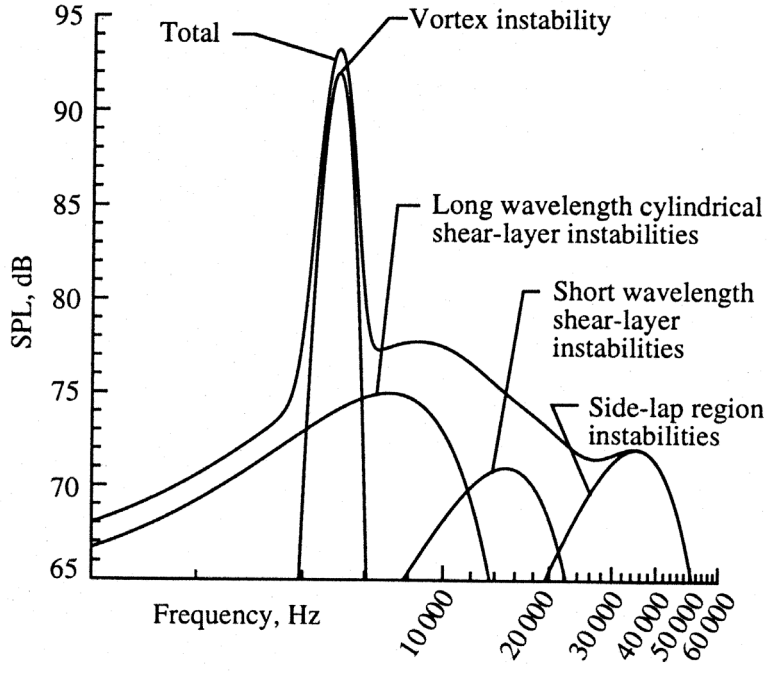

Figure 18 Schematic integrated 1/12-octave acoustic spectra of flap side-edge noise sources (from Ref. 72)

6.2.3 Trailing Edge Serrations and μ-Tabs

The effects of trailing edge serrations and μ-tabs ("micro tabs") are described in Ref. 72 (as well as in Ref. 48, C.L. Streett's presentation on "Physics of Flap-Edge Noise: Source and Reduction"). Figure 18 (taken from Ref. 72) shows the concepts as proposed in that reference where flap side edge noise generation is broken down into four components. The extremely strong tone-like 'vortex instability' source has been observed by AST workers only in the laboratory, and there only under rare conditions which are not fully understood. It is doubtful that this source would occur on actual transport aircraft, at least those of current design. Trailing edge serrations (also referred to as the 'noise weeder' in Ref. 72) are effective in suppressing this tone. However, no credit for such a suppression is assigned in this report.

μ-tabs are a row of trapezoidal fingers, slightly higher than the boundary layer thickness, attached to the pressure side of the flap close to its edge. Figure 24 of Ref. 72, reproduced here as Figure 19, shows the μ-tabs to have a noise reduction effect of 3 to 5 dB for the low and mid frequencies, and an increase of about 2.5 dB in the very high frequencies, presumably the 'side-lap region instabilities' (Figure 18). For the low frequencies, this is not consistent with information conveyed by C.L. Streett (NASA LaRC) in a telephone conversation that the 'long wavelength cylindrical shear-layer instabilities' provide a noise source that is very hard to suppress except by side edge fences or continuous mold technology. Also, data in Figure 19 was obtained on an unswept wing. A slide in Ref. 48, C.L. Streett's presentation on "Physics of Flap-Edge Noise: Source and Reduction", shows the effect of μ-tabs on a swept wing, reproduced here as Figure 20: only mid to high frequencies show a reduction. We assume that the frequency axis in Figure 20 does not reach far enough to show the increase at the very high frequencies. For the purposes of this report the μ-tab effect is estimated by the data in Figure 20 augmented by the very high frequency 'hump' of Figure 19. Furthermore, this effect is assumed to be omni directional. The frequencies were again scaled similarly to Section 6.2.2. The resulting noise reductions are shown in Figure 21.

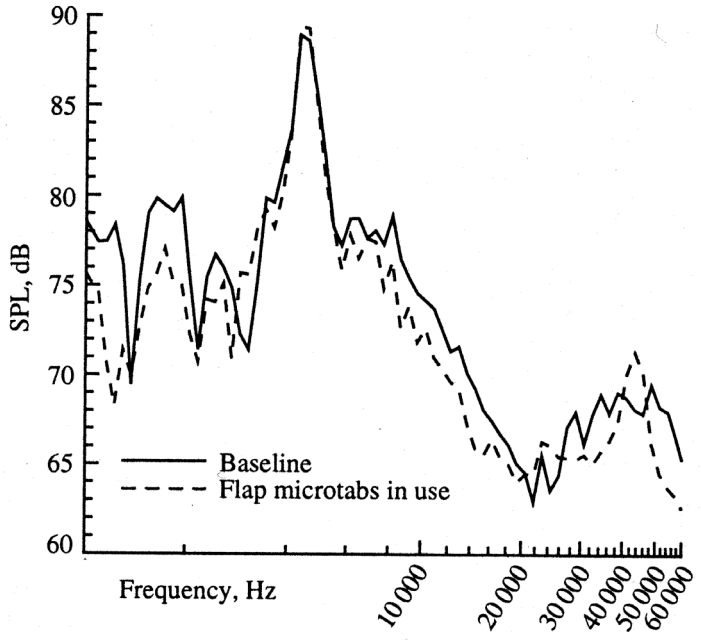

Figure 19 Integrated 1/12-octave acoustic spectra showing effect of μ-tabs

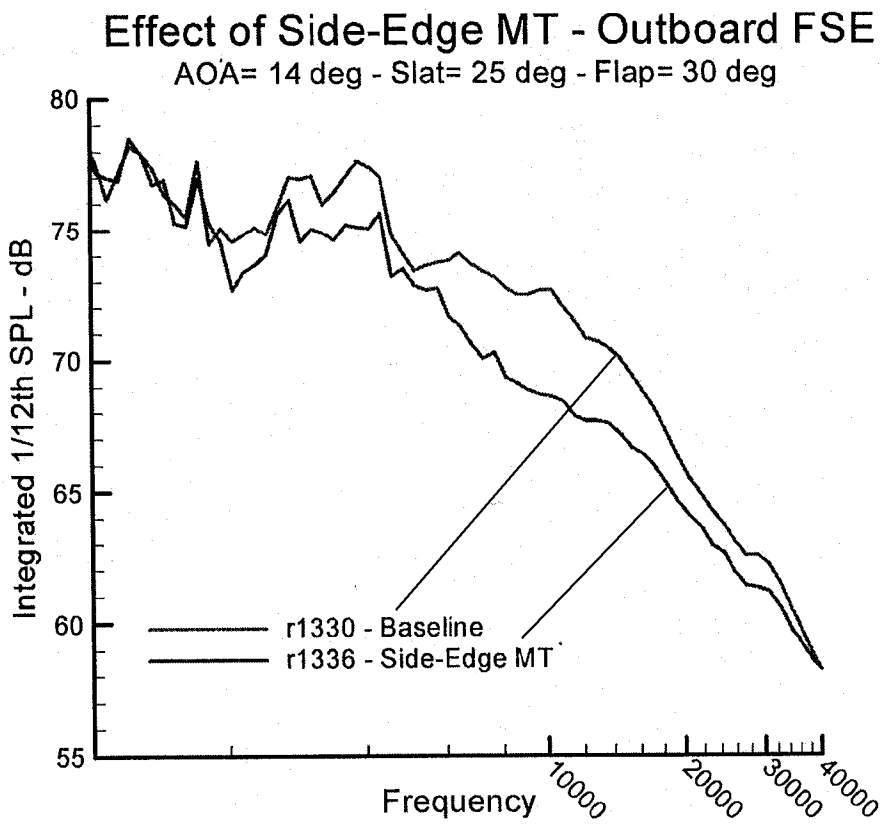

Figure 20 Effect of Side-Edge μ-Tabs

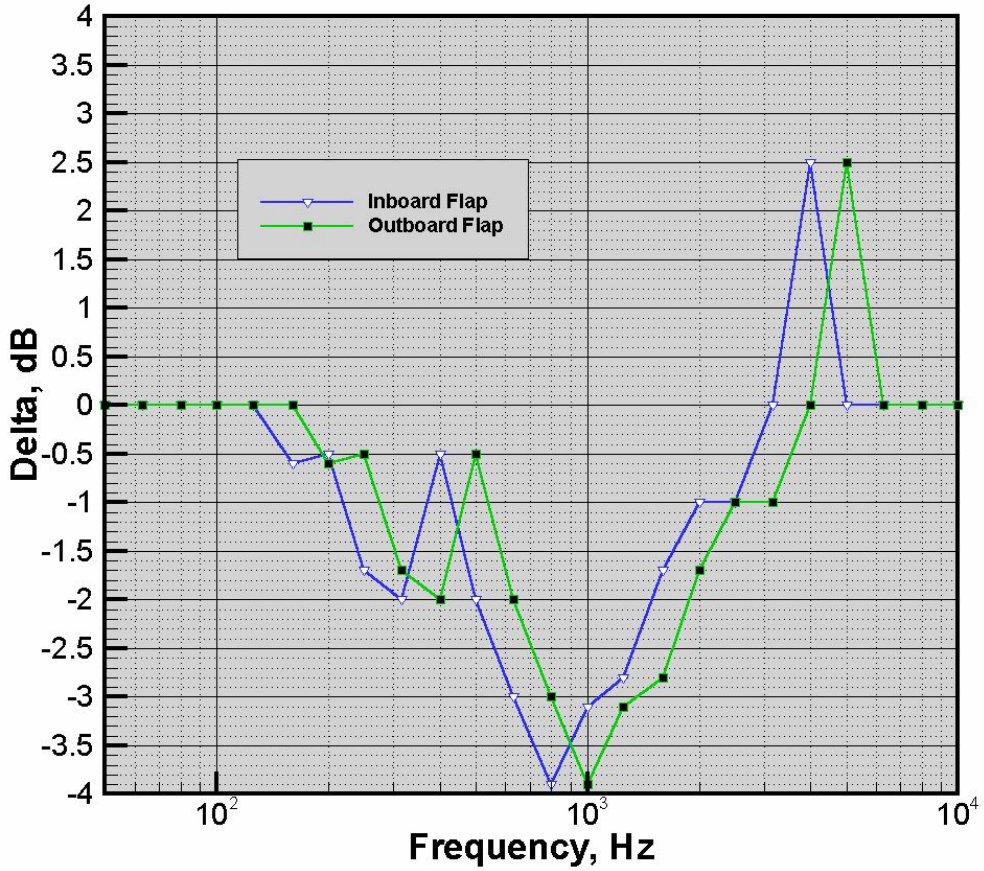

Figure 21 Delta Data for μ-Tabs on Flap Side Edge

For the Small and Medium Twin we proceed as we did for the flap side edge shaping noise reductions: the data for the Large Quad outboard flap are moved up in frequency by two 1/3-octave bands for both the Small and the Medium Twin.

6.2.4 Raked Tip

'Raked tip' means that the flap side edge is not aligned with the flow direction. Its rake angle is measured from the flap's leading edge. A rake angle of 90° is the 'un-raked' (baseline) tip shape.

Ref. 31 reports in a presentation by Bruce Storms et al., "Analysis of Flap-Tip Noise measurements from the Ames 7x10" (first in the conference proceedings) that raked flap tips can bring about noise reductions if the trailing edge is wider than the leading edge; data was acquired for a rake angle of 105°, flap deflection angle of 39°, angle of attack 10°. However, not enough data is available at the time of this writing in order to construct a noise reduction table.

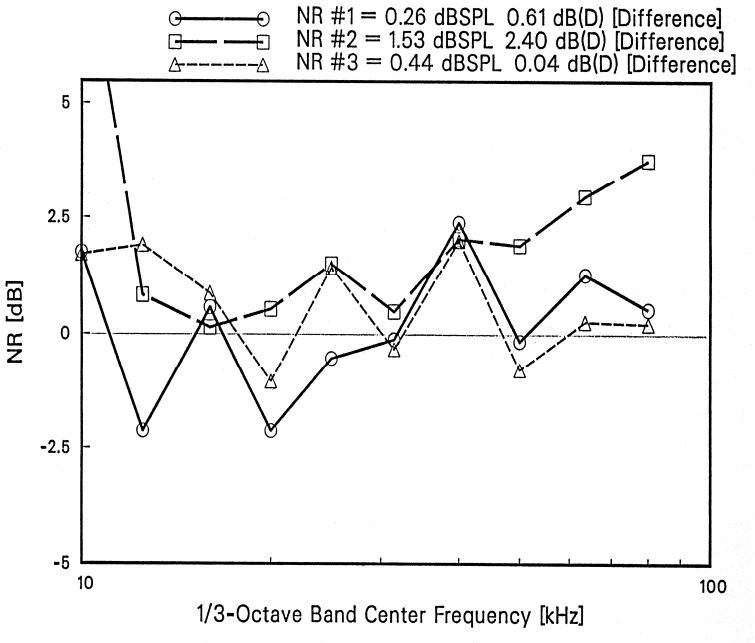

Figure 22 Noise Reduction Due to Porous Material Treatments on L1011 Flap Model (Ref. 9)

6.2.5 Porous Tip

In 1994, Lockheed investigated the effect on far field noise of treating L1011 model main flap surfaces with various porous materials (Ref. 9). The most promising of those treatments was 'NR#2' as shown in Figure 22. The authors do not comment on the high noise reduction of NR#2 in the 10KHz band. We believe that the extrapolation suggested in the figure leads to an unreasonably high noise reduction; we artificially cap the reduction at 3 dB, and assume 0dB reduction at lower frequencies. This may well miss the mark by a lot, but there is no other information available. At the high frequency end, however, it appears reasonable to let the noise reduction increase with higher frequencies by extrapolation.

In trying to apply these noise reductions to the Large Quad, we assume that appropriate materials could be found that reproduce the model data at large scale. We scale the frequencies using Eq. 1 on the basis of main flap element chord length. The chord of the model in Ref. 9 is 2.95 inches. For the 747-400, the length of the outboard edge of the inboard flap is 82.49", and the length of the inboard edge of the outboard flap is 62.14". Frequencies are then scaled according to

$$f_{FULL} = \left(\frac{2.95}{82.49}\right)^{0.8} f_{MODEL} = 0.0696 f_{MODEL} \quad \text{or} \quad f_{FULL} = \left(\frac{2.95}{62.14}\right)^{0.8} f_{MODEL} = 0.0873 f_{MODEL}$$

The above considerations lead to the noise reduction shown in Figure 23.

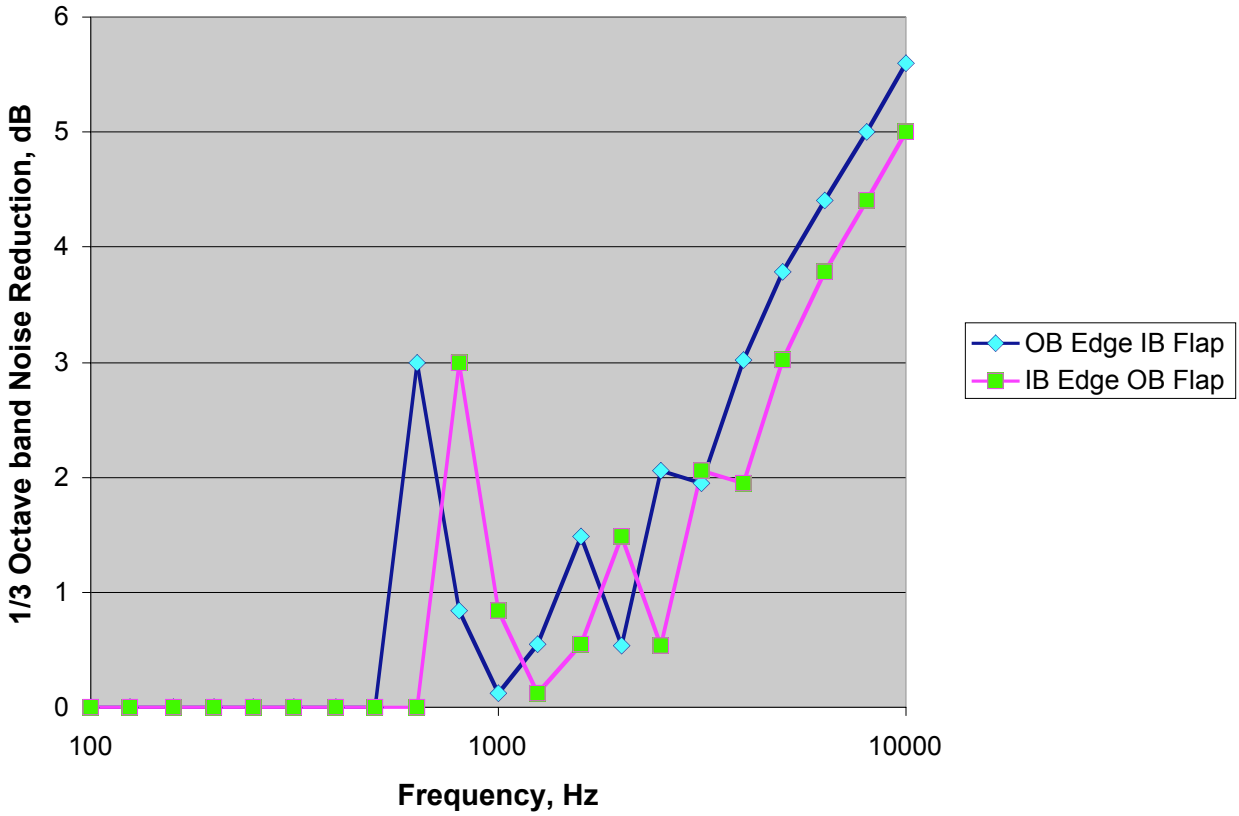

Figure 23 Noise Reduction Due to Porous Flap Treatment for Large Quad

Directivity data in Ref. 9 is not sufficiently reliable to be used here. The data in Figure 23 are assumed to apply omnidirectionally.

Ref. 19 also deals with 'acoustically treated flaps' but does not contain any far field sound radiation data and is therefore not used here.

Ref. 32 claims "… a minimum of aircraft performance penalties, since the resistance is large for the large mainstream flows at landing speeds". However, flow resistance through the porous material must be carefully controlled to provide high resistance to high speed flows (creating the aerodynamic forces) and low resistance to low speed flows (those due to acoustic motion). This can be achieved by taking advantage of nonlinear resistance behavior of porous materials: specific resistance increases with flow velocity.

For the Small and Medium Twin we proceed as we did for the flap side edge shaping noise reductions: the data for the Large Quad outboard flap are moved up in frequency by two 1/3-octave bands for both the Small and the Medium Twin.

6.2.6 No Span-wise Discontinuity

By eliminating flap side edges the associated noise source disappears. This can be achieved either by using a continuous main flap (as on the Airbus A340) or by CMT (Continuous Moldline Technol-

ogy). Ref. 66 reports that use of CMT caused flap side edge noise to be reduced to below measurable levels. This effect can therefore be modeled by omitting the flap side edge source.

6.2.7 Advances in High-Lift System Design

While there have been advances during the AST program in high lift system performance, a translation into quantifiable noise reduction has not been done. We confine our treatment here to general comments: a more effective high lift system provides more lift at the same speed. This allows reducing approach speed with an accompanying reduction in required thrust; this, in turn, reduces the total airplane noise. Also, if the high lift system could deliver less drag for the same lift, less thrust would be required for the same speed. However, engine thrust must not be reduced too much in order to be able to increase thrust quickly in an emergency without having to wait for the engine to spool up.

6.3 Leading Edge Devices

High lift devices at the wing's leading edge are either Kruegers or slats. Kruegers are devices consisting of a thin cambered surface, practically without thickness. Slats are devices with an airfoil cross-section having thickness and camber. So far in the AST program, only slats have been investigated as to their noise behavior. We therefore make the bold assumption that Kruegers behave the same way as slats.

In some slat noise experiments a strong very high frequency peak was observed with a bandwidth of about two third-octave bands. It was attributed to vortex shedding at the slat trailing edge. Such a tone has not been observed on transport aircraft in service. The probable difference is that the laboratory models had straight wings whereas actual aircraft have swept wings. In the laboratory, serrations at the slat trailing edge were effective in practically eliminating this tone. However, no credit for this noise reduction concept is assigned in this report.

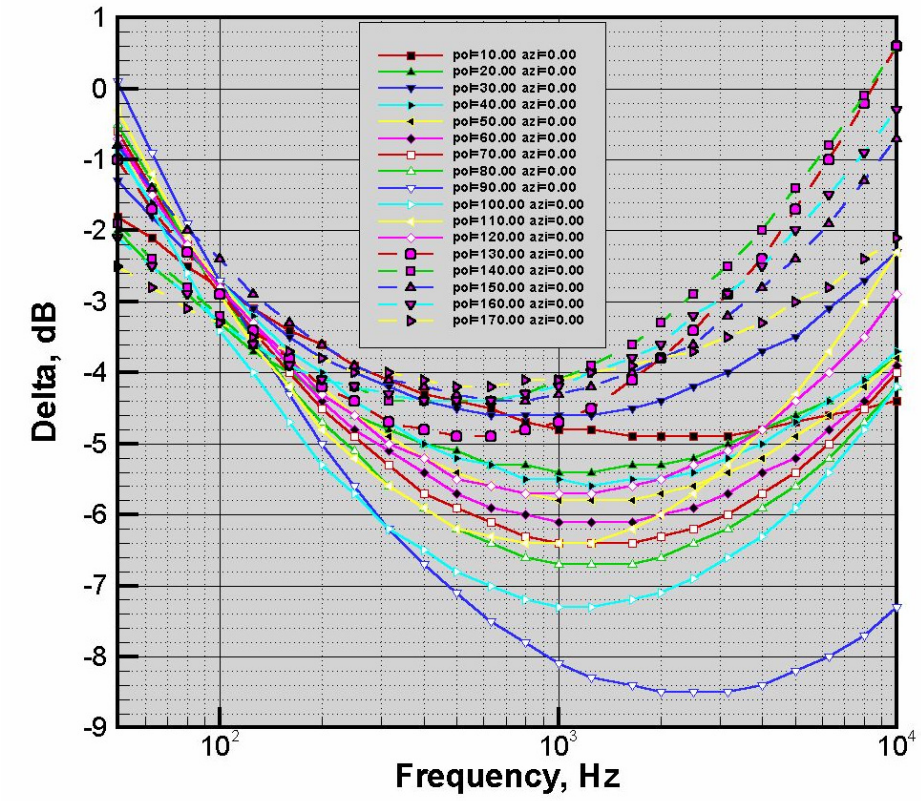

Figure 24 Delta Data for Reducing the Slat Gap by 1 Percent of Stowed Wing Chord.

6.3.1 Reduce Size of Gap

In Ref. 70 it is shown that very promising noise reduction comes from decreasing the slat gap. By reducing the slat gap by one percent of the stowed wing chord, it is shown that a noise reduction of about 5 dB can be achieved at the peak radiation angle, consistent with test data. No assessment is made here on the impact on aerodynamic performance. Using the methods of Ref. 70, the spectral details of this noise reduction have been predicted for the Large Quad, as shown in Figure 24. For the Small and Medium Twins, similar data were obtained; they are not shown here but are used in Sections 6.5 and 6.6.

6.3.2 Slat-Cove Filler

One of the sources of noise from a leading edge device is its 'cove' (see Figure 5) at the rear made necessary by the device to integrate smoothly into the main wing when it is not deployed. A large area of separated flow exists in the cove area causing mainly low frequency noise. Ref. 72 investigated filling the cove of a wind tunnel model and arrived at the results shown in Figure 25. How the cove would be filled in practice remains to be developed. One idea is to incorporate an inflatable device into the slat or Krueger. Another would be a spring-loaded thin metal sheet that would pop into place upon slat/Krueger deployment, and be pushed back into the slat/Krueger when it is stowed. As is apparent from these comments, there is a long way to go to flight status of this concept.

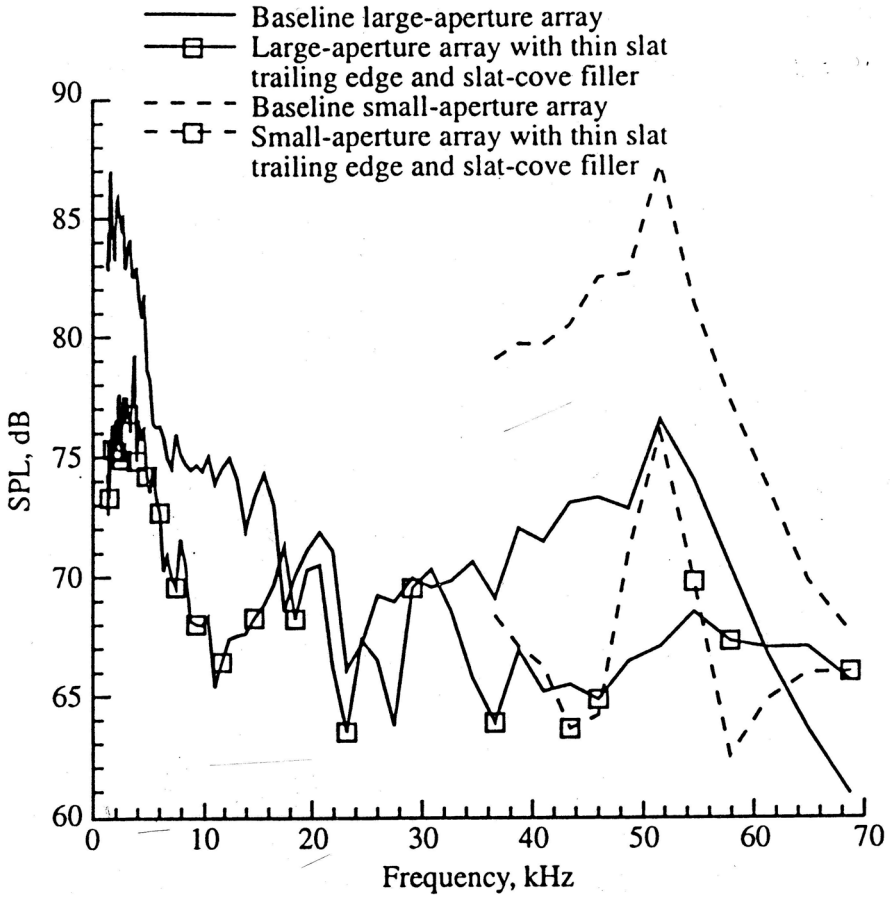

Figure 25 Integrated 1/12-octave spectra on slat (main wing angle of attack 6°, deployment angle 30°, Reynolds Number 14.4×10^6, Mach 0.2) (from Ref. 72)

Again, we scale frequencies on chord lengths: the model slat chord is approximately 5 inches. The 747-400's leading edge device chord is 31 inches. From Eq. 1:

$$f_{\text{FULL}} = \left(\frac{5}{31}\right)^{0.8} f_{\text{MODEL}} = 0.23 f_{\text{MODEL}}$$

Even though the large quad representative, the Boeing 747-400, only uses Kruegers, the effect of a slat cove filler can still be demonstrated in the hope that a Krueger cove filler's effect will not be much different from that of a slat cove filler. The noise reduction gleaned from Figure 25 is contained in Figure 26.

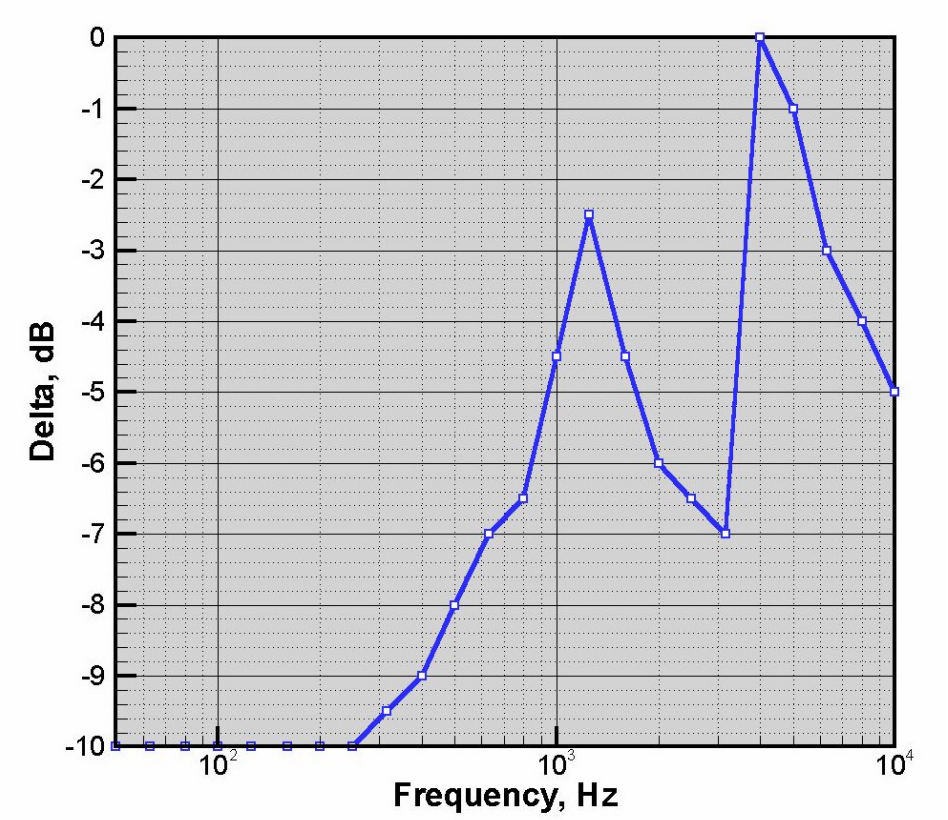

Figure 26 Delta Data for Cove Filler.

For the Small Twin, represented by the Boeing 737-300, the slat chord length is 13.12 inches. The frequency scaling becomes

$$f_{\text{FULL}} = \left(\frac{5}{13.12}\right)^{0.8} f_{\text{MODEL}} = 0.46 f_{\text{MODEL}}$$

which is double the scaling factor of the Large Quad, or one octave band, or three third-octave bands towards higher frequencies.

For the Medium Twin, represented by the Boeing 767-300, the slat chord for the inboard slat is 20 inches, and the one for the outer slat is 24 inches. We can use only one number in the present scheme; because the outer slat is much longer than the inner one we use the chord of the outer slat for frequency scaling:

$$f_{\text{FULL}} = \left(\frac{5}{24}\right)^{0.8} f_{\text{MODEL}} = 0.285 f_{\text{MODEL}}$$

which corresponds to shifting the Large Quad data by one third-octave band towards higher frequencies.

6.4 Landing Gear

Noise radiation from deployed landing gears has been subjected to much less investigation than flap side edges and leading edge devices; there exists comparatively little discussion in the literature. The following is a collection of some relevant comments.

From Ref. 59: A Boeing 737 landing gear was tested fully dressed, and then tested in a stripped condition: small hoses and tubes removed, cutouts removed, and open pin-holes taped over. The effect was that noise above 1000 Hz was reduced 2 to 3 dB.

From Ref. 62: Two landing gear configurations were examined during this test. The first configuration was a low-fidelity landing gear. The second configuration was a high-fidelity gear built using stereo lithography, which included many of the pieces present on the full-scale model. Results from acoustic testing show increased noise from the high-fidelity gear. Source location plots from phased array data confirm that ignoring the high frequency component for modeling 'cleaning up' is appropriate.

From Ref. 64: For the purpose of preliminary modeling, landing gear noise sources are broken down by low/med/hi frequency contributions, and, separately, tires. The low frequency component is assumed to come from the main strut; the medium frequencies are assumed to be dominated by the medium size components such as torque links; there is fairly good evidence that a lot of the high frequencies come from the small components (hoses, tubes, wires, etc.). The effect of 'cleaning up' the gear by bundling or hiding small tubes, hoses, and wires can be modeled approximately by ignoring the high frequency component (Figure 27). Not available at this time are models for the effects of aerodynamic shaping of struts and trucks, and partial aerodynamic enclosures for tires. Nevertheless, we make an attempt here to model this by ignoring the medium frequency component not contributed by the tires. Figure 28 shows the noise reductions when combining suppression of high and medium frequency components.

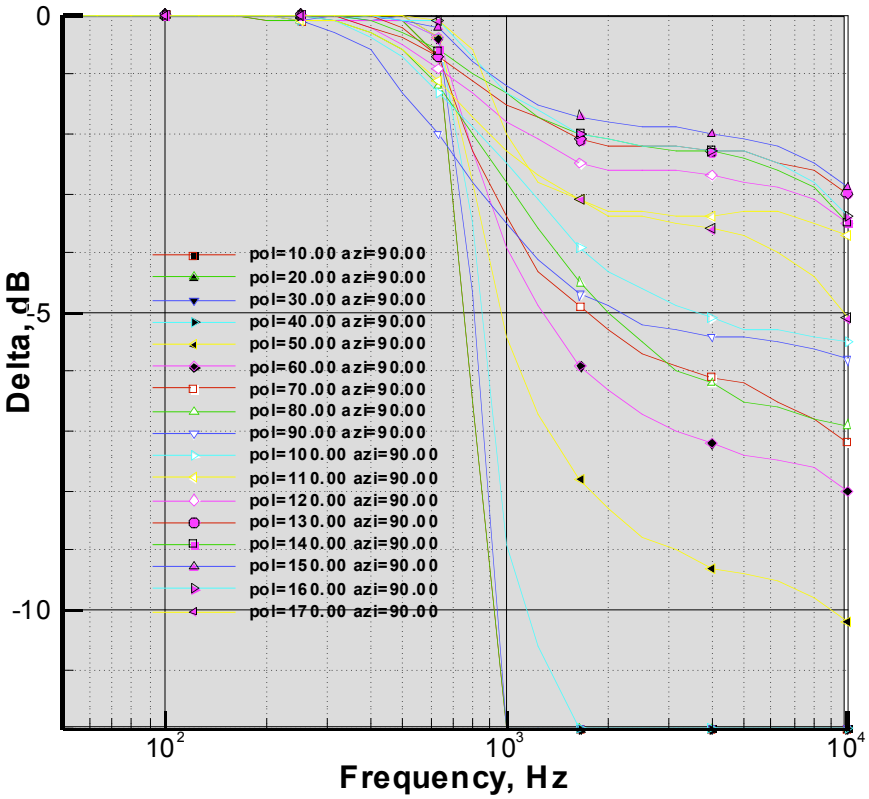

Figure 27 Delta Data for Large Quad Main Landing Gear High Frequency Portion.

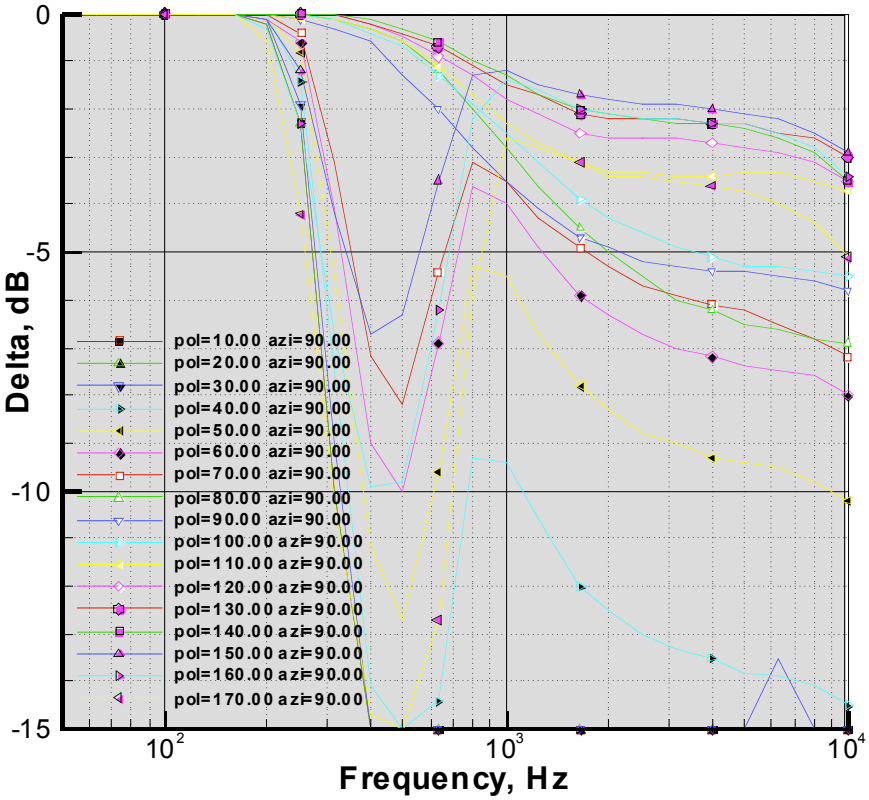

Figure 28 Delta Data for Large Quad Main Landing Gear High and Medium Frequency Portions.

At shallow polar radiation angles (i.e., close to horizontal) the wind tunnel measurements used in Ref. 64 are not considered adequate leading to unreasonably large differences between suppressed and unsuppressed conditions. To get around this, an arbitrary artificial suppression limit of 12 dB was imposed for the high frequency suppression, and 15 dB for the medium and high frequency suppressions together.

6.5 Airframe Noise Suppression Libraries

The noise reduction concepts discussed in Sections 6.2 through 6.4 were cast into library files for use with ANOPP. At the beginning of the project the thought was that ANOPP's general suppression module could not be used because it is not sensitive to Mach number, and we expected noise reductions to depend on Mach number. In the course of the investigations it became clear that desired Mach number dependencies could only be obtained for the baseline airframe noise predictions, and that we had to be content with cruder assessments for the noise reduction concepts, including no dependence on Mach number. This enabled the use of the general suppression module that provides deltas as a function of frequency, and polar and azimuthal angles.

The compact disk that accompanies this report contains files from which the desired libraries can be built by ANOPP runs. Table 4 shows the details. The names of the resulting libraries were formed thus: the first two letters designate the airplane; “AS” means airframe noise suppression; “2K” means year 2000.

Table 4 Noise Suppression Library Names

	File on Compact Disk	Name of Suppression Library
Large Quad	3_LargeQuad\5_NoiseReductionConcepts\LQAS2K_makelib.inp	LQAS2K.WRK
Medium Twin	2_MediumTwin\5_NoiseReductionConcepts\MTAS2K_makelib.inp	MTAS2K.WRK
Small Twin	1_SmallTwin\5_NoiseReductionConcepts\STAS2K_makelib.inp	STAS2K.WRK

6.6 Effects of Application of Noise Reduction Concepts

In this section, the effects of the noise reduction concepts are illustrated by reporting the results of ANOPP runs where the contents of the noise suppression libraries are applied. For sideline and cutback, only leading edge device noise reduction concepts are considered because the landing gear noise source does not exist, and for flap side edges there is no relevant data at the small deflection angles used during takeoff.

A summary of results is given in Table 5; its first column has pointers to figures with more details. We may make the following observations and comments:

- Flap side edge concepts Fences, μ-tabs, and porous surfaces all provide similar EPNL reductions ranging from 0.6 to 0.78 dB for LQ, 0.33 to 0.60 for MT, 0.42 to 1.17 dB for ST. The only one that stands out a little is the application of μ-tabs on the ST (1.17 dB).
- Eliminating flap side edge noise ('No noise from inboard/outboard flaps', for example by continuous moldline technology) is more effective the more the flap side edge contributes in the baseline; it is most helpful with LQ (5.17 dB), but still very noticeable with MT (1.94 dB) and ST (1.87 db).
- Side edge shaping unfortunately exhibits an EPNL increase for all three airplanes: 0.76 for LQ, 0.77 for MT, 1.27 for ST, even though the option with the most reduction potential was chosen (rounded edges with grit).
- 'All reduction concepts, most optimistic' means: no flap noise, both slat noise reductions applied, high and medium frequency noise reductions applied to main landing gear.
- 'All reductions concepts, near term' means: all inboard/outboard flap side edges with fences (height equal to double flap thickness), slat has cove filler only, and main gear has only high frequencies suppressed.
- The difference between 'most optimistic' and 'near term' application of all reduction concepts is large for all three airplanes: 7.76-1.55=6.21 dB for LQ, 6.13-1.97=4.16 dB for MT, 9.89-1.78=8.11 dB for ST. One may conclude that all noise sources must be reduced significantly together, otherwise at least one of them will be left dominating.
- The two slat noise reduction concepts provide similar amounts of reduction for all three airplanes. This is fortuitous in light of the rather arbitrary choice of reducing the gap size by 1% of the stowed wing chord. It does indicate that filling the cove and reducing the gap size need to be pursued simultaneously.
- On takeoff, leading edge device noise is more noticeable on the smaller airplanes. Its reduction brings these EPNL benefits at cutback: 1.18 dB for LQ, 4.33 dB for MT, and 6.67 dB for ST.

- The relationship of fence height with EPNL reduction is:

Fence Height (times flap thickness):		_	1	2
LQ	inboard:	0.73	0.96	1.12
	outboard:	0.91	1.17	1.36
MT	inboard:	1.09	1.39	1.62
	outboard:	1.30	1.65	1.90
ST	inboard:	0.73	0.97	1.14
	outboard:	0.87	1.12	1.31

While there is an increase of benefit with fence height, the presence of some kind of a fence is much more a factor than its height.

Table 5 Overflight Prediction With Noise Reduction Concepts

		Noise Reduction Concepts		Baseline EPNL	EPNL with Reduction	ΔEPNL	Compact Disk Path: 4_OverFlightSim\5_NoiseReductionConcepts\...
Figure 29	LQ	Leading Edge Device: cove filler and smaller gap	Sideline	86.11	84.79	-1.32	3_LargeQuad\1_Takeoff\sled\lqtko_sled.*
			Cutback	90.21	89.03	-1.18	
Figure 30			Approach	99.22	98.40	-0.82	3_LargeQuad\2_Approach\sled\lqapp_sled.*
Figure 31		No Noise from inboard/outboard flaps	Approach	99.22	94.05	-5.17	3_LargeQuad\2_Approach\noflaps\lqapp_noFlapNoise.*
Figure 32		Fences on all inboard/outboard flaps	Approach	99.22	98.44[(1)]	-0.78	3_LargeQuad\2_Approach\noflaps\lqapp_Fences.*
Figure 33		μ-tabs on all in board/outboard flaps	Approach	99.22	98.62	-0.60	3_LargeQuad\2_Approach\mtabs\lqapp_mtabs.*
Figure 34		Porous surfaces on all i/o flaps	Approach	99.22	98.48	-0.74	3_LargeQuad\2_Approach\porous\lqapp_porous.*
Figure 35		Side Edge Shaping of all i/o flaps	Approach	99.22	99.98	+0.76	3_LargeQuad\2_Approach\seshap\lqapp_seshap.*
Figure 36		Main Landing Gear Noise Suppression	Approach	99.22	98.39[(2)]	-0.83	3_LargeQuad\2_Approach\smaing\lqapp_smaing.*
Figure 37		All reduction concepts, most optimistic	Approach	99.22	91.46	-7.76	3_LargeQuad\2_Approach\allreds\lqapp_allreds.*
Figure 38		All reduction concepts, near term	Approach	99.22	97.67	-1.55	3_LargeQuad\2_Approach\allnear\lqapp_allnear.*

		Noise Reduction Concepts		Baseline EPNL	EPNL with Reduction	ΔEPNL	Compact Disk Path: 4_OverFlightSim\5_NoiseReductionConcepts\...
Figure 39	MT	Leading Edge Device: cove filler and smaller gap	Sideline	80.38	76.13	-4.25	2_MediumTwin\1_Takeoff\sled\mttko_sled.*
			Cutback	79.75	75.42	-4.33	
Figure 40			Approach	92.71	91.35	-1.36	2_MediumTwin\2_Approach\sled\mtapp_sled.*
Figure 41		No Noise from inboard/outboard flaps	Approach	92.71	90.77	-1.94	2_MediumTwin\2_Approach\noflaps\mtapp_noFlapNoise.*
Figure 42		Fences on all inboard/outboard flaps	Approach	92.71	92.20[(1)]	-0.51	2_MediumTwin\2_Approach\noflaps\mtapp_Fences.*
Figure 43		μ-tabs on all in board/outboard flaps	Approach	92.71	92.11	-0.60	2_MediumTwin\2_Approach\mtabs\mtapp_mtabs.*
Figure 44		Porous surfaces on all i/o flaps	Approach	92.71	92.38	-0.33	2_MediumTwin\2_Approach\porous\mtapp_porous.*
Figure 45		Side Edge Shaping of all i/o flaps	Approach	92.71	93.48	+0.77	2_MediumTwin\2_Approach\seshap\mtapp_seshap.*
Figure 46		Main Landing Gear Noise Suppression	Approach	92.71	91.85[(2)]	-0.86	2_MediumTwin\2_Approach\smaing\mtapp_smaing.*
Figure 47		All reduction concepts, most optimistic	Approach	92.71	86.58	-6.13	2_MediumTwin\2_Approach\allreds\mtapp_allreds.*
Figure 48		All reduction concepts, near term	Approach	92.71	90.74	-1.97	2_MediumTwin\2_Approach\allnear\mtapp_allnear.*

		Noise Reduction Concepts		Baseline EPNL	EPNL with Reduction	ΔEPNL	Compact Disk Path: 4_OverFlightSim\5_NoiseReductionConcepts\...
Figure 49	ST	Leading Edge Device: cove filler and smaller gap	Sideline	77.53	70.98	-6.55	1_SmallTwin\1_Takeoff\sled\sttko_sled.*
			Cutback	76.02	69.35	-6.67	
Figure 50			Approach	91.79	90.81	-0.98	1_SmallTwin\2_Approach\sled\stapp_sled.*
Figure 51		No noise from inboard/outboard flaps	Approach	91.79	89.82	-1.87	1_SmallTwin\2_Approach\noflaps\stapp_noFlapNoise.*
Figure 52		Fences on all inboard/outboard flaps	Approach	91.79	91.06[(1)]	-0.73	1_SmallTwin\2_Approach\noflaps\stapp_Fences.*
Figure 53		μ-tabs on all in board/outboard flaps	Approach	91.79	90.62	-1.17	1_SmallTwin\2_Approach\mtabs\stapp_mtabs.*
Figure 54		Porous surfaces on all i/o flaps	Approach	91.79	91.37	-0.42	1_SmallTwin\2_Approach\porous\stapp_porous.*
Figure 55		Side Edge Shaping of all i/o flaps	Approach	91.79	93.06	+1.27	1_SmallTwin\2_Approach\seshap\stapp_seshap.*
Figure 56		Main Landing Gear Noise Suppression	Approach	91.79	91.63[(2)]	-0.16	1_SmallTwin\2_Approach\smaing\stapp_smaing.*
Figure 57		All reduction concepts, most optimistic	Approach	91.79	81.90	-9.89	1_SmallTwin\2_Approach\allreds\stapp_allreds.*
Figure 58		All reduction concepts, near term	Approach	91.79	90.01	-1.78	1_SmallTwin\2_Approach\allnear\stapp_allnear.*

[(1)] Data for fence height equal to flap thickness used.
[(2)] Data for suppression of high and medium frequencies used.

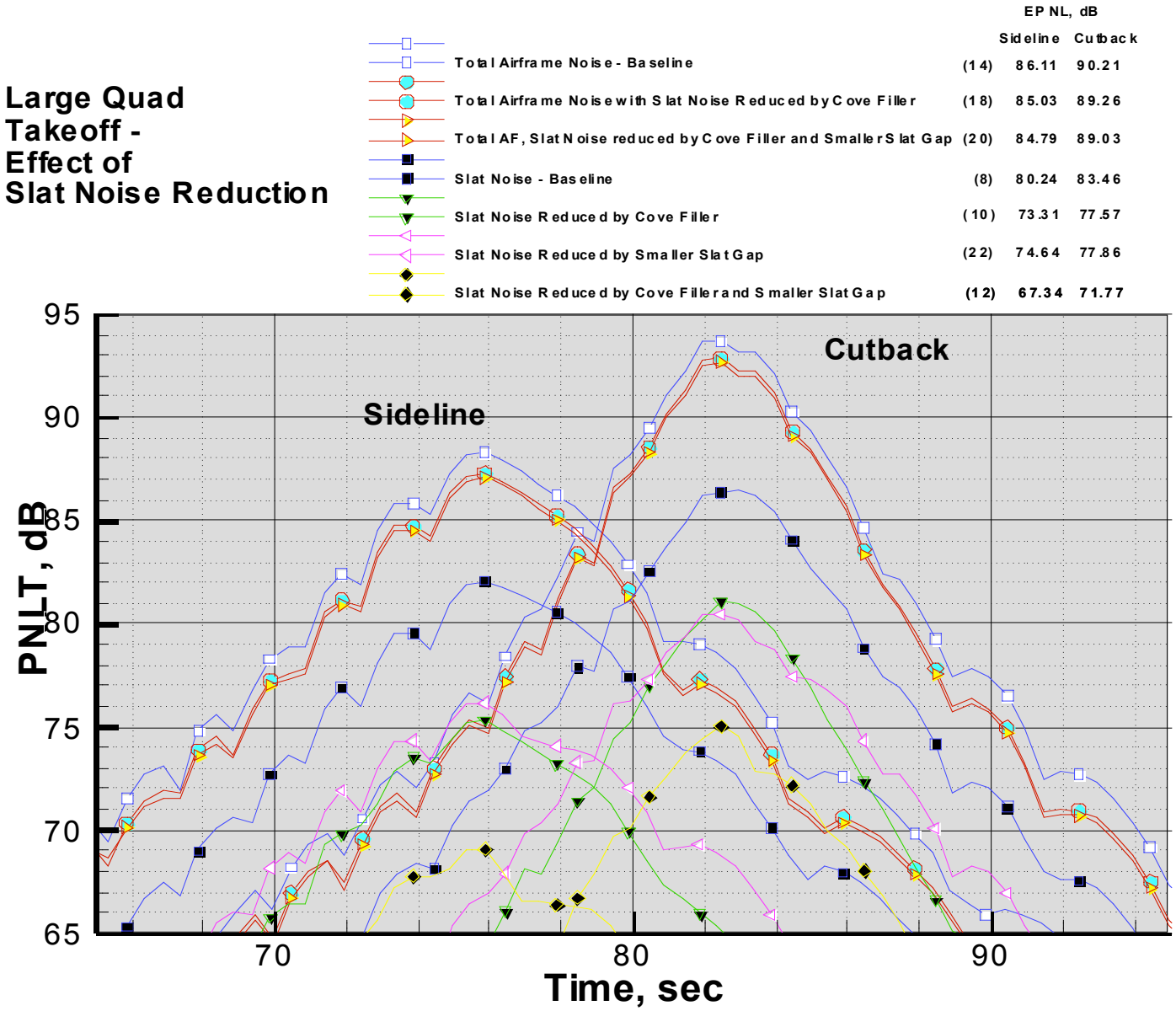

Figure 29 PNLT vs time for Large Quad Takeoff – Leading Edge Device Noise Reduction.

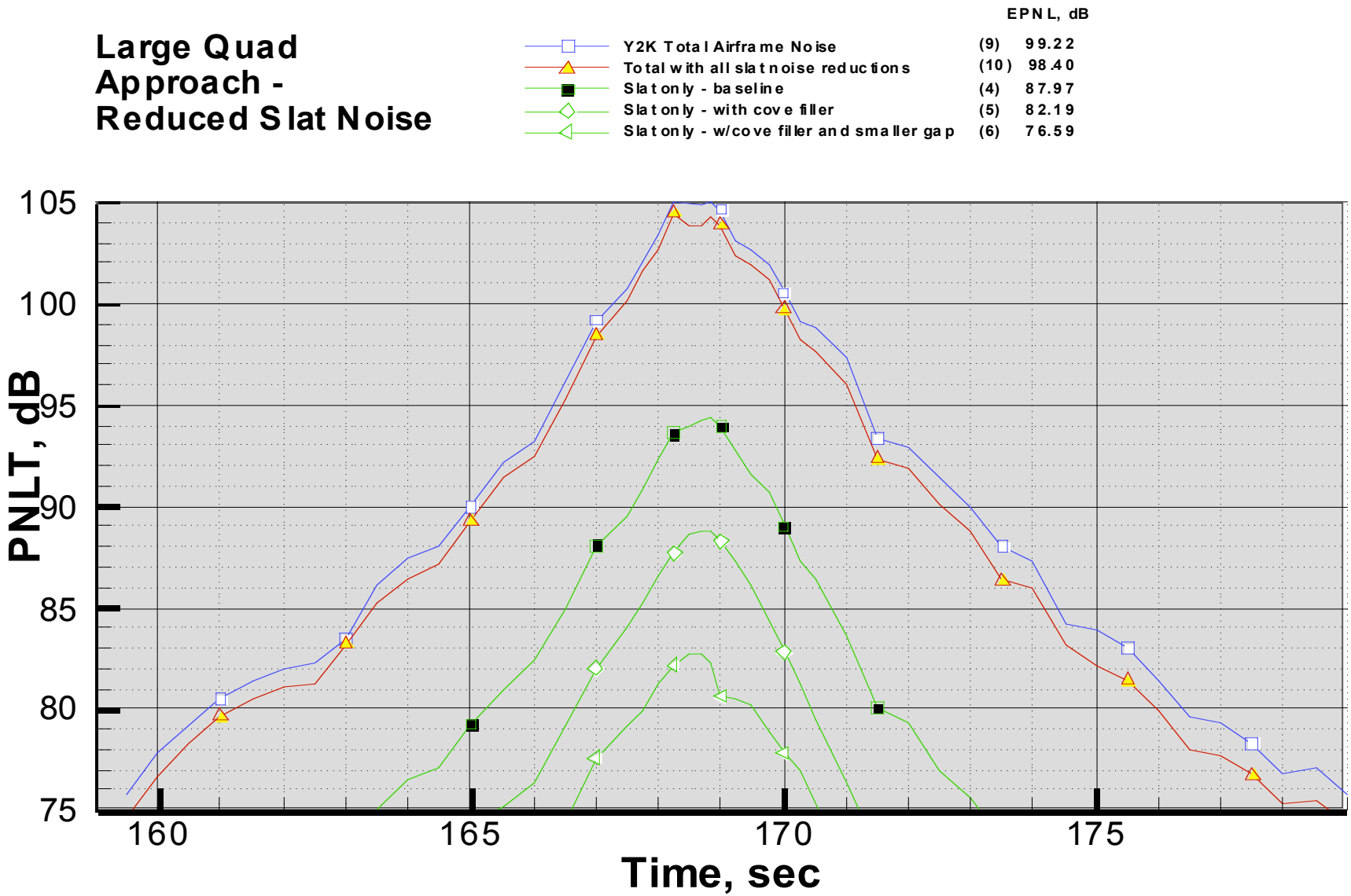

Figure 30 PNLT vs time for Large Quad Approach – Leading Edge Device Noise Reduction.

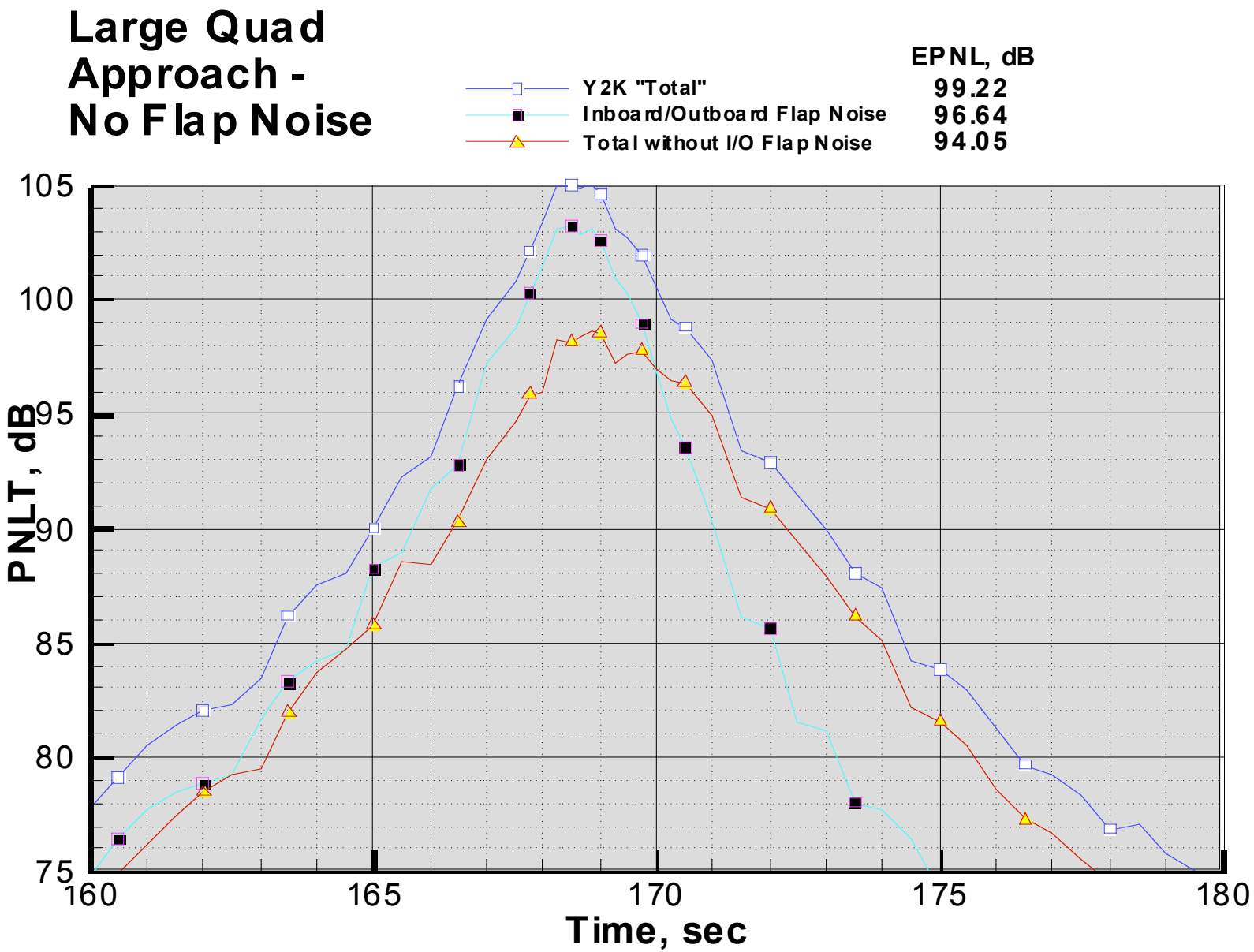

Figure 31 PNLT vs time for Large Quad Approach – Inboard/Outboard Flap Noise Eliminated

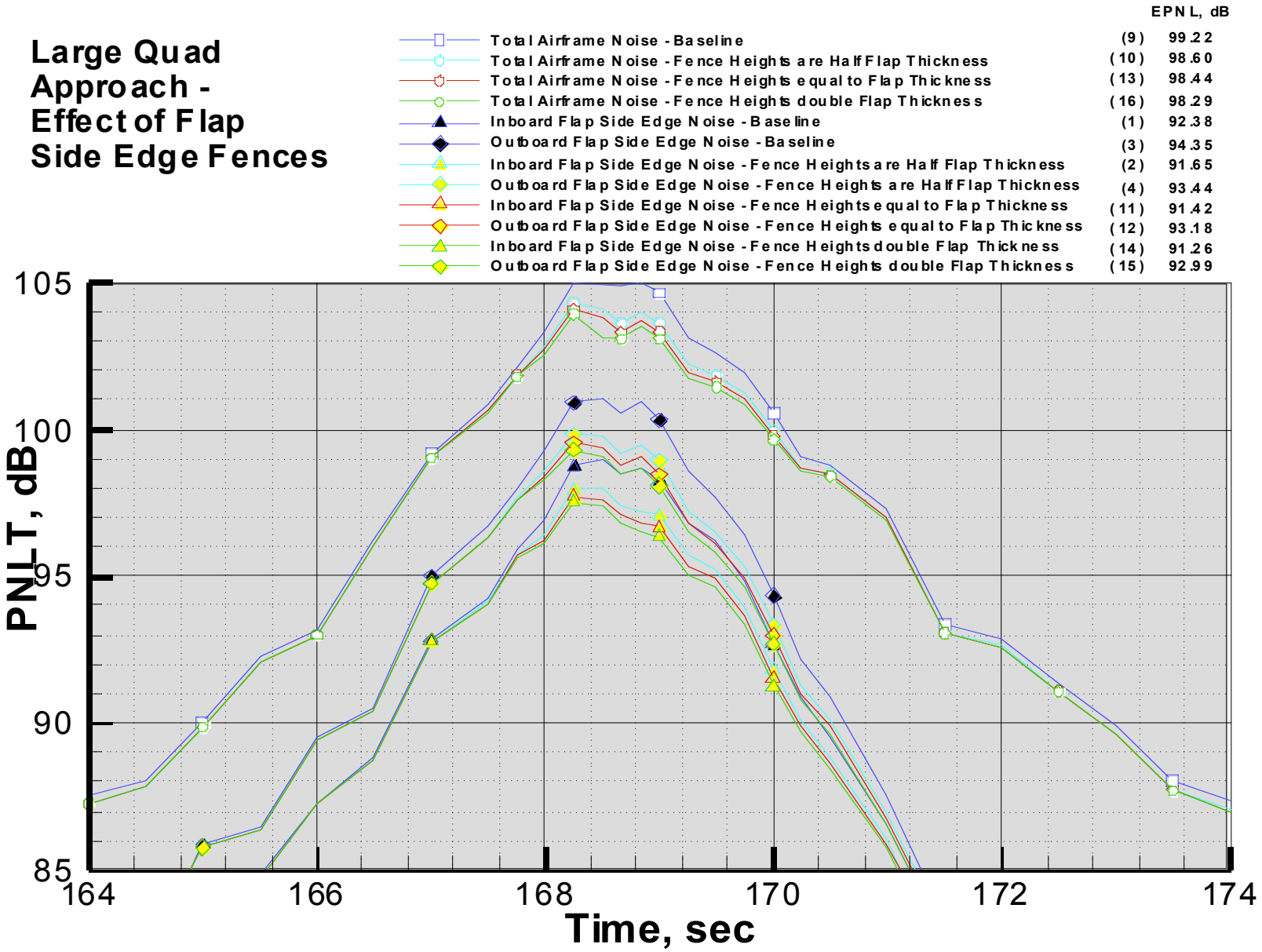

Figure 32 PNLT vs time for Large Quad Approach – Fences on Inboard/Outboard Flaps

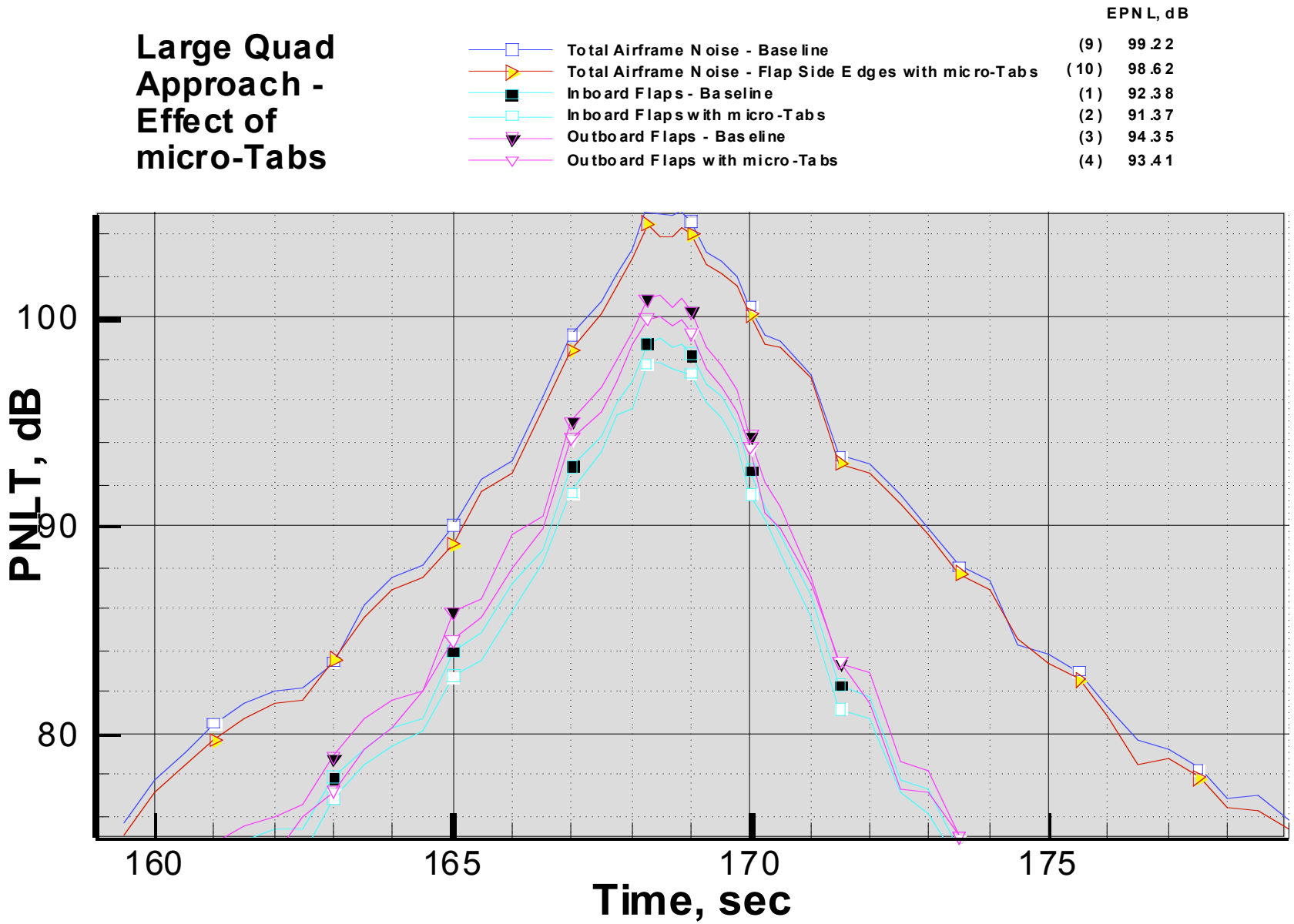

Figure 33 PNLT vs time for Large Quad Approach – μ-tabs on Inboard/Outboard Flap Side Edges

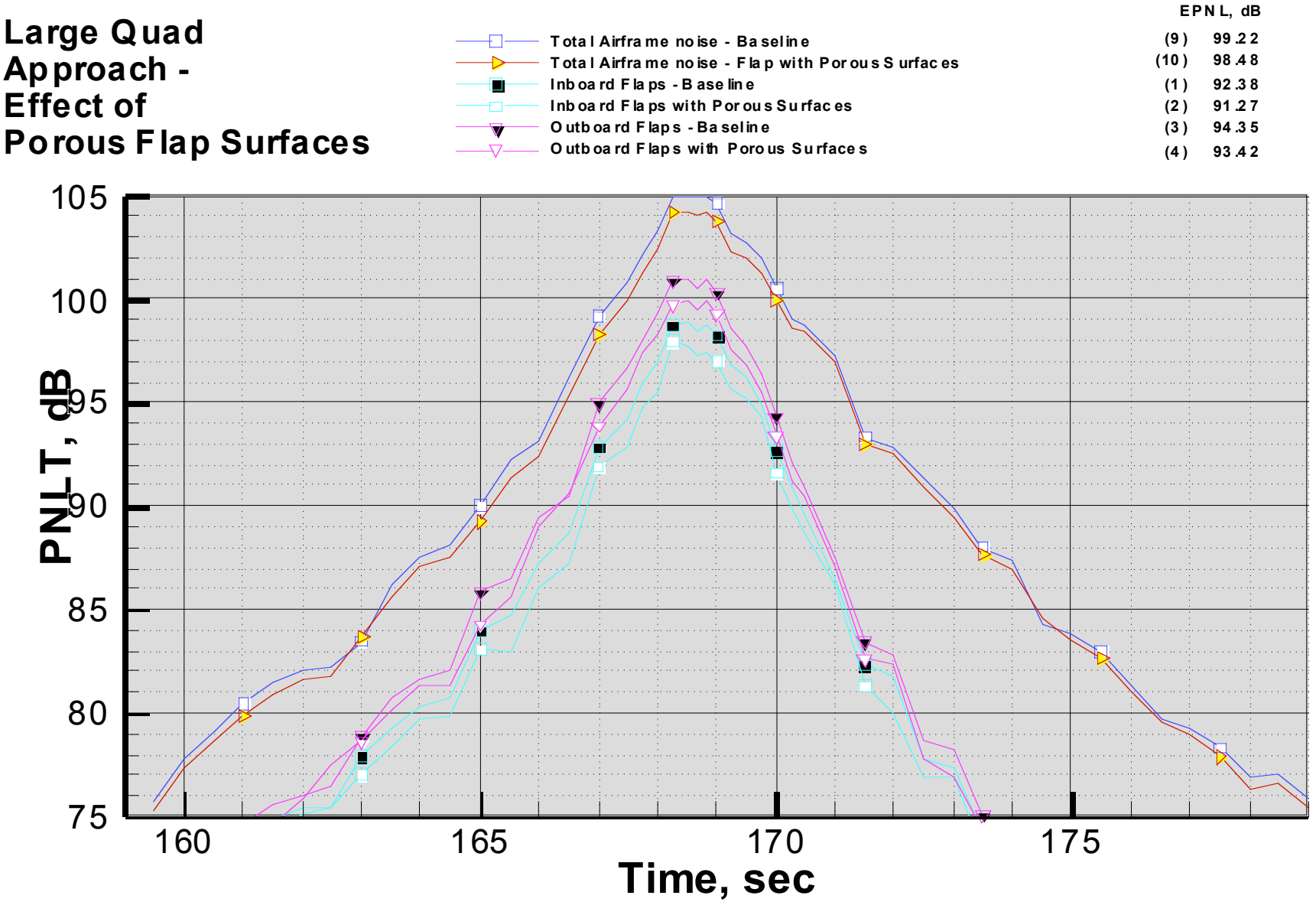

Figure 34 PNLT vs time for Large Quad Approach – Porous Surfaces on Inboard/Outboard Flaps

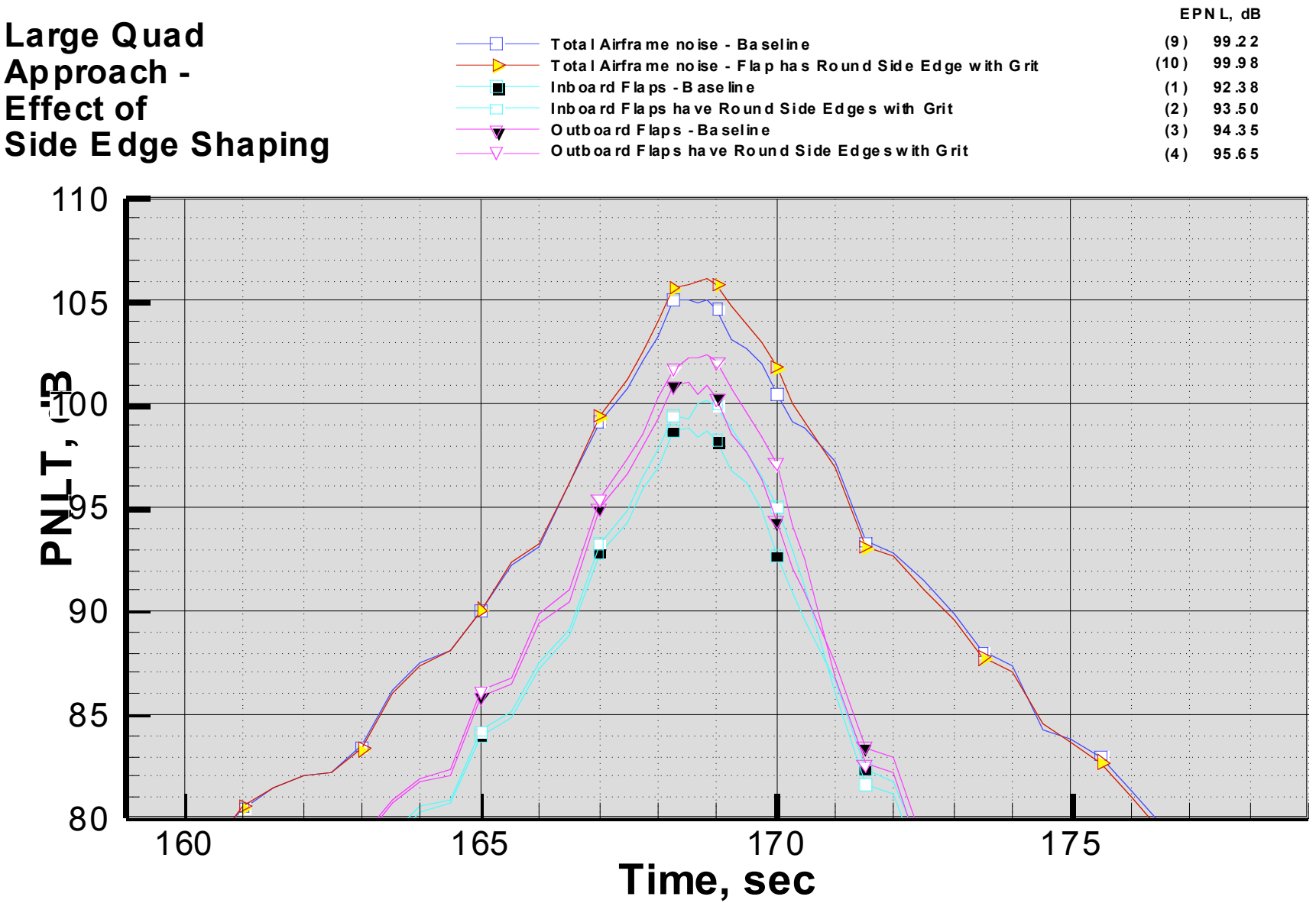

Figure 35 PNLT vs time for Large Quad Approach – Side Edge Shaping of all Inboard/Outboard Flaps

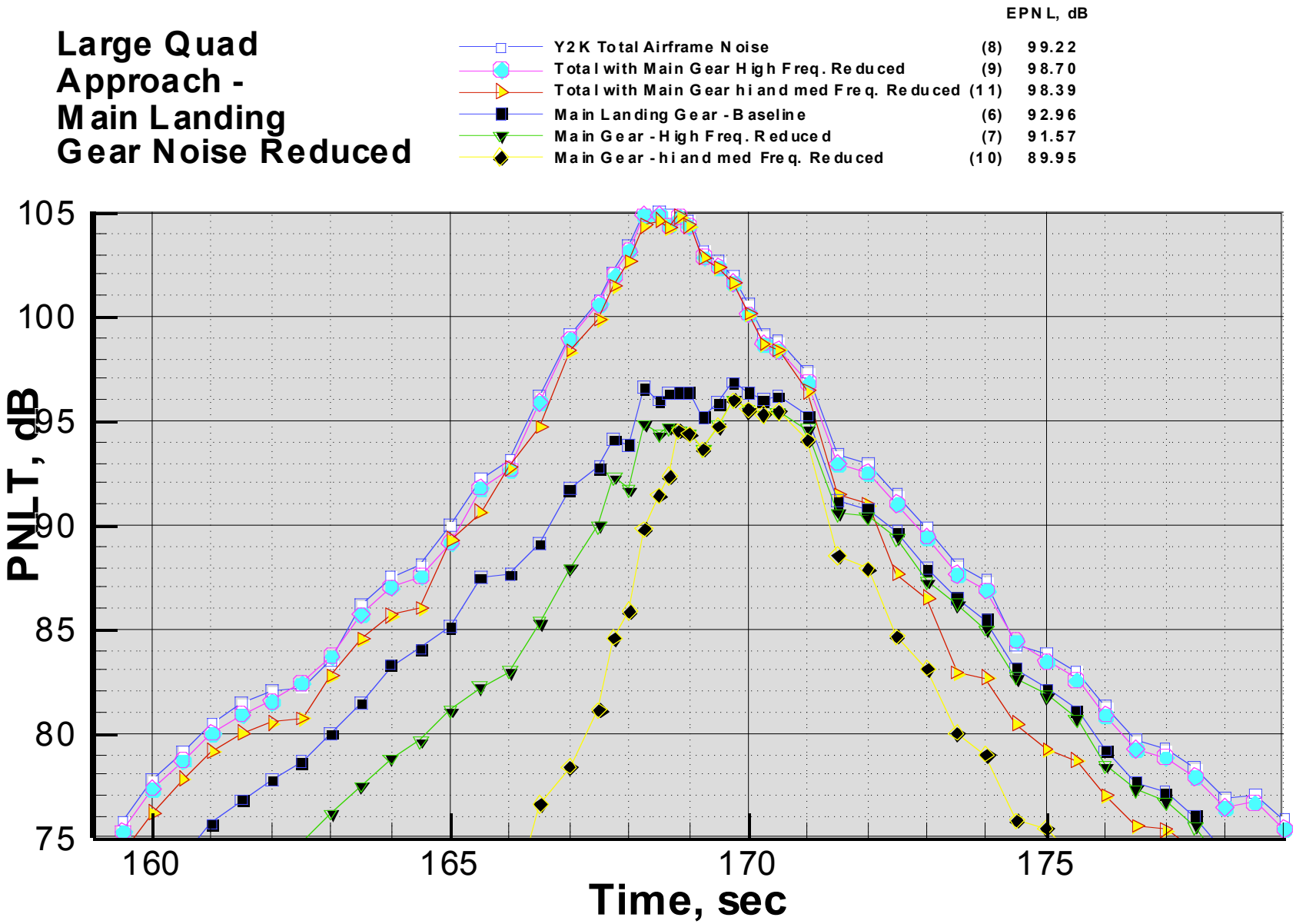

Figure 36 PNLT vs time for Large Quad Approach – Main Landing Gear Noise Suppression

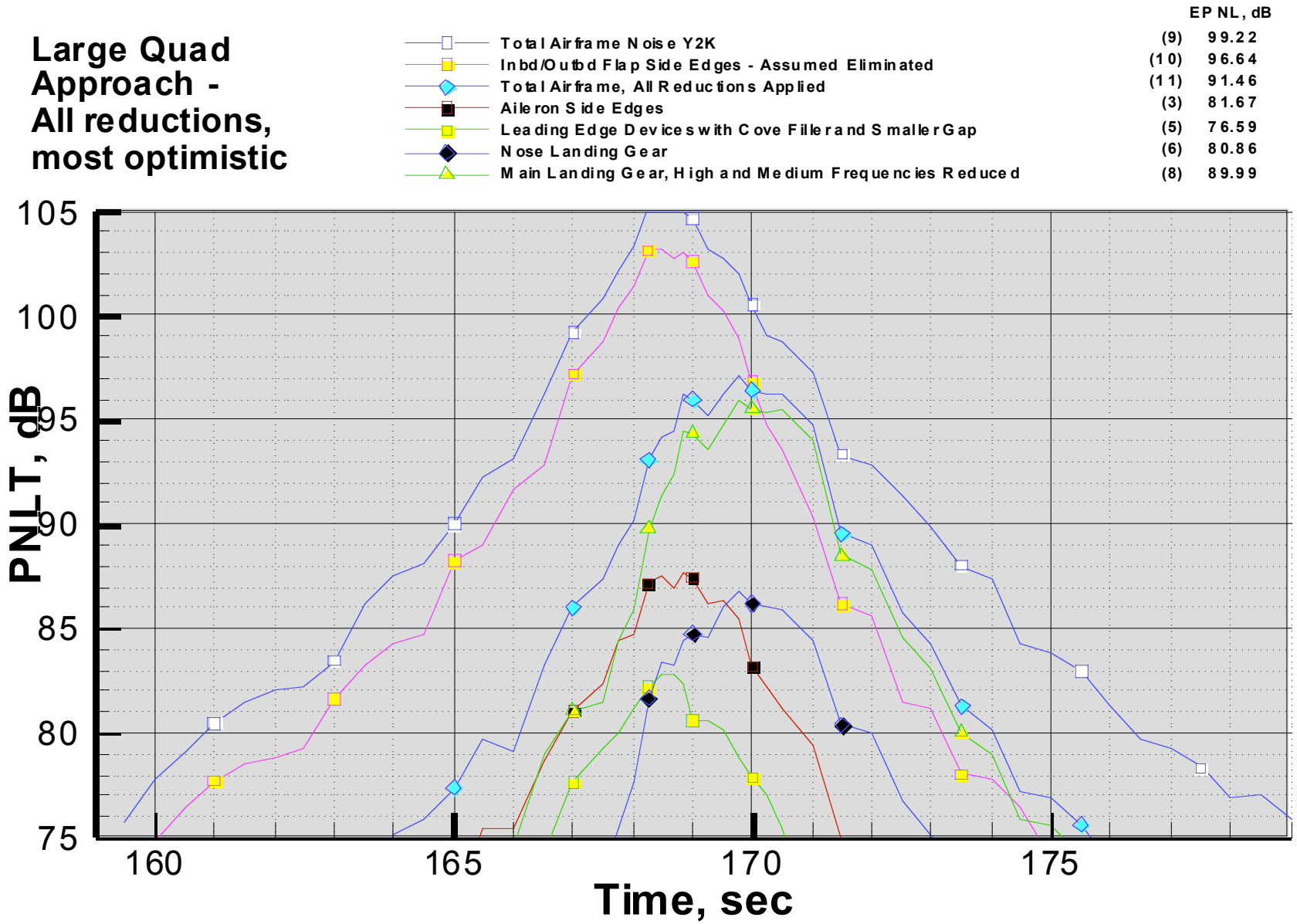

Figure 37 PNLT vs time for Large Quad Approach – All Concepts, Most Optimistic

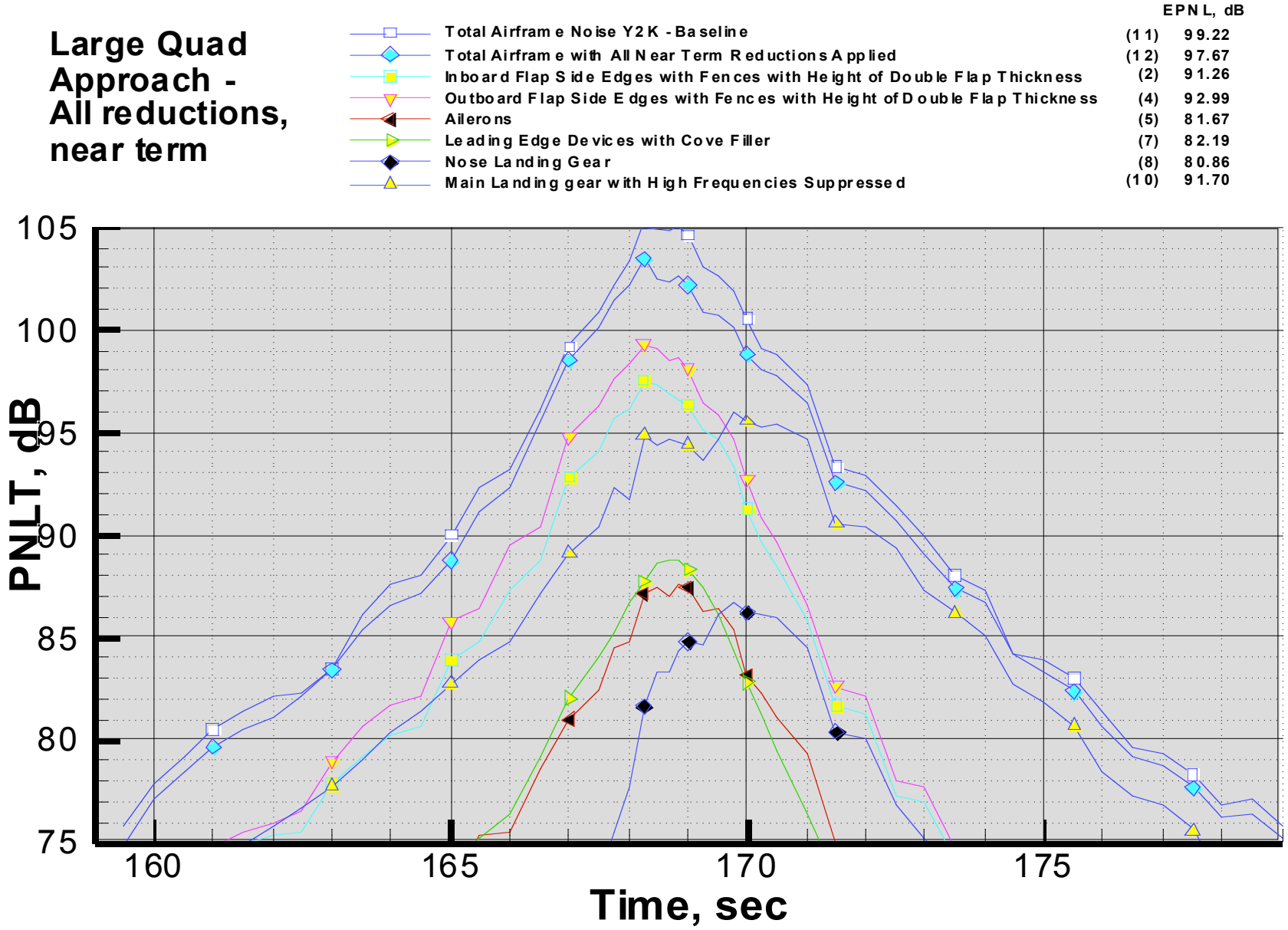

Figure 38 PNLT vs time for Large Quad Approach – All Concepts, Most Optimistic

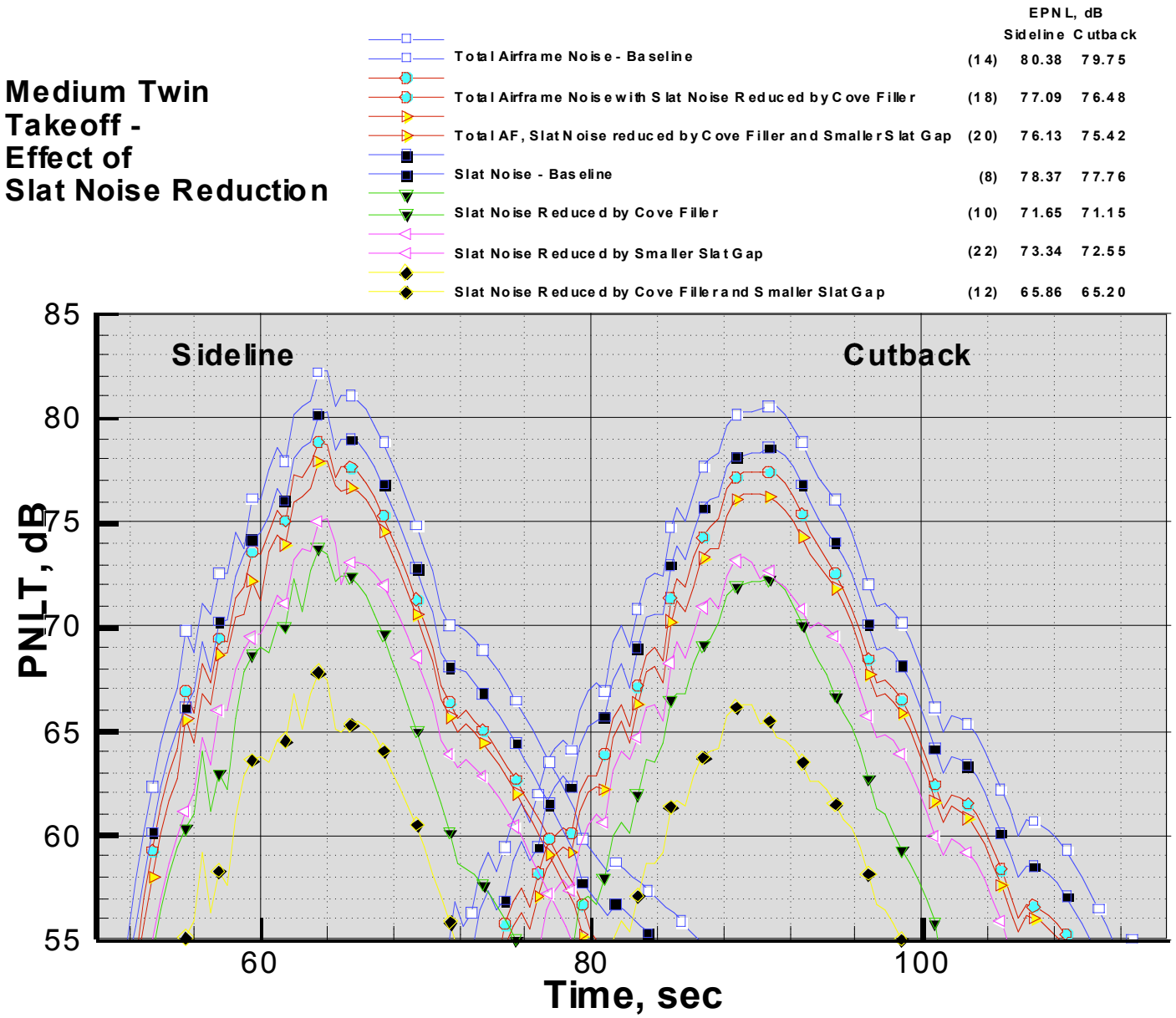

Figure 39 PNLT vs time for Medium Twin Takeoff – Leading Edge Device Noise Reduction.

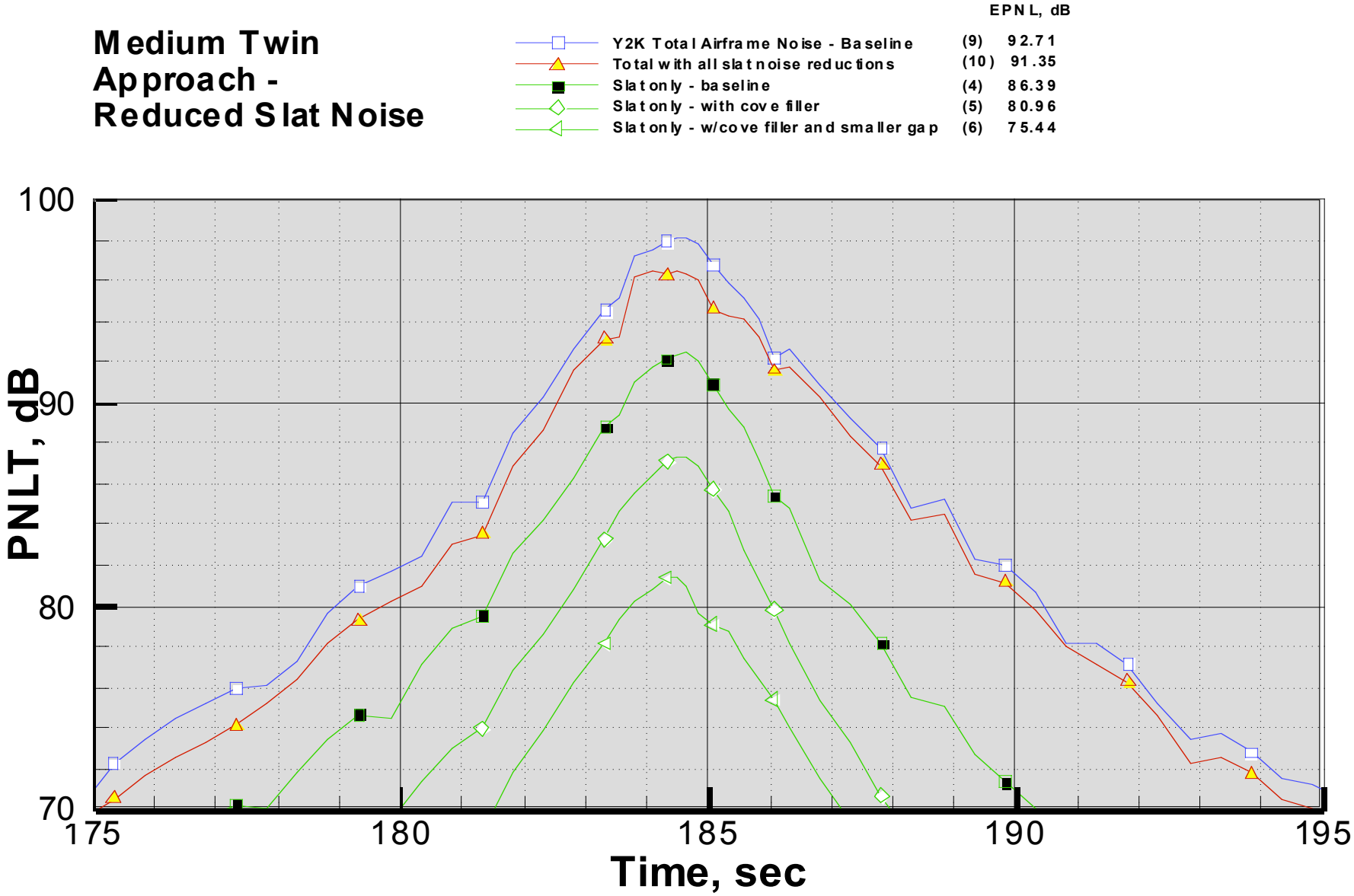

Figure 40 PNLT vs time for Medium Twin Approach – Leading Edge Device Noise Reduction.

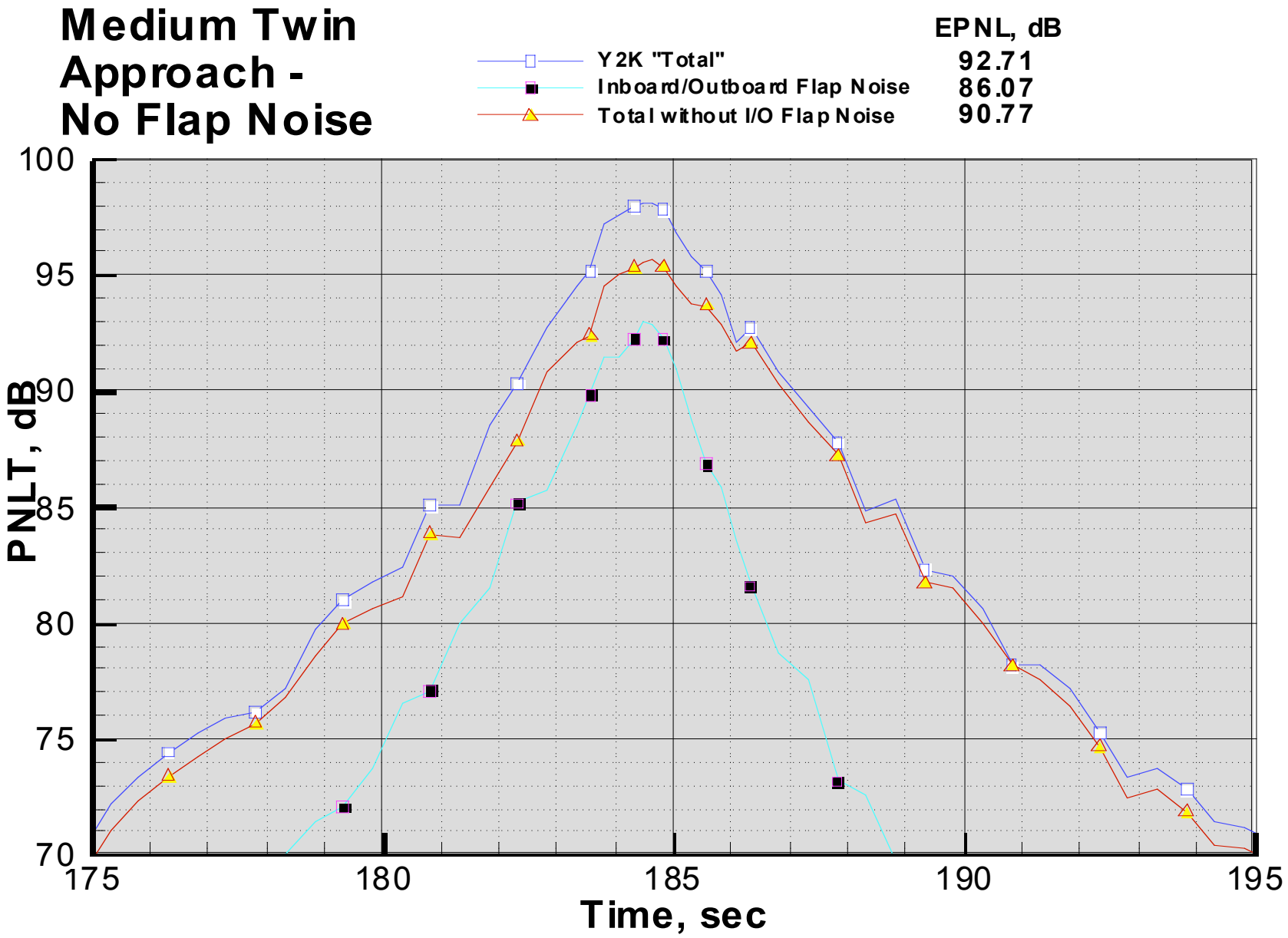

Figure 41 PNLT vs time for Medium Twin Approach – No noise from inboard/outboard flaps.

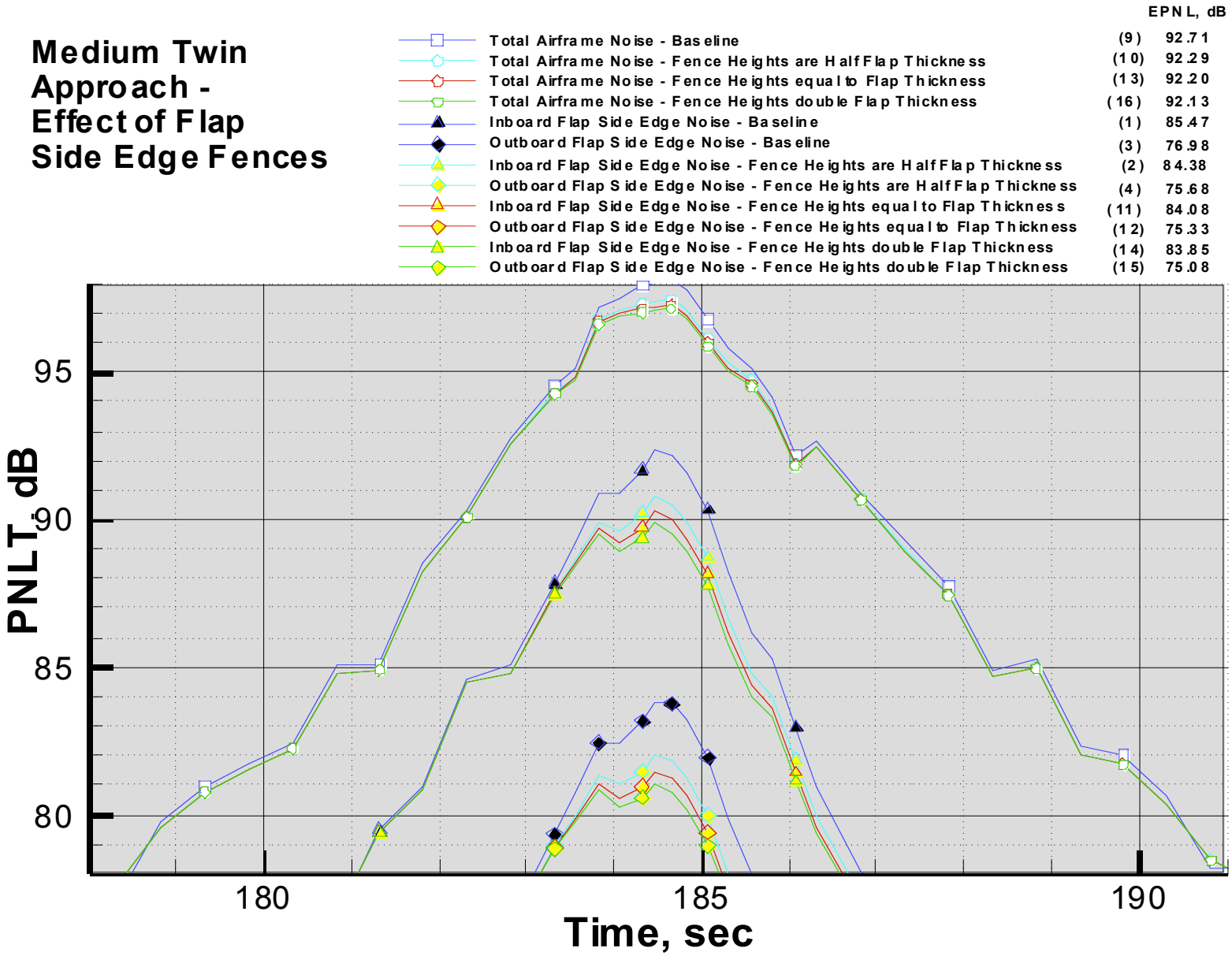

Figure 42 PNLT vs time for Medium Twin Approach – Fences on inboard/outboard flaps.

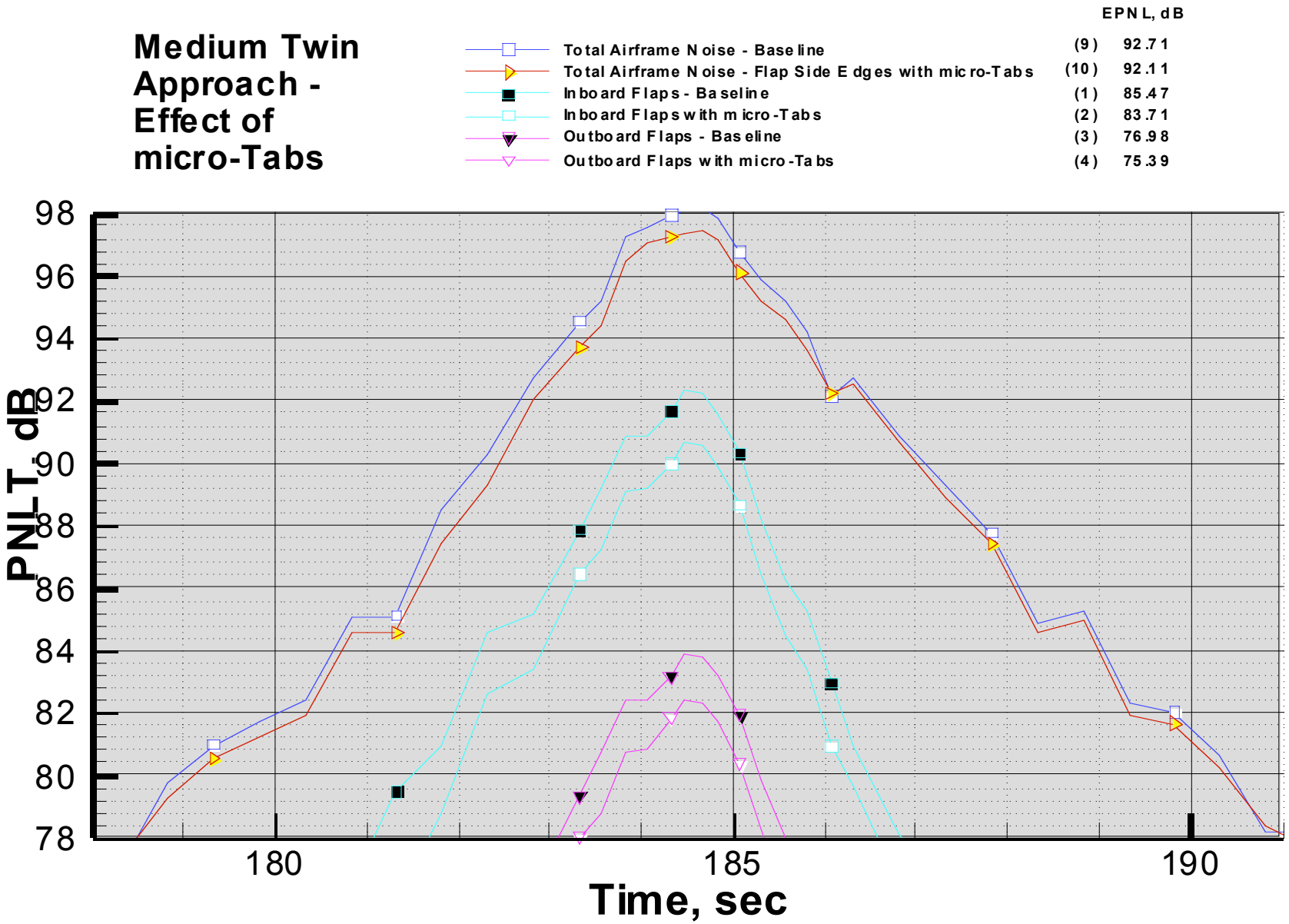

Figure 43 PNLT vs time for Medium Twin Approach – μ-tabs on inboard/outboard flaps.

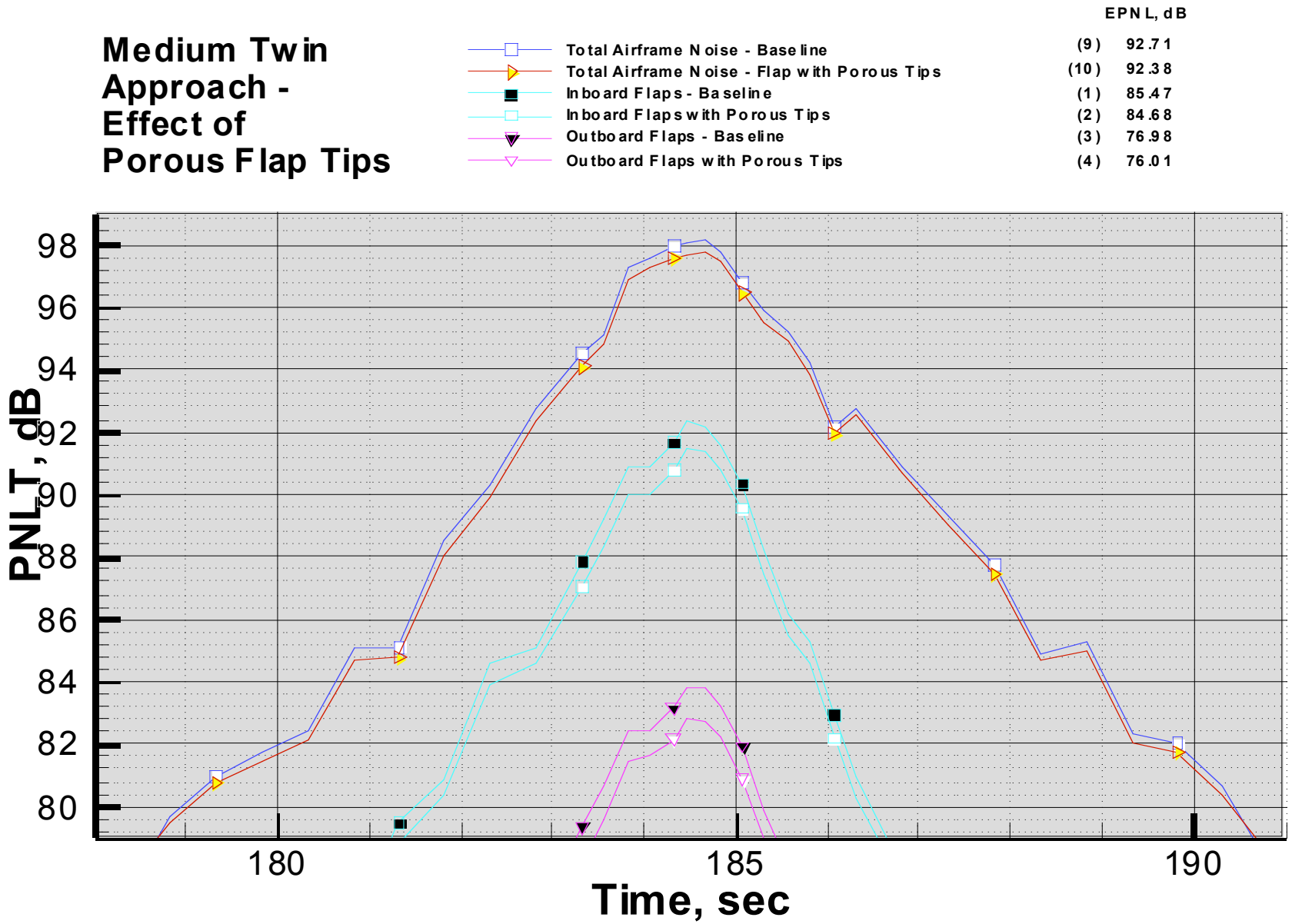

Figure 44 PNLT vs time for Medium Twin Approach – Porous surfaces on inboard/outboard flap tips.

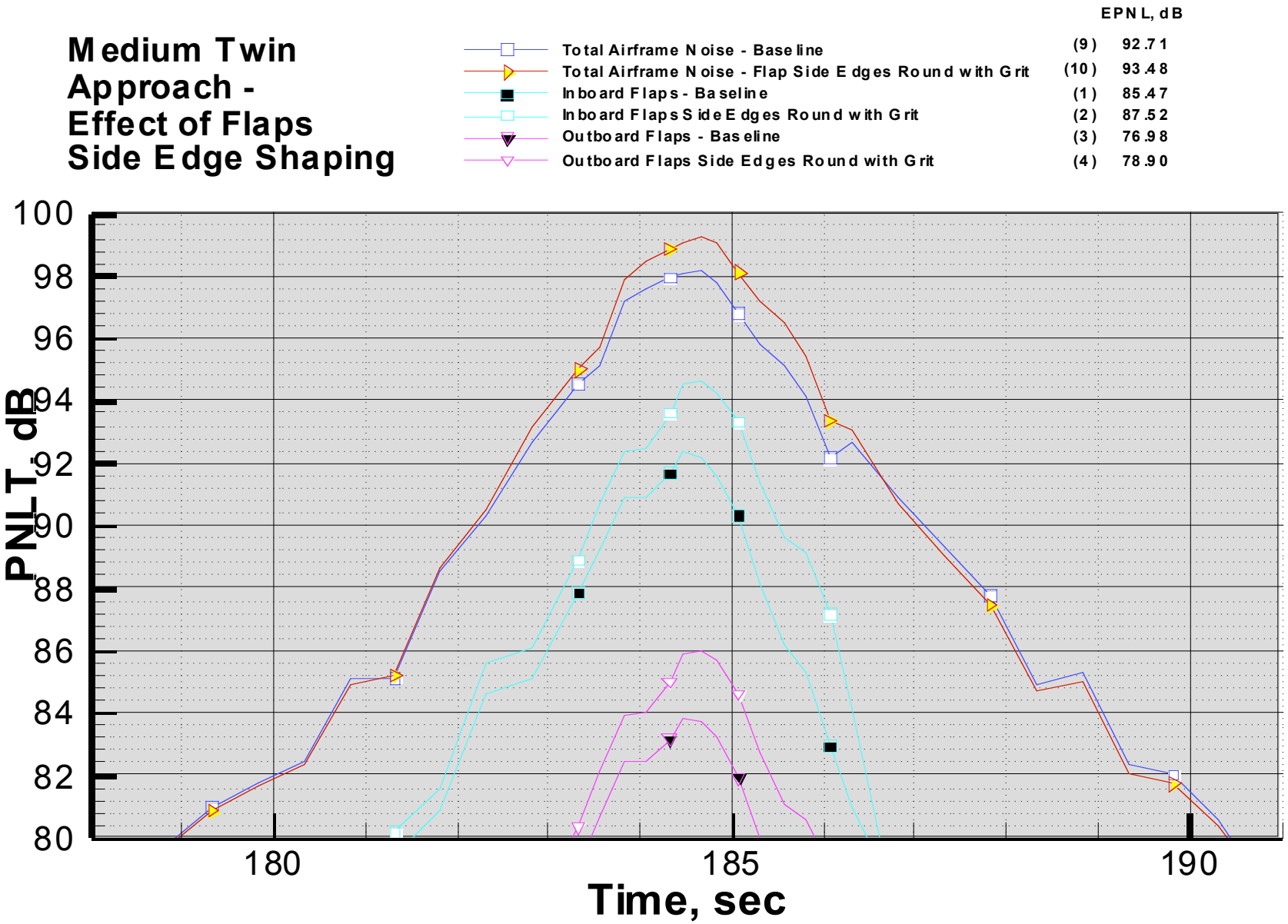

Figure 45 PNLT vs time for Medium Twin Approach – Side edge shaping on inboard/outboard flaps.

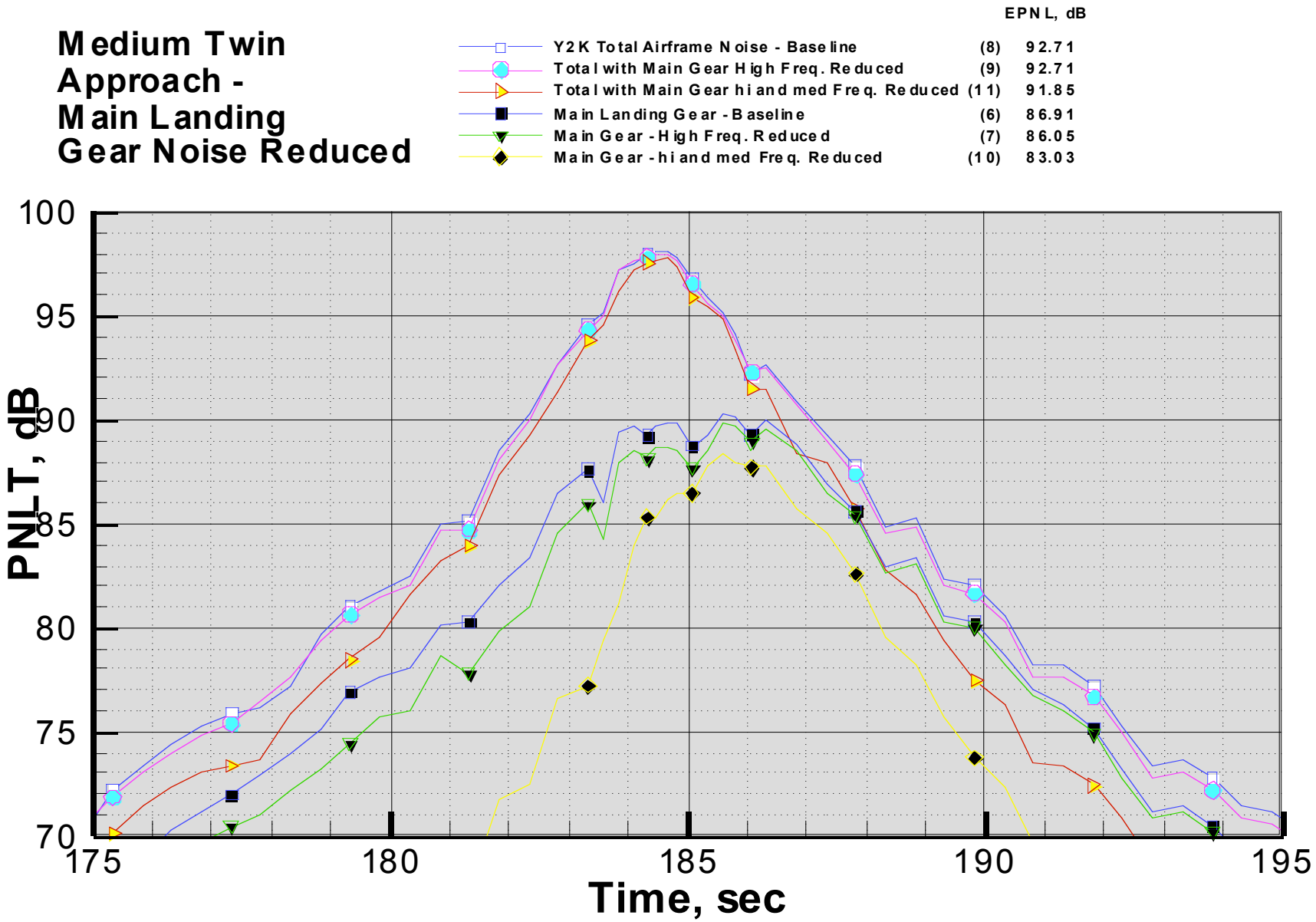

Figure 46 PNLT vs time for Medium Twin Approach – Main landing gear noise reductions.

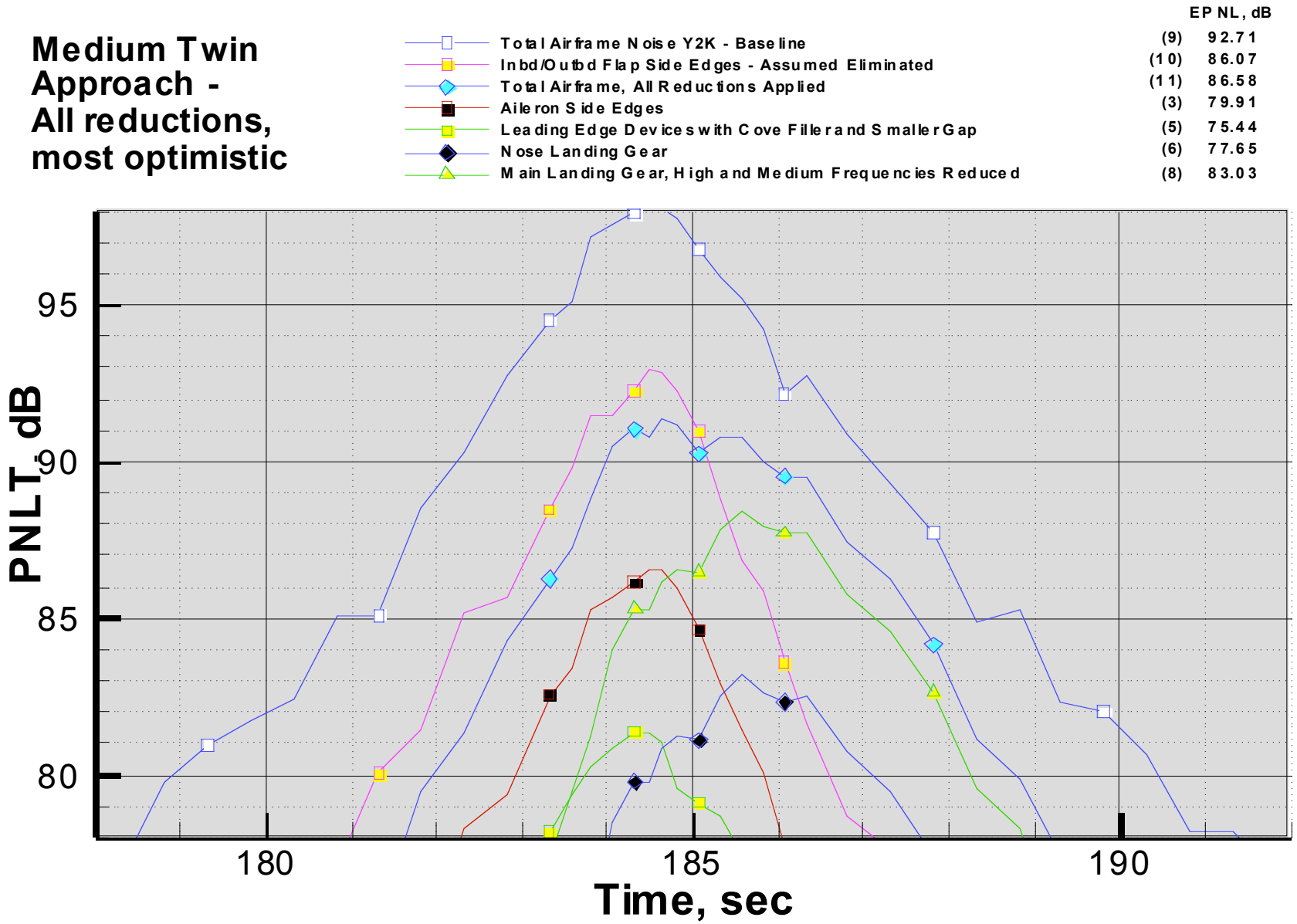

Figure 47 PNLT vs time for Medium Twin Approach – All reduction concepts, most optimistic.

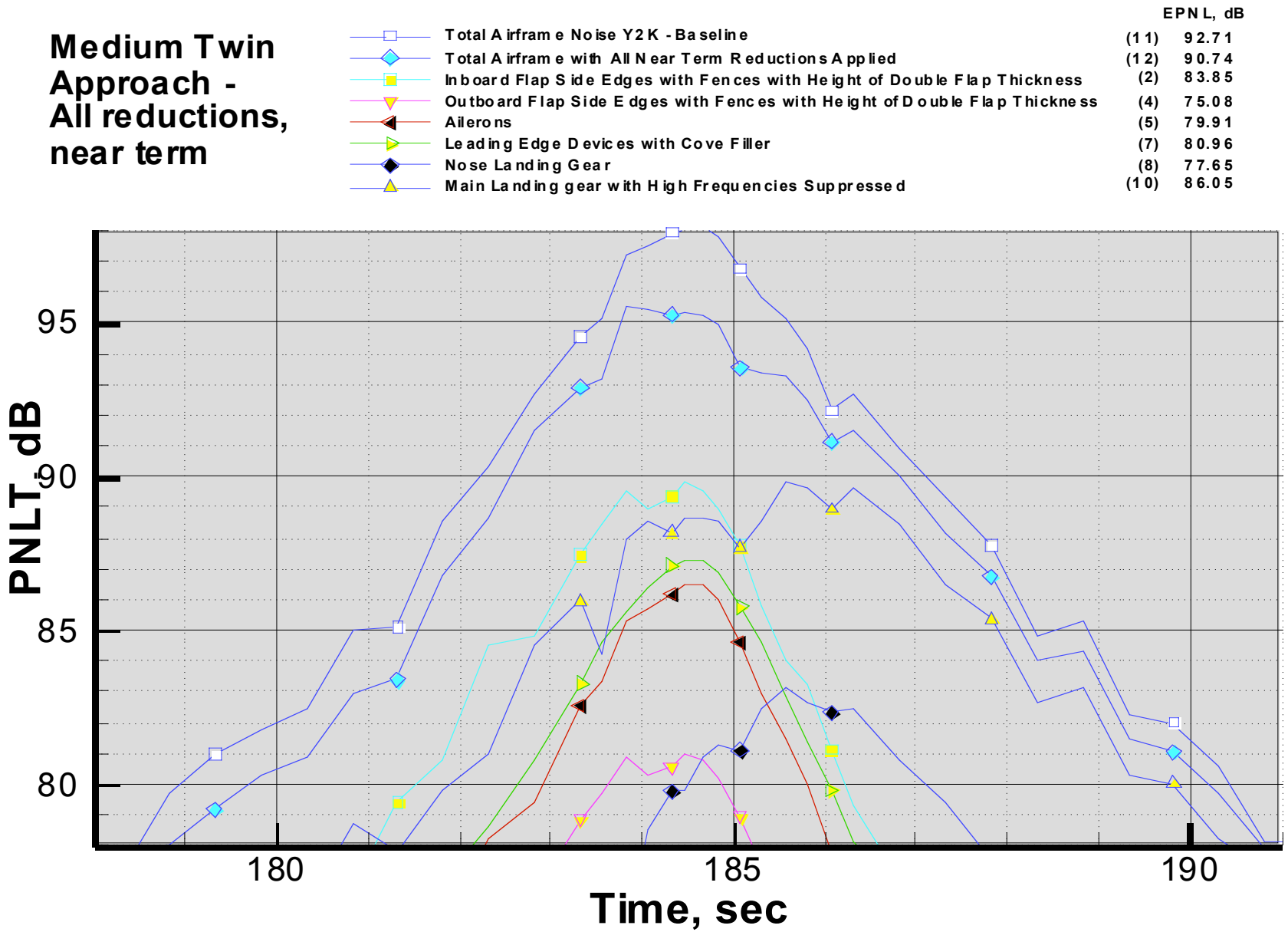

Figure 48 PNLT vs time for Medium Twin Approach – All reduction concepts, near term.

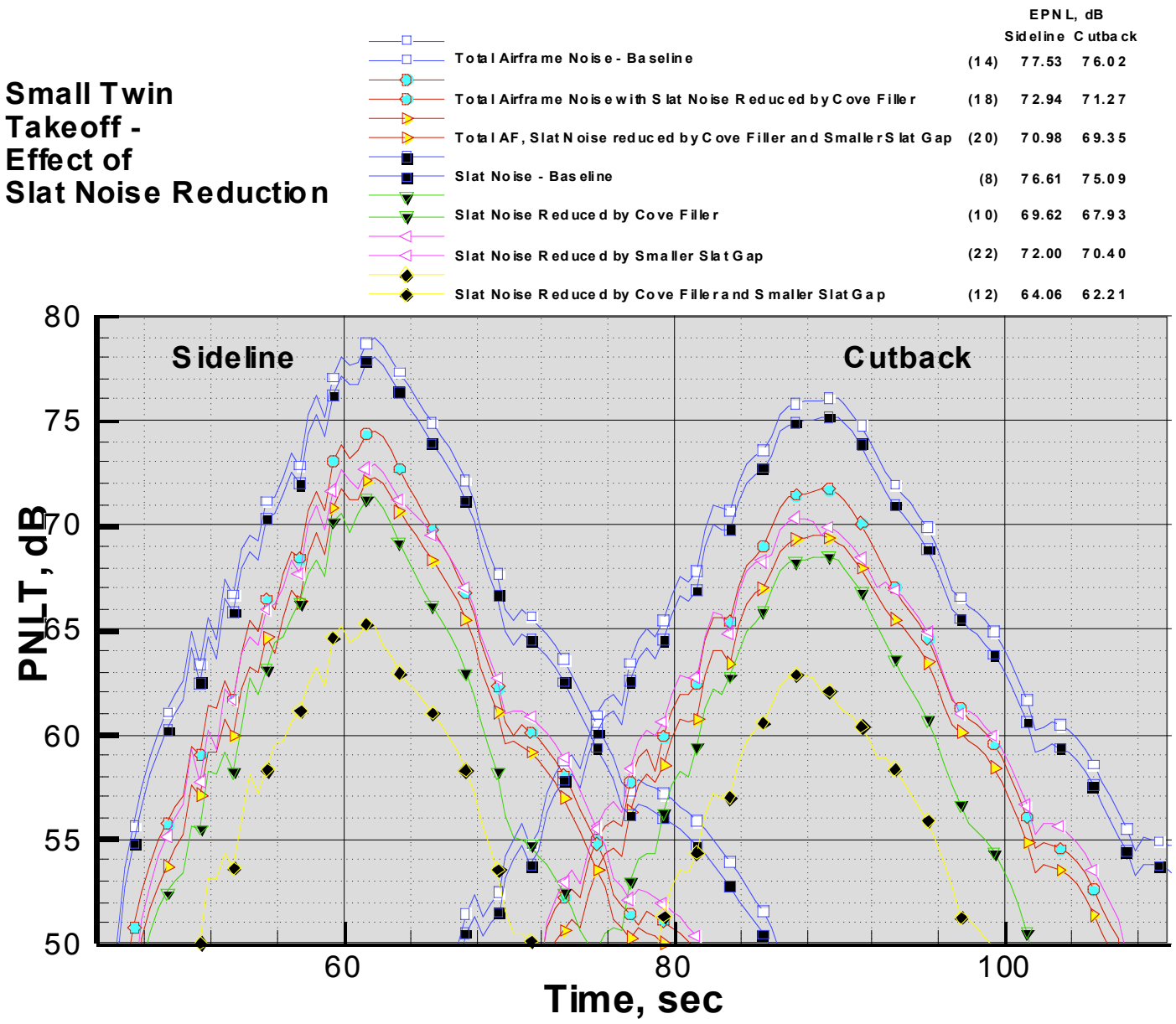

Figure 49 PNLT vs time for Small Twin Takeoff – Leading Edge Device Noise Reduction.

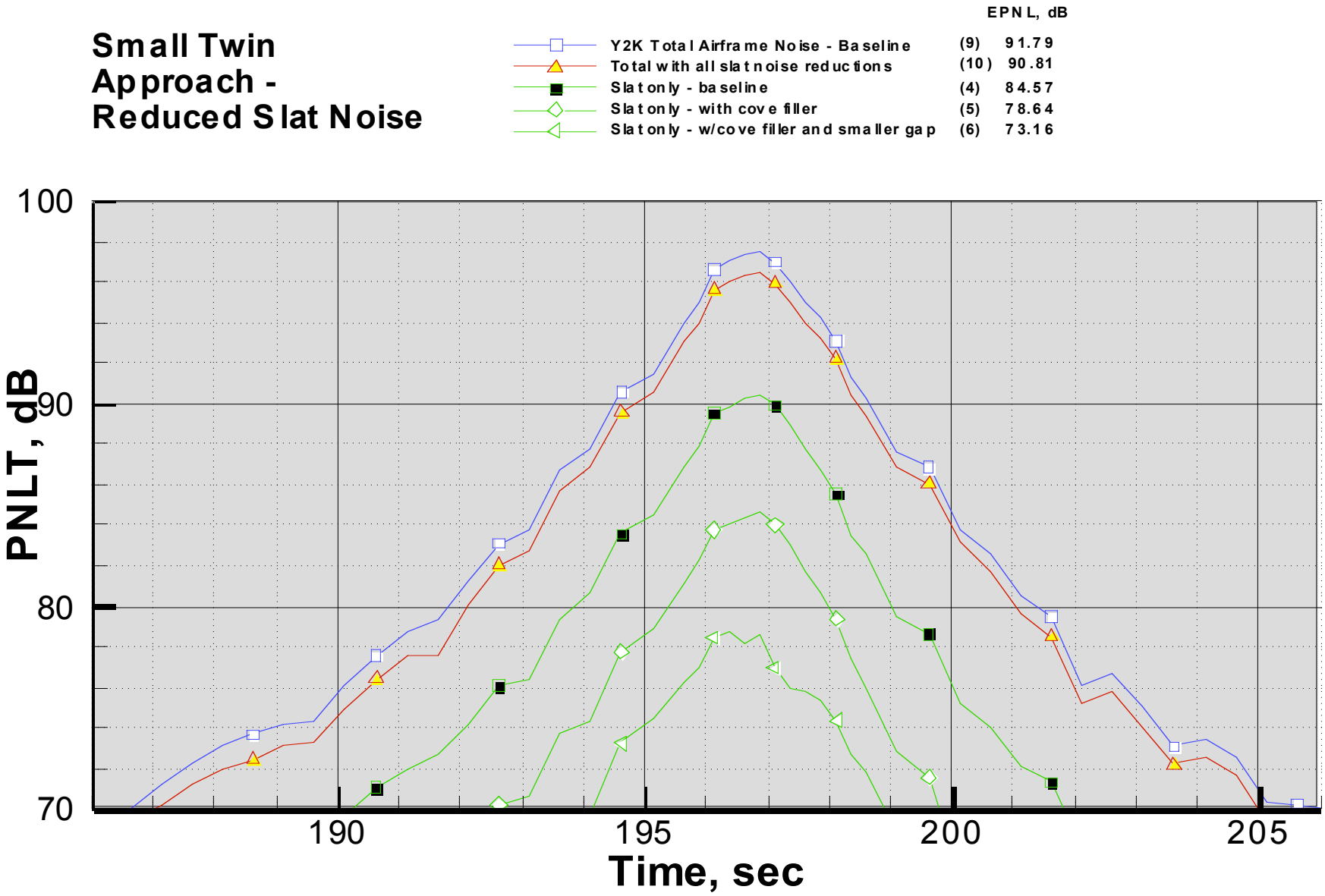

Figure 50 PNLT vs time for Small Twin Approach – Leading Edge Device Noise Reduction.

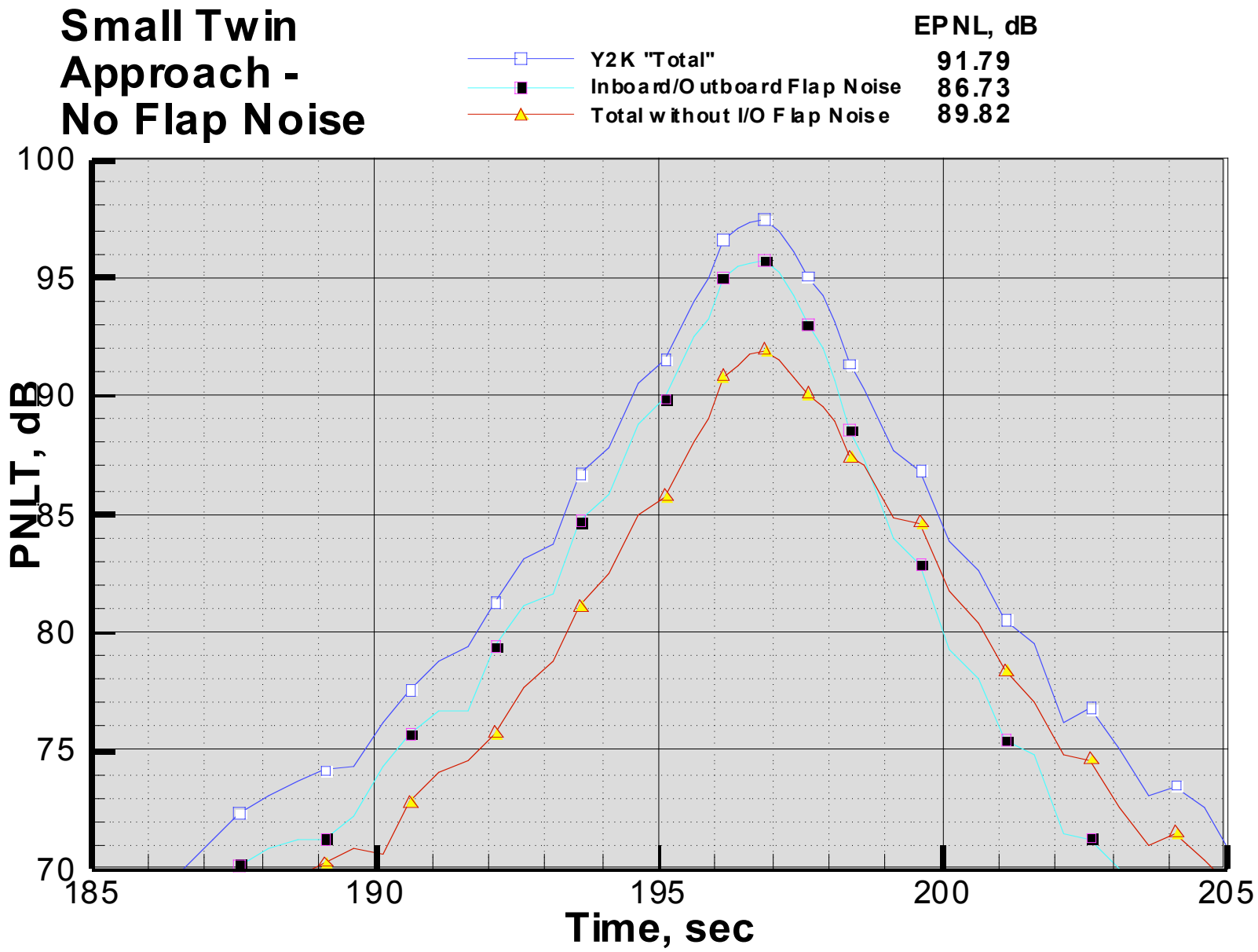

Figure 51 PNLT vs time for Small Twin Approach – No noise from inboard/outboard flaps.

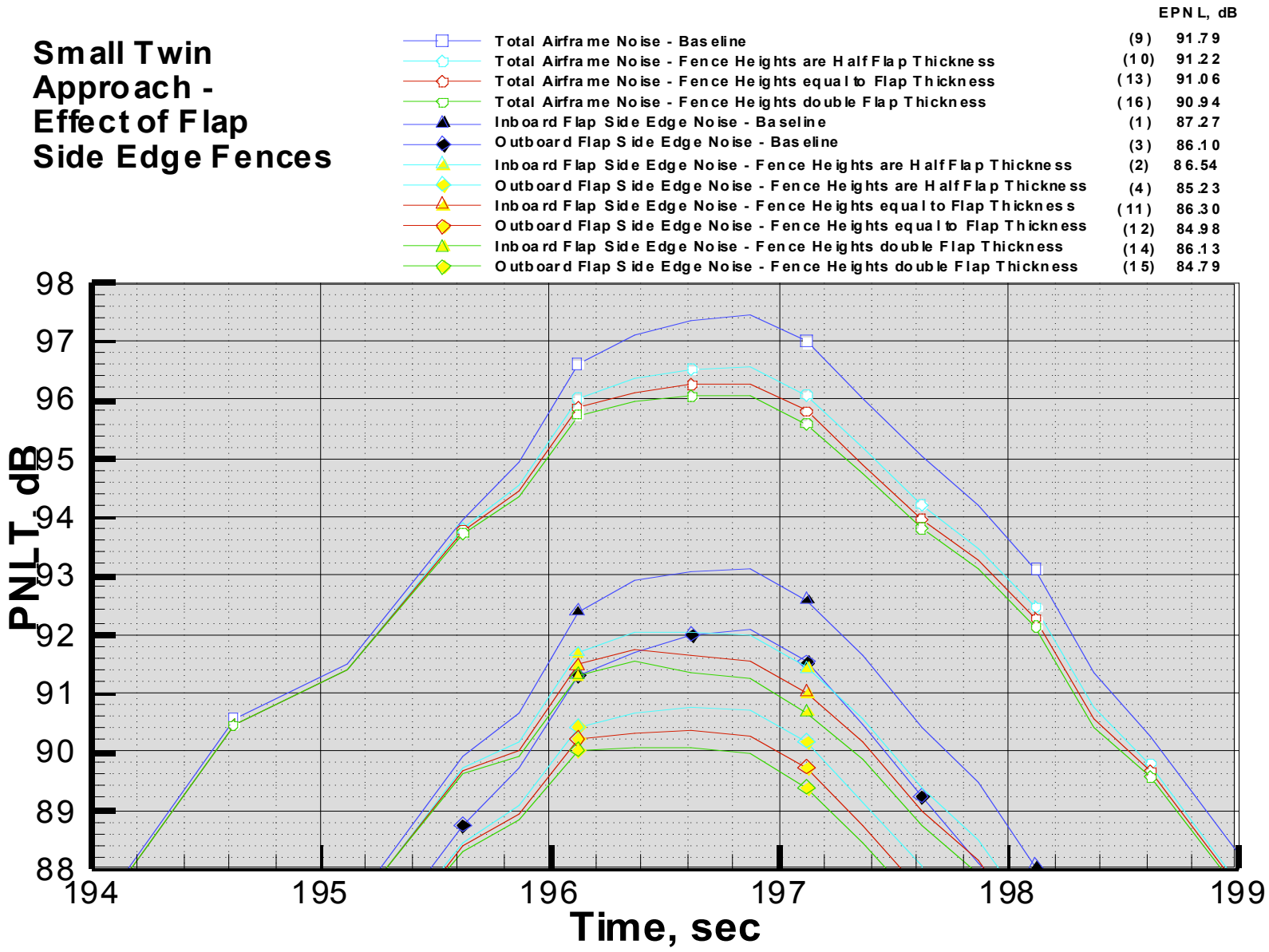

Figure 52 PNLT vs time for Small Twin Approach – Fences on inboard/outboard flaps.

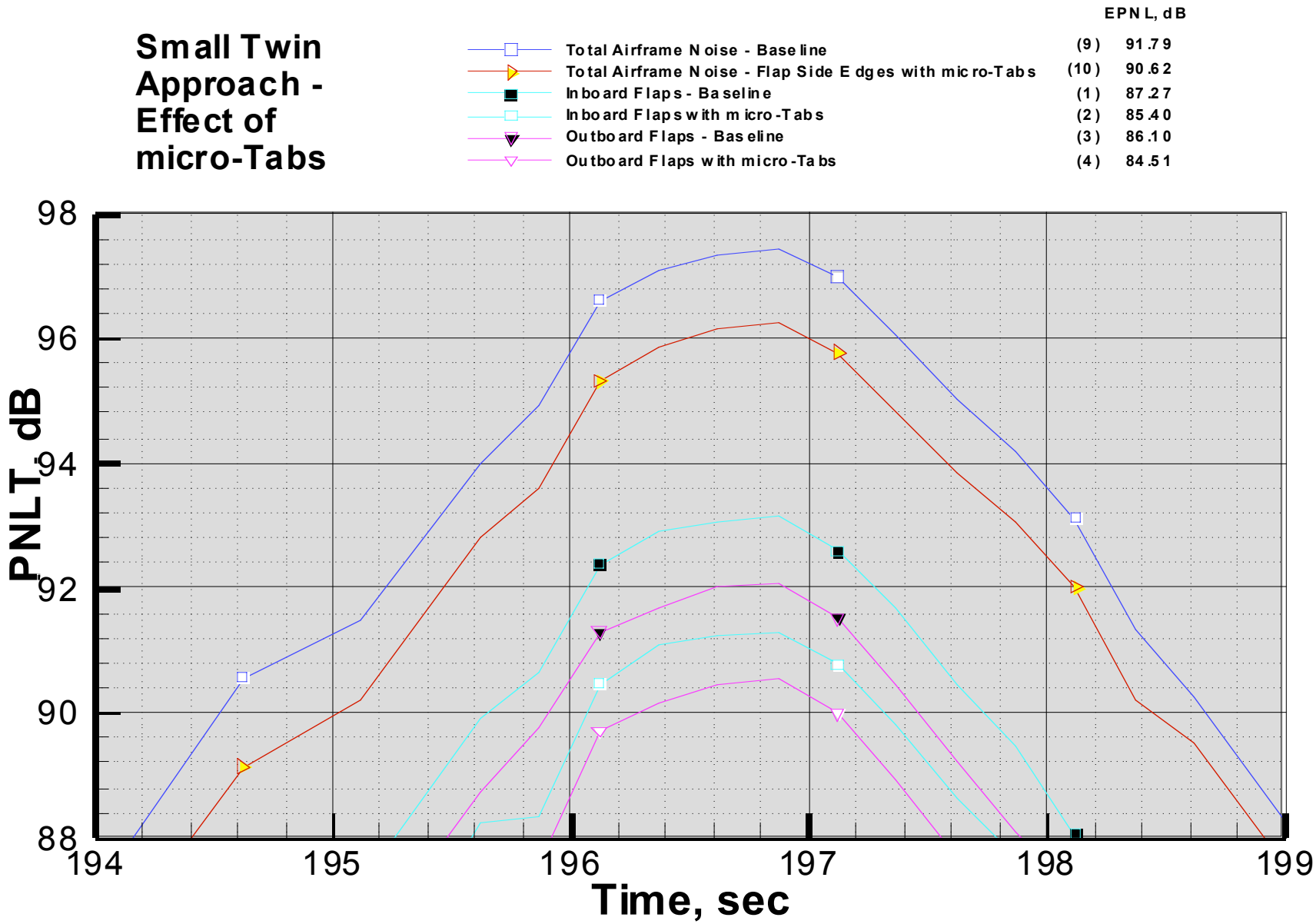

Figure 53 PNLT vs time for Small Twin Approach – μ-tabs on inboard/outboard flaps.

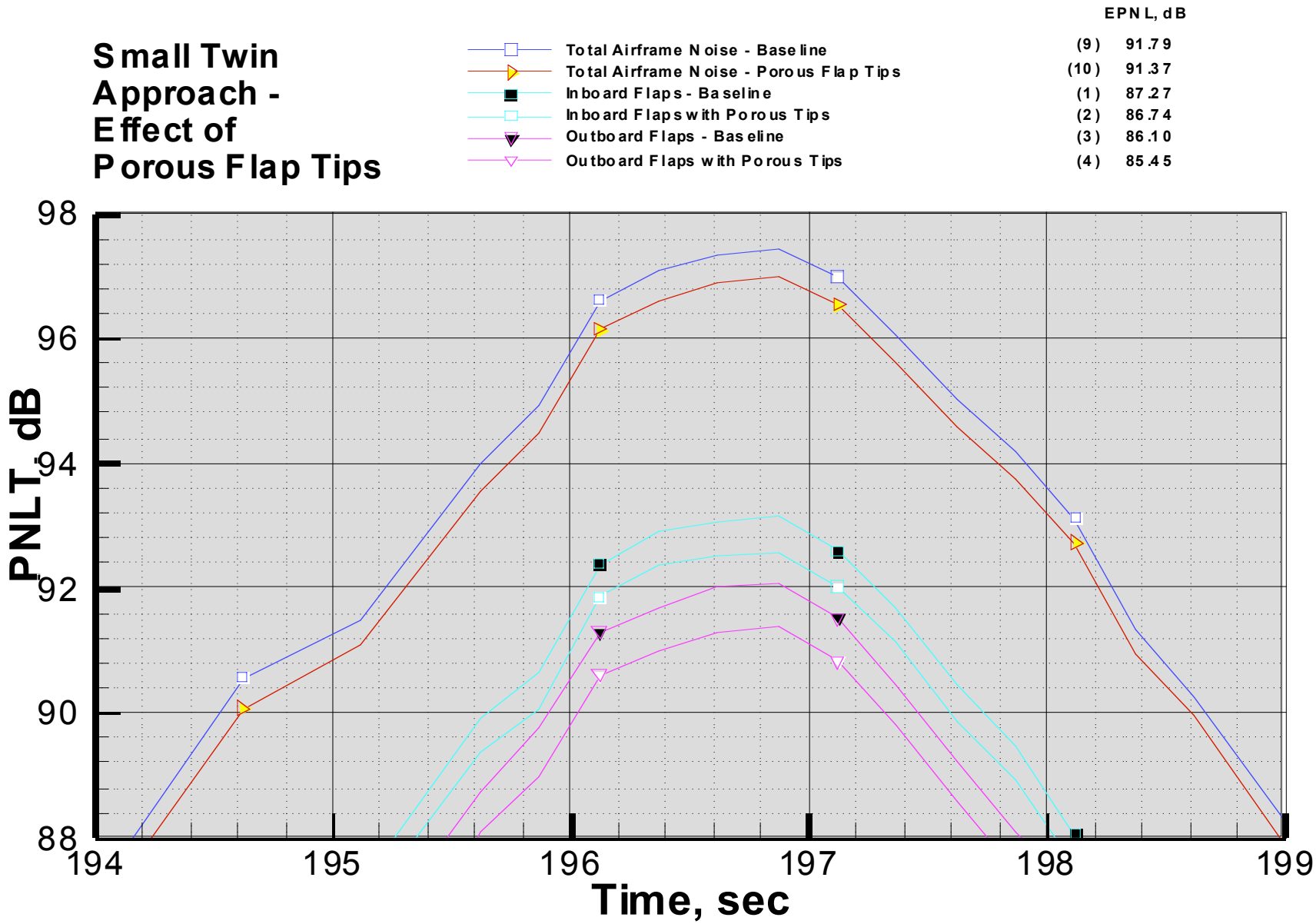

Figure 54 PNLT vs time for Small Twin Approach –Porous surfaces on inboard/outboard flap tips.

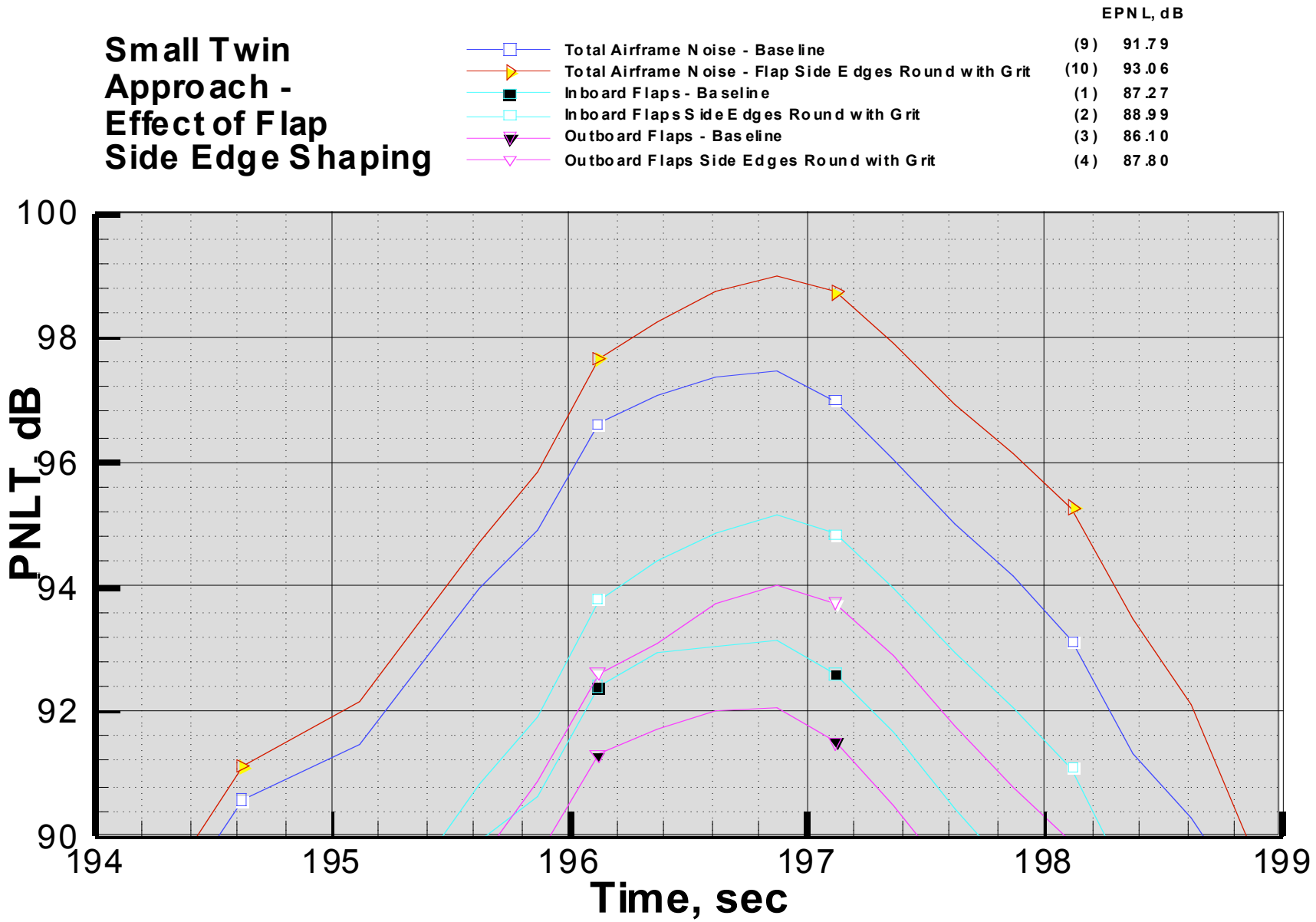

Figure 55 PNLT vs time for Small Twin Approach –Side edge shaping on inboard/outboard flaps.

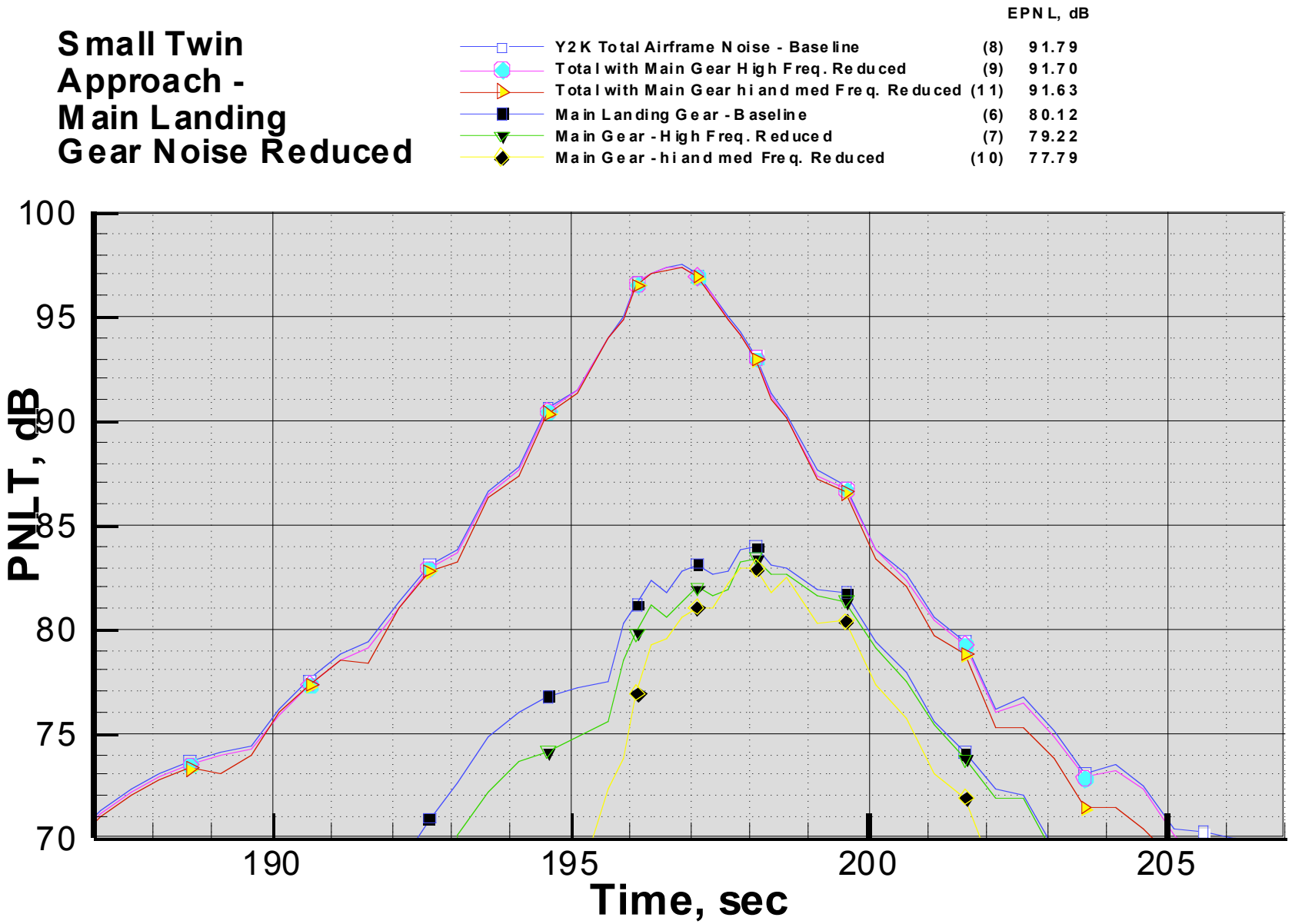

Figure 56 PNLT vs time for Small Twin Approach – Main landing gear noise reductions.

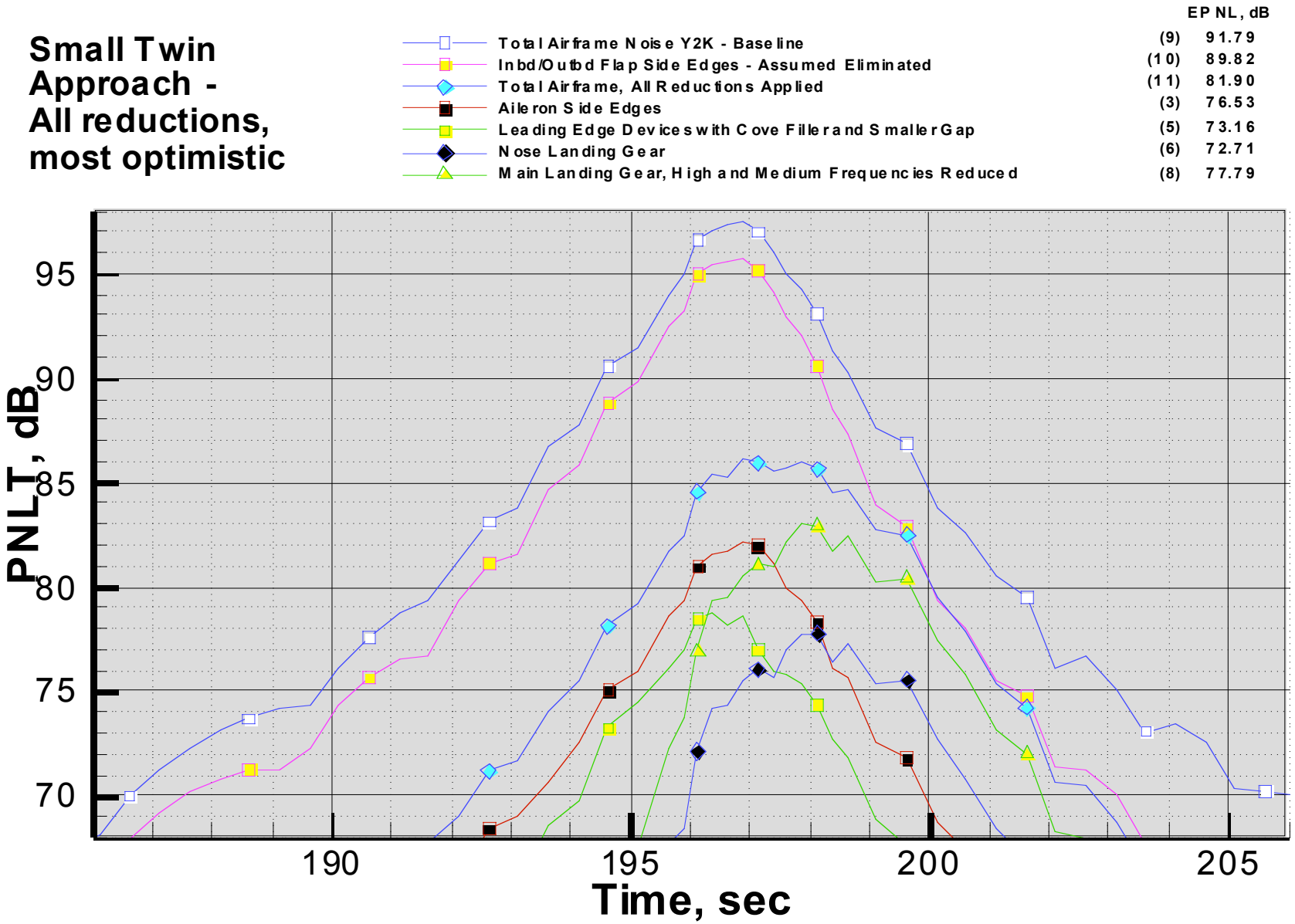

Figure 57 PNLT vs time for Small Twin Approach – All noise reduction concepts, most optimistic.

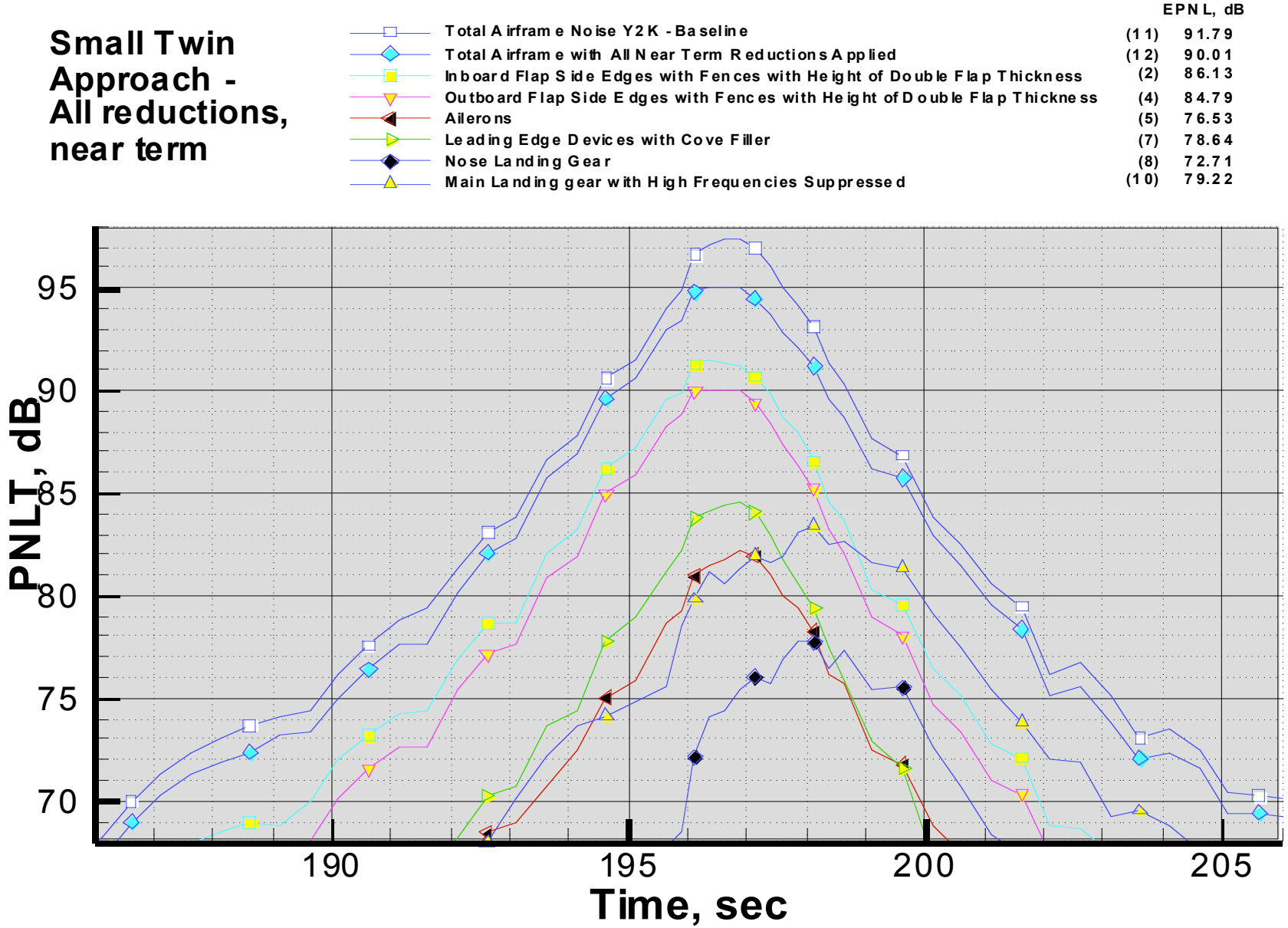

Figure 58 PNLT vs time for Small Twin Approach – All noise reduction concepts, near term.

7 Recommendations for Future Airframe Noise Reduction Research

Table 6 Compendium of Concepts and Ideas for Future Activities

Description	Pay-off	Time Horizon
PREDICTION METHODS		
General needs: ♦ Improve acoustic modeling capability, based on source physics ♦ Improve unsteady CFD methods with emphasis on understanding behavior of acoustic sources ♦ Improve empirical prediction tools	Reduces need for expensive experimentation and provides impetus for new noise reduction concepts	On-going into distant future
Flaps		
Need design tool for assessing treatment effects (fences, porous treatment, μ-tabs etc): Use data collected under AST to derive empirical prediction tool for treatment effects	Enable quick turn around assessment of noise reduction both for retrofit and for new production development	Soon
Extend acoustic modeling capability for noise reduction treatment: (e.g. combine vortex method with a finite impedance surface to model porous surface treatment)	Enable, and improve quality of, design and trade-off studies	Not too far into the future
Explore feasibility of advanced unsteady flow simulations (e.g. by Detached Eddy Simulation)	Provide tools for the future	Later
Slats		
Need design tool that is sensitive to changes to gap, cove filler and trailing edge geometry (thickness, serrations): Use data collected under AST to derive empirical prediction tool for these effects	Enable quick turn around assessment of noise reduction both for retrofit and for new production development	Soon
Improve and extend acoustic modeling methods such as the vortex method	Enable, and improve quality of, design and trade-off studies	Not too late
Develop DES for slat flow applications	Provide tools for flow physics understanding and provide numerical database	Fairly soon
Incorporate effects of support brackets into slat noise prediction	Improve realism	Later

Description	Pay-off	Time Horizon
Landing Gear		
Validate and improve statistical model with experimental and numerical data	Tool for noise prediction, noise reduction assessment and new product development	Very soon
Determine level of detail required for adequate prediction results	Guidance for subsequent prediction model development	Very soon
Continue refining CFD methods		
Assess DES as the provider of flow fields for first-principle noise prediction. Compare incompressible and compressible solutions. Design, code, and shake down a practical far-field noise-prediction approach.	Use for creating empirical model/design tool	On-going
Integrate with the high lift system	Combined aero/noise evaluation of hi-lift devices	Later
Improve existing empirical modeling by including data from: DERA (747 model), recent NASA Ames tests (737), upcoming STAR tests (777).	Enable, and improve quality of, design and trade-off studies	Soon
EXPERIMENTS		
Flaps		
Porous tips: optimize porosity, determine influence on cruise drag	Data for improved prediction models	Later
μ-tabs: apply on swept wings and on larger scale; determine influence on cruise drag		Later
Slats		
Krueger slats: need fundamental investigation	Generate basic insights	Very soon
Determine whether slat brackets are a major noise source	Guide future activities	Soon
Model slat in more detail, such as cove seal, trailing edge bulb seal	Data for improved prediction models	Later
Landing Gear		
Wheel well cavities:		
Determine when they contribute significantly	Guide future activities	Later
Model cavities faithfully, especially for the nose gear	Data for improved prediction models	Later

Description	Pay-off	Time Horizon
Flight testing of noise reduction concepts – try for 2001 on 777 and leverage STAR test	Model and flight test data would become available at about the same time – unique opportunity to investigate scaling/Reynolds # effects, validate prediction models, and provide guidance for future research	Very soon
Wind tunnel testing:		
Models with great detail	Answer the burning question of how much detail is sufficient	Soon
Surface treatment of fuselage/wing panels close to landing gear	Determine probable effectiveness of each option, provide guidance for future research	Later
Roughness on struts and/or trucks		Later
Partial fairing of truck		Soon
DESIGN OPTIONS		
Flaps		
Improve wing design so highly loaded flaps are not required (see **Note 1**)	Less noise due to smaller flaps or less flap deflection	Next new wing
Continuous moldline technology:	Eliminate the flap edge noise source	Later
Materials research		
Designs for multi-element flaps		
Retrofit		
Replace flaps by trailing edge blowing		Futuristic
Slats		
Expand use of 'auto gap' (slat would be sealed at approach; in an emergency the slat would automatically gap.)	Much of slat noise eliminated in routine operation	Later
Cove filling materials that still allow mating with the main wing at cruise	Eliminate low frequency portion of slat noise	Later
Landing Gear		
Reduce complexity of landing gear; fewer hoses and tubes	Eliminate high frequency portion of landing gear noise	Soon

Description			Pay-off	Time Horizon
		Reduce the number of small openings and cavities on the landing gear	Reduce tones from organ pipe/Helmholtz resonator effects	Later
		Fairings (Issues: weight, access, shrapnel due to tire blow)	Reduced levels at all frequencies	Later
		Virtual fairings by blowing/exhausting in front of strut and truck		Futuristic
	Plasma: generate plasma flow with, hopefully, greatly reduced turbulence around airframe sources		Remains to be seen	Futuristic
OPERATIONAL OPTIONS				
	Slats			
		Expand use of 'auto gap' (slat would be sealed at approach; in an emergency the slat would automatically gap)	Much of slat noise eliminated in routine operation	Later
	Landing Gear			
		Deploy late (way beyond approach certification point)	Landing gear noise source eliminated possibly up to airport property boundary	Futuristic

Note 1 An idea about the flap side edge noise reduction potential due to improved wing design can be gleaned from the noise prediction formula given in Section 3.2.2 of Ref. 64 and from page 29 of Ref. 30 which discusses two important required data items: the cross-flow velocity at the flap side edge (depends on the slope of the span load [wing loading as a function of spanwise distance]), and the circulation indicating the strength of the flap side edge vortex (depends on the span load discontinuity at the flap side edge).

8 References

Ref. #	Citation	Year
Ref. 1	Gillian, R. E., "ANOPP User's Manual", NASA TM-84486, 1982	1983
Ref. 2	Goldhammer, M.I., "User's Manual for Computer Program A449B Advanced Lifting Surface Methods," Boeing internal document D6-46987, 1979.	1979
Ref. 3	Kendall, J.M., Ahtye, W.F., "Noise Generation by a Lifting Wing/Flap Combination at Reynolds Numbers to $2.8x10^6$", AIAA Paper 80-0035, AIAA 18^{th} Aerospace Sciences Meeting, Jan 14-16, 1980, Pasadena California.	1980
Ref. 4	Miller, W.R., "Flap Noise Characteristics Measured by Pressure Cross-Correlation Techniques," Ph.D. Thesis, UCLA, 1980.	1980
Ref. 5	Fink, M.R., Bailey, D.A., "Airframe Noise Reduction Studies and Clean-Airframe Noise Investigation," NASA CR-159311 (April 1980).	1980
Ref. 6	S.A. McInerny, et al., "An Experimental Investigation of Wing Tip Turbulence with Application to Aerosound," AIAA-86-1918	1986
Ref. 7	Soderman, P.T., Allen, C.S., "On The Scaling Of Small-Scale Jet Noise To Large Scale," AIAA 92-02-109.	1992
Ref. 8	Revell, J. D., Kuntz, H.L., Balena, F.J. , Hickmon, F.O., Lackey, D.F., Feltz, E.P.: "Contract NAS1-20102, Task 3 Interim Report for FY1994, Airframe Noise Reduction Studies for Advanced Subsonic Transport (AST) Aircraft (L-1011 Noise Reduction Study)", Lockheed-Martin Skunkworks, Oct. 31, 1994	1994
Ref. 9	Revell, J. D., Kuntz, H.L., Balena, F.J. , Hickmon, F.O., Lackey, D.F., Feltz, E.P., "Contract NAS1-20102, Task 3 Interim Report for FY1994, Airframe Noise Reduction Studies for Advanced Subsonic Transport (AST) Aircraft", Lockheed-Martin Skunkworks, Revised November 30, 1995.	1995
Ref. 10	Sen, Rahul, "Assessment of the NASA ANOPP Method of Airframe Noise Prediction from a Noise Reduction Standpoint," Boeing Document D6-81619TN, under NASA Contract NAS1-20900 Task 2 (1993-94).	1995
Ref. 11	Blackner, A.M., Davis, C.M., "Airframe Noise Source Identification Using Elliptical Mirror Measurement Techniques," Inter-Noise 95, Newport Beach CA, July 10-12, 1995.	1995
Ref. 12	Mathias, D.L., Roth, K.R., Ross, J.C., Rogers, S.E., and Cummings, R.M.: "Navier-Stokes Analysis of the Flow About a Flap Edge", AIAA-95-0185, 33^{rd} Aerospace Sciences Meeting, Reno, NV, Jan. 1995.	1995
Ref. 13	Reed, David H., et al., "Airframe Noise Workshop", collection of viewgraphs of a NASA AST Workshop held October 17-19, 1995, in Renton, Washington.	1995
Ref. 14	Storms, B. L., Takahashi, T. T., and Ross, J. C., "Aerodynamic Influence of a Finite-Span Flap on a Simple Wing," SAE Paper 95-1977, September 1995.	1995
Ref. 15	Revell, J.D., Kuntz, H.L.,: "Contract NAS1-20102, Task 3 Interim Report for FY1995, Modified Drag Element Method of Airframe Noise Prediction", Lockheed-Martin Skunkworks, April 30, 1996.	1995

Ref. 16	Kumasaka, Henry A., Martinez, Michael M., Weir, Donald S., “Definition of 1992 Technology Aircraft Noise Levels and the Methodology for Assessing Airplane Noise Impact of Component Noise Reduction Concepts,” NASA CR 198298, June 1996.	1996
Ref. 17	Sen, R., “Local Dynamics and Acoustics in a Simple 2D Model of Airfoil Lateral-Edge Noise, AIAA-96-1673, AIAA/CEAS 2nd Aeroacoustic Conference, State College, PA, 1996.	1996
Ref. 18	Revell, J.D., Kuntz, H.L., Balena, F.J., “Prediction of Airframe Noise Radiation from Flap Side-Edges, Using Vortex Flow Data from a CFD Solution,” report by Lockheed-Martin to NASA Ames, contract NAS2-20102, Task 3, September 1996.	1996
Ref. 19	Revell, J.D., et al., “Contract NAS1-20102, Task 3 Interim Report for FY1996, Airframe Noise Reduction Studies for Advanced Subsonic Technology Aircraft, L-1011 Flap Noise Reduction using Acoustically Treated Flaps”, Lockheed-Martin Skunkworks, Sept., 1996.	1996
Ref. 20	Sen, Rahul, “Interpretation of Acoustic Source Maps Made with an Elliptic-mirror Directional Microphone System,” AIAA 96-1712, 2nd AIAA/CEAS Aeroacoustics Conference, May 1996.	1996
Ref. 21	Storms, B. L. and Ross, J. C., "Aerodynamic Effects of Flap-Tip Treatments on an Unswept Wing," AIAA Paper 96-2372, June 1996.	1996
Ref. 22	Allen, C.S., Soderman, P.T., “Scaling and Extrapolating Small-scale in-Flow Wind Tunnel Jet Noise to Full0scale Flyover Jet noise,” AIAA-97-1602-CP.	1997
Ref. 23	Sen, R., “Vortex-Oscillation Model of Airfoil Side-Edge Noise”; AIAA Journal vol. 35, no. 3, March, 1997.	1997
Ref. 24	Meadows, KR., Brooks, T.F., Humphreys, W.M., Hunter, W.W., and Gerhold, C.H., "Aeroacoustic Measurements of a Wing-Flap Configuration", AIAA Paper 97-1595, 3rd AIAA/CEAS Aeroacoustics Conference, Atlanta, Georgia, May, 1997.	1997
Ref. 25	Hayes, J., Horne, W.C., Soderman, P., and Bent, P., “Airframe Noise Characteristics of a 4.7% DC-10 Model, AIAA-97-1594, AIAA/CEAS 3rd Aeroacoustics Conf., Atlanta, GA, May, 1997.	1997
Ref. 26	Horne, W.C., Hayes, J., Ross, J.C., and Storms, B.L.: “Measurements of Unsteady Pressure Fluctuations of an Unswept, Multi-Element Airfoil”, 3rd AIAA/CEAS Aeroacoustics Conference, Atlanta, Georgia, May, 1997, AIAA-97-1645-CP.	1997
Ref. 27	Guo Y.: “On sound generation by unsteady flow separation at airfoil sharp edges, AIAA Paper 97-1697, 3rd AIAA/CEAS Aeroacoustics Conference, Atlanta, Georgia, May, 1997.	1997
Ref. 28	Mosher, M., Watts, M., Jovic, S., and Jaeger, S.: “Calibration of Microphone Arrays for Phased Array Processing”, 3rd AIAA/CEAS Aeroacoustics Conference, Atlanta, Georgia, May, 1997, AIAA-97-1678-CP.	1997
Ref. 29	Sen, R.: “A Study of Unsteady Fields Near Leading-edge Slats,” AIAA 97-1696, 3rd AIAA/CEAS Aeroacoustics Conference, Atlanta, Georgia, May, 1997.	1997

Ref. 30	Sen, R., Blackner, A., Yee, P., and Stoker, R., “Airframe Noise Generation and Radiation”, NASA Contract NAS1-20090, Task 2 Informal Report, Boeing Commercial Airplane Company, Jan. 1997.	1997
Ref. 31	Anon., “NASA AST Program, Noise Reduction Technology, Proceedings of Airframe Noise Workshop,” Long Beach CA, collection of viewgraphs, June 1997.	1997
Ref. 32	Revell, J.D., Kuntz, H.L., Balena, F., Horne, W.C., Storms, B.L., and Dougherty, R.: "Trailing Edge Flap Noise Reduction by Porous Acoustic Treatment”, 3rd AIAA/CEAS Aeroacoustics Conference, Atlanta, Georgia, May, 1997, AIAA-97-1646-CP.	1997
Ref. 33	Sen, R., et al, “Airframe Noise Baseline Scale Effects/Analytical and Empirical Models-Progress Toward a Second Generation Flap-Edge Noise Model,” NASA Contract NAS1-90740, Boeing Commercial Airplane Company, December 1997.	1997
Ref. 34	Shivashankar, B., and Blackner, A.: “Installed Jet Noise”, AIAA-97-1601, 3rd AIAA/CEAS Aeroacoustics Conference, Atlanta, Georgia, May 1997.	1997
Ref. 35	Khorrami, M.R., Singer, B.A, Takallu, M.A., “Analysis of Flap Side-Edge Flowfield for Identification and Modeling of Possible Noise Sources,” SAE Paper 971917, Traverse City MI, May 1997.	1997
Ref. 36	Streett, C.L.: “Numerical Simulation of Fluctuations Leading to Noise in a Flap-Edge Flowfield,” AIAA 98-0628, 36th Aerospace Sciences Meeting and Exhibit, Reno, Nevada, January 1998.	1998
Ref. 37	Radeztsky, R.H., Singer, B.A., and Khorrami, M.R.: "Detailed measurements of a flap side-edge flow field," AIAA Paper 98-0700, 36th Aerospace Sciences Meeting and Exhibit, Reno, Nevada, January, 1998.	1998
Ref. 38	Humphreys, W.M., Brooks, T.F., Hunter, W.W., and Meadows, K.R: "Design and Use of Microphone Directional Arrays for Aeroacoustic Measurements", AIAA Paper 98-0471, 36th Aerospace Sciences Meeting and Exhibit, Reno, Nevada, January, 1998.	1998
Ref. 39	Storms, B.L., et al., “An Aerodynamic Study of an Unswept Wing with a Three-Dimensional High-lift System,” NASA/TM-1998-112222, February 1998.	1998
Ref. 40	Khorrami, M.R., and Singer, B.A.: "Stability analysis for noise-source modeling of a part span flap," AIAA Paper 98-2225, June 1998.	1998
Ref. 41	Macaraeg, M.G., “Fundamental Investigation of Airframe Noise,” AIAA-98-2224, 4th AIAA/CEAS Aeroacoustics Conf., Toulouse, FR, June 1998.	1998
Ref. 42	Streett, C.L.: “Numerical Simulation of a Flap-Edge Flowfield,” AIAA 98-2226, 4th AIAA/CEAS Aeroacoustics Conf., Toulouse, FR, June 1998.	1998
Ref. 43	Guo, Y., Hardy, B., Bent, P., Yamamoto, K., Joshi, M., “Noise Characteristics of the DC-10 Aircraft High Lift System,” Boeing Report No. CRAD-9310-TR-4893, Sept. 1998.	1998
Ref. 44	Guo, Y., Bent, P., Yamamoto, K., Joshi, M., “Surface Pressure Fluctuations on DC-10 High Lift System and Their Correlation with Far Field Noise,” Boeing Report No. CRAD-9310-TR-4872, September 1998.	1998
Ref. 45	Guo, Y., Stoker, R., Hardy, B., Bent, P., Joshi, M., “DC-10/MD-11 Acoustic Test in NASA Ames 12-ft Pressurized Wind Tunnel,” Boeing Report No. CRAD-9310-TR-4894, September 1998.	1998

Ref. 46	Guo, Y., “A semi-analytical/semi-empirical model for flap side edge noise prediction”, NASA Contract NAS1-20103, Task 2, Report CRAD-9310-TR-3765, The Boeing Company, Sept. 1998.	1998
Ref. 47	Sen, R.: “Theoretical Investigation of Slat Noise”, NASA Contract NAS1-97040, Task 2, Boeing Commercial Airplane Company, December 1998.	1998
Ref. 48	Anon., “NASA AST Program, 3rd Airframe Noise Workshop.” collection of viewgraphs, Boeing-Seattle November 1998.	1998
Ref. 49	Khorrami, M.R., Singer, B.A., and Radeztsky, R.H.: "Reynolds Averaged Navier-Stokes computations of a flap side-edge flow field," AIAA J., Vol.37, No.1, pp. 14-22, January 1999.	1999
Ref. 50	Singer, B.A., Brentner, K.S., Lockard, D.P. and Lilley, G.M., “Simulation of Acoustic Scattering from a Trailing Edge,” AIAA-99-0231. – Also: Singer, B.A., Brentner, K.S., Lockard, D.P. and Lilley, G.M., “Simulation of Acoustic Scattering from a Trailing Edge,” J. Sound & Vibration (2000) 230(3), 541-560.	1999
Ref. 51	Berkman, M.E., Khorrami, M.R., Choudhari, M., and Sadowski, S.S.:"Investigation of high-lift flow field of an energy efficient transport wing," AIAA Paper 99-0926, January 1999.	1999
Ref. 52	Brooks, T.F., Humphreys, W.M., "Effect of Directional Array Size on the Measurement of Airframe Noise Components", AIAA paper 99-1958, presented at 5th AIAA/CEAS Aeroacoustics Conference in Seattle, May 1999.	1999
Ref. 53	Dong, T.Z., Tam, C.K.W., and Reddy, N.N.: “Direct Numerical Simulation of Flap Side Edge Noise”, AIAA-99-1803, presented at 5th AIAA/CEAS Aeroacoustics Conference in Seattle, May 1999.	1999
Ref. 54	Singer, B.A., Lockard, D.P., Brentner, K.S., Khorrami, M.R., Berkman, M.E., and Choudhari, M.: “Computational Acoustics Analysis of Slat Trailing-Edge Flow” AIAA Paper No. 99-1802, presented at AIAA Aeroacoustic Conference, Seattle, May 1999.	1999
Ref. 55	Korari, M.R., Beckman, M.E., Chuddar, M., Singer, B.A., Locker, D.P., and Brenner, K.S.: "Unsteady flow computations of a slat with blunt trailing edge," AIAA Paper 99-1805, presented at 5th AIAA/CEAS Aeroacoustics Conference in Seattle, May 1999.	1999
Ref. 56	Guo, Y.: “Prediction of flap side edge noise”, AIAA Paper 99-1804, presented at 5th AIAA/CEAS Aeroacoustics Conference in Seattle, May 1999.	1999
Ref. 57	Guo Y., “Application of Ffowcs Williams/Hawkings equation to two-dimensional problems”, report by The Boeing Co. to NASA LaRC, contract NAS1-20268, Task 20, June 1999. – Also: Guo, Y.P., “Application of the Ffowcs Williams/Hawkings equation to two-dimensional problems,” J. Fluid Mech. (2000), vol. 403, pp.201-221.	1999
Ref. 58	Guo, Yueping, “Modeling of Noise Reduction by Flap Side Edge Fences,” report by The Boeing Co. to NASA LaRC, contract NAS1-20268, Task 20, June 1999.	1999
Ref. 59	Stoker, R.W., “Landing Gear Noise Test Report”, report by Boeing Co. to NASA LaRC under Contract NAS1-97040, Task 8, February 1999.	1999

Ref. 60	Storms, B.L., Ross, J.C., Hayes, J., and Moriarty, P.: "Acoustic Measurements of Slat Noise on a Three-Dimensional High-Lift System", AIAA-99-1957, presented at 5th AIAA/CEAS Aeroacoustics Conference in Seattle, May 1999.	1999
Ref. 61	Hayes, J.A., Horne, W.C., Jaeger, S.M., Soderman, P.T., "Measurement of Reynolds Number Effect on Airframe Noise in the 12-foot Pressure Wind Tunnel," AIAA-99-1959, 5th AIAA/CEAS Aeroacoustics Conference, Seattle, May 1999.	1999
Ref. 62	Sen, Rahul, and Stoker, Robert W., "Airframe Noise Test of a 0.063-scale 777 Model: Test Report," report by The Boeing Co. to NASA LaRC, contract NAS1-97040, Task 2, December 1999.	1999
Ref. 63	Tam, C.K.W., Pastouchenko, N., "Gap Tones: A Component of Airframe Noise'", AIAA 2000-0606, January 2000.	2000
Ref. 64	Sen, Rahul, Hardy, Bruce, Yamamoto, Kingo, Guo, Yueping, Miller, Gregory, "Airframe Noise Subcomponent Definition and Model," NASA Contractor Informal Report, Contract NAS1-97040, Task 9, January 2000.	2000
Ref. 65	Tam, C.K.W., Pastouchenko, N., "Gap Tones: A Component of Airframe Noise," AIAA 2000-0606, 38th Aerospace Sciences Meeting and Exhibit, January 2000, Reno NV.	2000
Ref. 66	Storms, Bruce L., Hayes, Julie A., Jaeger, Stephen M., Soderman, Paul T., "Aeroacoustic Study of Flap-Tip Noise Reduction Using Continuous Moldline Technology," AIAA 2000-1976, 6th AIAA/CEAS Aeroacoustics Conference, June 12-14, 2000, Lahaina HI.	2000
Ref. 67	Guo, Y.P., "Ffowcs Williams/Hawkings Equation for Two-Dimensional Problems," AIAA 00-2066, 6th AIAA/CEAS Aeroacoustics Conference, Lahaina HI, June 2000.	2000
Ref. 68	Guo, Y.P., Joshi, M.C., Bent, P.H., Yamamoto, K.J., "Surface pressure fluctuations on aircraft flaps and their correlation with far-field noise," J. Fluid Mechanics (2000), vol. 415, pp. 175-202.	2000
Ref. 69	Guo, Y.P., Modeling of Noise Reduction by Flap Side Edge Fences," AIAA 00-2065, 6th AIAA/CEAS Aeroacoustics Conference, Lahaina HI, June 2000.	2000
Ref. 70	Guo, Yueping, "A Discrete Vortex Model for Slat Noise Prediction", report CRAD-9402-TR-5170 by The Boeing Company to NASA Langley Research Center, September 2000.	2000
Ref. 71	Brooks, T.F., Humphreys, W.M.Jr., "Flap Edge Aeroacoustic Measurements and Predictions," AIAA 2000-1975, 6th AIAA/CEAS Aeroacoustics Conference, Lahaina HI, June 2000.	2000
Ref. 72	Choudhari, M.M., Lockard, D.P., Macaraeg, M.G., Singer, B.A., Streett, C.L., Neubert, G., Stoker, R.W., Underbrink, J., Berkman, M.E., Khorrami, M.R., Sadowski, S.S., "Aeroacoustic Experiments in the NASA Langley Low-Turbulence Pressure Tunnel," NASA TM-2002-211432, February 2002.	2000
Ref. 73	Guo, Yueping, "A Statistical Model for Landing Gear Noise Prediction," Journal of Sound and Vibration, Volume 282, pp. 61-87	

9 Appendix: Abstracts and Review Notes of AST Airframe Noise Literature

Ref. 9 Revell, J. D., Kuntz, H.L., Balena, F.J., Hickmon, F.O., Lackey, D.F., Feltz, E.P., "Contract NAS1-20102, Task 3 Interim Report for FY1994, Airframe Noise Reduction Studies for Advanced Subsonic Transport (AST) Aircraft", Lockheed-Martin Skunkworks, Revised November 30, 1995.

Summary: Noise reduction tests were conducted on a 1/20 scale semi-span model of the L-1011 in a free jet wind tunnel within the acoustic anechoic chamber at the Lockheed Rye Canyon test facility in Valencia, Ca, now being operated by NTS. This report describes the results of far-field noise tests conducted in August of 1994. A second series of tests were conducted in July of 1995, primarily to verify the surface pressure fluctuation data. During the 1995 tests, three additional noise reduction. Treatments were evaluated. These results will be presented in a separate report.

The nozzle cross section is 35 inches by 16 inches. Test data were obtained over a range of 0.135 to 0.194 Mach number. Fifteen configurations were tested, including seven noise reduction configurations, and two baseline repeat tests at the end of the program. Only the inboard flaps were deflected in these tests. The wing was mounted between sidewall boundary layer diverter plates, leaving a net wingspan of 31 inches exposed to the potential core of the free jet. The exposed 31-inch span represents about 76.4% of the exposed L-1011 semi-span, or 79.4 % of the full semi-span when the fuselage is present.

The instrumentation consisted of seven far-field microphones at a sideline distance of 6.71 ft (134 ft full-scale), and 14 surface pressure transducers, two on the main wing and 12 on the trailing edge flap surfaces.

Preliminary analysis indicates worthwhile noise reductions, for the inboard flaps alone, of up to 1.5 dB in OASPL and 2.4 dBD (D-weighted OASPL, which is used to approximate PNL).

The model scale data were scaled to full size for comparison with flyover data published by Fethney and Jelly of the RAE. The OASPL and D-weighted OASPL agreed within 0.87 dB and 0.83 dBD, respectively with the flyover data for 42° flaps plus leading edge slats. Projections for TE flaps plus LE slats (landing gear retracted) to FAR-36 landing approach conditions at 79.7 m/s gave 94.5 EPNL from scaled wind tunnel data vs. 95.9 EPNdB for the velocity-adjusted RAE prediction. These levels are 9.3 and 7.9 EPNdB below the FAR-36 Stage 3 allowance for the L-1011 (at 430,000 lb takeoff gross weight). Inclusion of the landing gear using RAE data adjusted to 79.7 m/s puts the total airframe noise signature at 98.3 EPNdB using RAE data (5.5 EPNdB below the Stage 3 allowance), or 97.4 EPNdB (6.4 EPNDB below Stage 3) using scaled wind tunnel data.

The present results, although preliminary, strongly suggest that if the total landing approach noise goal for the AST is to be in the range of FAR-36 Stage 3 minus 6 EPNdB, then the total airframe noise reduction needs to be at least 4 dB, with emphasis on flap noise reduction. Recommended future effort includes further work on flap noise reduction, emphasizing side edge effects, and landing gear noise reduction, via drag-reducing fairings.

Ref. 10 Sen, Rahul, "Assessment of the NASA ANOPP Method of Airframe Noise Prediction from a Noise Reduction Standpoint," Boeing Document D6-81619TN, under NASA Contract NAS1-20900 Task 2 (1993-94).

The airframe-noise module of the NASA ANOPP method of airplane-noise prediction is considered. This report is concerned with the suitability of the method as a design tool for low airframe-noise design studies. Attention is restricted to source models for wing and high-lift noise. On comparing the conceptual basis of these models to prevalent theoretical ideas and to source behavior suggested by model-scale data, we find that many important features are ignored in ANOPP. Three such features are discussed in detail: spanwise variation of noise source strength, flap side-edge

sources, and interaction effects. It is argued that viable design concepts can be based on exploiting such features, leading to significant airframe-noise reductions. Since these and other aspects of airframe-noise are not represented in ANOPP we conclude that it is unsuitable as a design tool for noise-reduction studies.

Discusses Fink's airframe noise module from 1977. Does not address landing gear noise at all, only wings and high lift devices. Contains a lot of elliptic mirror source location measurement data.

Ref. 11 Blackner, A.M., Davis, C.M., "Airframe Noise Source Identification Using Elliptical Mirror Measurement Techniques," Inter-Noise 95, Newport Beach CA, July 10-12, 1995.

Used elliptic mirror in LSAF to produce noise source maps of airframe noise on various Boeing airplane models. Identified as major sources: landing gear (dominating low frequencies), main wing leading edge (contributing mostly in the mid frequencies), flap edges (dominating the high frequencies). Establishes some trends with Mach number and angle of attack. Investigates influence of flap edge treatments: round edge and large fence.

Ref. 12 Mathias, D.L., Roth, K.R., Ross, J.C., Rogers, S.E., and Cummings, R.M.: "Navier-Stokes Analysis of the Flow About a Flap Edge", AIAA-95-0185, 33rd Aerospace Sciences Meeting, Reno, NV, Jan. 1995.

Used 3D, incompressible NS solver, Baldwin/Barth turbulence model. Results shown as particle traces. Demonstrates vortex formation. Does not mention noise in abstract or conclusions.

Ref. 13 Reed, David H., et al., "Airframe Noise Workshop", collection of viewgraphs of a NASA AST Workshop held October 17-19, 1995, in Renton, Washington.

1993/94 airframe noise tests in LSAF using elliptic mirror -> The flap side edge noise source was determined to be the highest priority for evaluation. – Flap edge empirical model tries to collapse location of peak frequency on local steady flow parameters. – Leading edge noise source is second priority in evaluation. – Attempts to predict noise from steady flow parameters (but I saw a note somewhere that said one needs unsteady measurements/parameters for a successful prediction). Yueping Guo seems to do just that using DC-10 data. – Flap tip fences on lower surface reduce noise significantly.

Paper by M.G. Macaraeg: Overview of LaRC Airframe Noise Effort

> Layout of 5-year program for systematically attacking airframe noise from fundamental perspective including experimental, numerical and analytical work.

Paper by Kazuhiro Kusunose: Overview of Preliminary Design Process and Tools for High-Lift Systems

> Catalog of high lift devices. Boeing numerical methods for high lift aerodynamics (Paul Meredith is referenced). [There are two papers by Kazu on this subject in these proceedings.]

Paper by Rahul Sen: Elliptical Mirror Source Imaging

> See discussion of Ref. 20.

Paper by Jim Underbrink: Phased Array Data System Development

> Gives system requirements and touts several successful applications.

Paper by T. F. Brooks: Microphone Array Technology Development at NASA LaRC

> Microphones on standoffs in front of supporting grid (Boeing's microphones are in a solid plane surface). Codename MAPPS (Microphone Array Phased Processing System). No data directly applicable to airframe noise.

Paper by Chris Tam: Flap-Edge Noise: Physics and Computational Model

Refers to Ref. 3. Asserts that flap-edge noise is not generated by flow sources (turbulence), but most likely by flow-wing/flap surface interaction (vortex shed from deflected flap edge impinges on non-deflected trailing edge of wing). Modeling uses CAA with grid of 6.15 million points. No results shown.

Paper by Thies, A.T., Tam, C.K.W., Reddy, N.N.: Direct Numerical Simulation of Edge Noise as Related to Airframe Noise

(continuation of previous paper.) 2D only. Angle of attack 6°, M=0.15: noise from gap between wing and flap dominates (consistent with Ref. 3). Angle of attack 0°: flap trailing edge noise dominates. Acoustic mean squared pressure scales with **fifth** power of Mach number (experiment and simulation agree pretty well). 3D work planned.

Paper by Barry Lazos: Flap Edge Noise Research at NASA LaRC

Starts with aerodynamic flow characterization, overall and in detail through flow viz. Also measured fluctuating surface pressures. Shows setups, but experiments still to come – no results.

Paper by Kristine Meadows, Thomas Brooks, and Michael Marcolini: Risk Reduction Acoustic Tests in the Quiet Flow Facility

Quarter scale wing with flap model blown at by a jet. Shows results, but too little text to make sense of them. Lack of color in paper reproduction leaves ambiguities. Extracts from their summary: low frequency amplitude increases with flap angle and reduced gap flow; mid frequency amplitude increases with gap flow; high frequency (aeroacoustic feedback loop) amplitude depends on gap size and tripping.

Paper by Bruce Storms, Jim Ross, and Cliff Horne: Flap Edge Experiment Phase II

Presents only plans – no results.

Paper by Storms, Ross, Horne, Dougherty, Underbrink, and Takahishi: Flap Tip Treatments for the Reduction of Lift-Generated Noise

Adding a full or lower flap tip fence reduced noise in all frequency bands: 4 dB at 3 KHz, 1 dB at 5 KHz, 4 dB at 10 KHz. Fence heights are comparable to airfoil thickness. Lower fence only is acoustically hardly different from full fence. Lower fence only provided drag reduction.

Paper by Horne, Storms, Hayes, Hamid: Measurement of Unsteady Pressures at the Edge of a Deployed Fowler Flap

Shows spectral details of effect of installing a lower fence on unsteady surface pressures. Nothing on radiated noise. Lower flap fence is significant in reducing upper flap surface spectral levels as well as reducing peak coherence levels.

Paper by Jim Revell: Analysis of Acoustical Data from NASA/Ames Flap Side Edge Experiment Using the Modified Drag Element Method

Not enough text to make sense of the slides. From the ‘conclusions’:

1/3-OB spectra relative to OASPL collapse fairly well re Strouhal number = freq*FlapChordLength/FreeStreamVelocity.

OASPL has some correlation with wing lift coefficient, total drag, and viscous drag.

Paper by Kenneth Jones: Preliminary Results from a Recent Subsonic Transport investigation in the Langley 14x22 Foot Subsonic Tunnel

Tries to integrate into high lift systems design methodology more encompassing requirements, including reduced noise and wake vortex alleviation. Obtained data from microphone array, but no reporting of results.

Paper by Yueping Guo: An Analytical Study of Flap Side Edge Noise

Relates radiated sound to surface pressure fluctuations in a simple formula. But it is not clear how this can be sensitive to design features such as fences at flap side edges.

Paper by Jay Hardin and James Martin: Acoustic Computations for Sen's Flap Edge Flow Model

Not enough text to understand gist of this paper.

Paper by Rahul Sen: Flap-Edge Noise Analytical Model Development

See discussion of Ref. 17.

Paper by W.K. Anderson and M.A. Takallu: Computations for Part-Span Experiment in Quiet Flow Facility

One of the objectives was to provide data for improved source analytic models and correlations. A picture shows streamlines in the vicinity of a flap tip (or edge); the streamlines form a vortex caused by the flap tip. They calculate shear layer and vortex instabilities relevant to acoustics, but no acoustic results are shown.

Paper by Revell, Kuntz, Lackey, Balena, Hickmon: L-1011 Flap Noise Reduction Using Acoustically-Treated Flaps

See discussion of Ref. 19.

Paper by Tony Blackner: Flap Edge Source Behavior

Used elliptic mirror in LSAF. Detailed parametrics on flap edge noise. Scales with 58 log(M). Slight increase of noise in mid frequencies with angle of attack. Dependency on flap deflection: 3-5 dB increase from flap 25 to 40 at mid to high frequencies for Small Twin; 1 dB increase at mid frequencies from flaps 24 to 40 at mid frequencies for Large Quad (newer high lift technology). Fences did quite well in reducing noise radiation (max 1.4 EPNdB).

Paper by Rahul Sen: Flap-Edge Noise Empirical Model Development

Multiple peaks in flap-edge noise spectra suggest several noise generation mechanisms are involved. Tries to postulate a hypothesis by breaking fluctuating velocity down into a local and an upstream portion but does not arrive at convincing trends in the data (elliptic mirror measurements). Recommends further experimental work and some help from theoretical/numerical investigations.

Paper by Tony Blackner: Leading Edge Source Behavior

Used elliptic mirror in LSAF. Detailed parametrics on leading edge data (not as extensive as for flap edge). Scales with 51 log(M). Sealing a normally open slat gap decreases noise dramatically. Effect with angle of attack is subtle and similar to flap edge behavior. Recommends further work.

Paper by Hayes, Jaeger, Horne, Allen: DC10 Airframe Noise Study, Test Description and Preliminary Traversing Microphone Results

Used 4.7% scale model in 40x80 tunnel. By comparing to full-scale data, establishes usefulness of wind tunnel scale model testing for flap edge noise, but not for landing gear noise.

Paper by Paul Bent and Clifton Horne: Model DC10 Airframe Noise Test, Status Report

Used 4.7% scale model in 40x80 tunnel. Three Flap edge fence heights compared: 0.5, 1, and 2 times flap thickness – height equal to thickness was best (at M 0.275). Graphs seem to have used color originally – difficulty identifying curves in black and white. Uses cross-correlation to help identify source mechanisms.

Paper by Phil Yee: Validation of Sub-Scale Measurement and Extrapolation

Concludes that an acceptable estimate can be obtained of in-flight airframe noise from the wing using data from sub-scale models under low Reynolds number conditions. Uses data from Boeing models measured in LSAF. The shear layer correction is a crucial data analysis step. Whether this is also applicable to landing gear was not investigated.

Paper by Phil Yee and Rahul Sen: Boeing Technical View

Rule-of-thumb design guidelines are available: double or single inboard flap, continuous main flap (no cutouts), single outboard flap and drooped ailerons (for these two, distribute span load, reduce vorticity), seal leading edge devices. Future airframe design trends are towards simpler trailing edge high lift designs. Talks about empirical models still in the future tense.

Ref. 14 Storms, B. L., Takahashi, T. T., and Ross, J. C., "Aerodynamic Influence of a Finite-Span Flap on a Simple Wing," SAE Paper 95-1977, September 1995.

Wind tunnel test. Half-span flap creates span-wise pressure gradients on main wing element. Flow viz shows two co-rotating vortices near flap tip that merge before reaching the trailing edge. Reference Ref. 12 does not mention noise in abstract or conclusions.

Ref. 16 Kumasaka, Henry A., Martinez, Michael M., Weir, Donald S., "Definition of 1992 Technology Aircraft Noise Levels and the Methodology for Assessing Airplane Noise Impact of Component Noise Reduction Concepts," NASA CR 198298, June 1996.

The Statement of Work for Task 12 of Contract NAS1-97040 states that this reference must be used for defining received times, acoustic angles, and propagation distances when providing spectral data in this report. There is no airframe noise technology per se discussed.

Ref. 17 Sen, R., "Local Dynamics and Acoustics in a Simple 2D Model of Airfoil Lateral-Edge Noise, AIAA-96-1673, AIAA/CEAS 2nd Aeroacoustic Conference, State College, PA, 1996.

Contends that acoustical predictions can make use of existing scattering theories of a vortex in the vicinity of an edge. The source mechanism is the oscillation of the roll-up vortex at the flap tip. Even though the problem is formulated as only in two dimensions, the math is involved and hard to follow. Refers to Ref. 6, among others.

Ref. 18 Revell, J.D., Kuntz, H.L., Balena, F.J., "Prediction of Airframe Noise Radiation from Flap Side-Edges, Using Vortex Flow Data from a CFD Solution," report by Lockheed-Martin to NASA Ames, contract NAS2-20102, Task 3, September 1996.

Developed an empirical prediction scheme for flap side edge noise in a two-step process:

(1) estimate OASPL from

$$OASPL = OASPL_{\text{Reference at } 40^\circ \text{ Flap Deflection}} + (20 \text{ or } 30) * \log_{10}\left(\frac{\text{Cross - flow velocity on the flap}}{\text{Free Stream Velocity}}\right)$$

(2) estimate spectral shape from

$$SPL_{1/3} = OASPL + \Delta SPL_{1/3}$$

where $\Delta SPL_{1/3} = -\left(a + b\chi + c\chi^2\right)$, with Strouhal number $\chi = \frac{\text{Frequency} \times \text{Vortex Radius}}{\text{Free Stream Velocity}}$. Constants *a, b, c* are determined from correlations in the experimental data.

This scheme works well for large flap deflection angles (greater than 25°).

Ref. 19 Revell, J.D., et al, "Contract NAS1-20102, Task 3 Interim Report for FY1996, Airframe Noise Reduction Studies for Advanced Subsonic Technology Aircraft, L-1011 Flap Noise Reduction using Acoustically Treated Flaps", Lockheed-Martin Skunkworks, Sept., 1996.

Summary: During 1994 and 1995 Lockheed tested a 1/20th scale semi-span model of the L1011 wing to acquire farfield acoustic data and surface pressure data. The model was mounted in an anechoic free-jet facility at the Lockheed-Martin Rye Canyon Research Center, Santa Clarita, CA. Seven noise reduction (NR) configurations were tested in 1994. The farfield sound pressure level (SPL) measurement results were presented in the previous interim report. In 1995 two new NR configurations were tested and three NR configurations were retested. The NR treatment configurations consisted of porous acoustic materials mounted in various configurations on the aft element of the inboard segment of the double-slotted, trailing-edge flap system. Surface pressure transducers were used to measure the strength of the flap generated noise, via pressure fluctuation spectra. In the present interim report the nearfield pressure fluctuations are analyzed with respect to the effects of the various noise reduction treatments. In addition, flow resistance and specific acoustic impedance measurement results are presented for each material.

Summary (continued): Porous materials of several resistances (from 420 through 1070 MKS rayls) were used for the resistive elements of the flap surface modifications. Modification of the flap surface impedance appeared to have only a minor effect on the surface pressure fluctuation levels (FPL). Cut-off trailing-edges with acoustic surface treatments appeared to have some positive acoustical effects, but may generate the most detrimental aeronautical effects. Adding trailing-edge resistance may reduce some of the aeronautical degradation, but may reduce the acoustical advantages of the concept. The trailing- edge corner modification appears to have the most generally positive reduction of FPL and it is anticipated that aeronautical effects will be minimal. Nonlinear behavior of the resistive materials was applied in an advantageous fashion. These results tend to indicate that full-scale flaps may still use standard surfaces, and only a section of the trailing edge corners may need to be modified. Streamlining the under-wing cove area decreased the surface pressure fluctuations.

Notes: Using 1/20-th scale model of L-1011 wing in a 16”x35” free jet exhausting at M 0.23 into anechoic chamber (18’x18’x14’) with cutoff frequency **60** Hz [REALLY? That’s extremely low!]. Spectra of surface pressure fluctuations have a narrow peak; surface treatments are generally effective below and above this peak, but not at it. Exception is corner/cove resistive treatment; confusing dB scale on graphs. Streamlining under-surface of wing increases noise reduction. The results of these tests and the results of Fink and Bailey Research (Ref. 5) led to conclusion that the trailing edge is not the place where most of the sound is generated, and led to other noise reduction options, e.g., porosity around the side/trailing edge which permits dc flow normal to the surface diminishing the strength of the roll-up vortex and the upper-lower surface pressure differentials. The choice of the proper porous material is touchy. This work had not yet the benefit of noise source location work using the elliptic mirror or acoustical phased array; the importance of the flap tip as a noise source was not yet fully realized, therefore the porous treatment extended over the whole length of the flap.

It is not clear whether a shear layer correction was performed to account for the refraction of the very high frequency sound (Figure 12 shows a frequency range from 10 to 100 KHz) through the free jet shear layer as it propagates to the far field microphones.

Ref. 20 Sen, Rahul, “Interpretation of Acoustic Source Maps Made with an Elliptic-mirror Directional Microphone System,” AIAA 96-1712, 2nd AIAA/CEAS Aeroacoustics Conference, May 1996.

Better discrimination in transverse direction than longitudinally. Resolution and gain increase with frequency linearly. Boeing mirror focal length ~60 inches. Data can be integrated to yield subcomponent source strengths, or whole wing predictions. Provided useful insight, but its limitations need to be overcome by use of phased array methods.

Ref. 21 Storms, B. L. and Ross, J. C., "Aerodynamic Effects of Flap-Tip Treatments on an Unswept Wing," AIAA Paper 96-2372, June 1996.

The effect of six flap tip configurations on the aerodynamics of an unswept wing with a half span flap was studied experimentally. Five flap tip geometries, including three tip fences, a rounded tip, and a raised perimeter, were compared to the blunt-tipped baseline. The major conclusions:

- Significant drag reduction (20%) is achieved with a lower flap tip fence. The drag of the round-tipped flap and the blunt-tipped baseline are comparable.
- All 5 flap-tip treatments marginally increase maximum lift relative to the baseline flap with minimal effects on the lift curve at lower angles of incidence. Surface pressure measurements, however, show that the flap tip flow field is significantly altered.
- Pressure distributions and flow viz reveal multiple flap tip vortices whose relative strengths and locations are modified by the flap tip treatments. In particular, any fence extending below the flap lower surface blocks spanwise flow and produces a more diffuse vortex structure at the flap tip.

Ref. 23 Sen, R., "Vortex-Oscillation Model of Airfoil Side-Edge Noise"; AIAA Journal vol. 35, no. 3, March 1997.

This is Ref. 17 converted into a Journal paper. The author does not point out a way to use this theory in a practical prediction technique. Asked Yueping Guo whether he sees a way to prediction from this. Reply from Yueping Guo in June 2000:

> Rahul's paper, together with others under NASA AST, brought out the importance of the side edge vortex in flap-related noise. The model he used is not suitable to implement for practical noise prediction, mainly because too many assumptions and approximations are made in the model so that it is too far away from practical situations.
>
> However, the idea of relating the vortex to the noise makes physical sense. That is why we have been developing an empirical prediction code, following the same idea, but using an empirical approach. This task is also under NASA AST (Task 9). The code is basically functional now, though we have some ideas to improve it.

Ref. 24 Meadows, KR., Brooks, T.F., Humphreys, W.M., Hunter, W.W., and Gerhold, C.H., "Aeroacoustic Measurements of a Wing-Flap Configuration", AIAA Paper 97-1595, 3rd AIAA/CEAS Aeroacoustics Conference, Atlanta, Georgia, May, 1997.

Points out that noise radiation from wing tips is dealt with in prediction of radiation from helicopter rotors. Used a model (~6% of full scale) wing section with a 30 percent chord half span flap in flow speeds up to Mach 0.17 in a NASA Langley open jet wind tunnel facility (QFF); chord Reynolds numbers up to 1.7×10^6. Measurement of surface and far field pressures. Use of phased array for source localization.

Ref. 25 Hayes, J., Horne, W.C., Soderman, P., and Bent, P., "Airframe Noise Characteristics of a 4.7% DC-10 Model, AIAA-97-1594, AIAA/CEAS 3rd Aeroacoustics Conf., Atlanta, GA, May, 1997.

This Paper reports the results of the NASA Ames/McDonnell-Douglas 4.7% scale DC-10 model Airframe Noise Study conducted in the NASA Ames 40- by 80-Foot Wind Tunnel. The study successfully identified noise sources generated by the airframe using in-flow measurements with a phased array of microphones. More specifically, the study identified the noise generating airframe components (slats and flaps), source location (leading, trailing, and side edge), and source directivity. Particular attention was given to flap side edges - a region previous studies identify as a dominant noise source. The results of this study confirmed these previous results. Landing gear showed little contribution to the overall broadband spectrum. While this result contradicts field data, it was not unexpected due to the model landing gear's simple geometry and low Reynold's number. Scaled levels from the model study were comparable to a full-scale DC-10 flight test at low frequencies, with less agreement at high frequencies. Factors that may account for the discrepancy are

discussed. Finally, the noise reduction potential of various flap-tip fences were examined for the reduction of flap side-edge noise. A trend of increased noise reduction with increasing fence size was measured.

Ref. 26 Horne, W.C., Hayes, J., Ross, J.C., and Storms, B.L.: "Measurements of Unsteady Pressure Fluctuations of an Unswept, Multi-Element Airfoil", 3rd AIAA/CEAS Aeroacoustics Conference, Atlanta, Georgia, May 1997.

Abstract: This paper presents an analysis of unsteady pressure measurements in noise source regions of an unswept wing equipped with a part-span flap and with full- and part-span slats. The test was conducted in the NASA Ames 7- by 10-Foot Wind Tunnel, at Mach Numbers up to 0.22 and Reynolds Numbers up to 3.7×10^6 based on wing chord. Signal processing methods included autospectra, coherence between adjacent sensors, and cross-correlation between the time derivative of surface pressure sensors and one of the microphones of a phased array which was mounted in the test section wall. The spectra of signals from sensors near the flap side-edge, which were similar in shape to preliminary acoustic spectra obtained from the phased microphone array, generally decayed monotonically with frequency. Signals from sensors located in the slat region also exhibited similar features in comparison to preliminary phased microphone array spectra, including high frequency noise associated with a low slat loading condition. Modifications to the flap-edge and slats which resulted in reduced radiated noise levels generally had the effect of reducing the autospectral levels of individual sensors as well as reducing the coherence between adjacent sensors in the noise source regions.

Significant attenuations due to notches cut into slat.

Uses cross-correlations between derivative of surface pressure and far field sound. Interpretation of those data seems incomplete.

Ref. 27 Guo Y.: "On sound generation by unsteady flow separation at airfoil sharp edges: AIAA Paper 97-1697, 3rd AIAA/CEAS Aeroacoustics Conference, Atlanta, Georgia, May, 1997.

Copy of the abstract: This paper studies sound generation by unsteady flow separation at the sharp trailing edge of an airfoil which is subject to the incidence of an incoming vortex. The flow separation is modeled by unsteady vorticity production at the trailing edge, in the form of a vortex sheet originating from the sharp edge, which rolls up into discrete vortex cores. Fully nonlinear motions are allowed for the vortex cores, as well as strength fluctuations with time. The latter models the unsteady injection of vorticity into the flow by the flow separation process. The model thus addresses a nonlinear generation mechanism for airfoil trailing edge noise that captures both the contribution due to unsteady vortex motions and that due to vorticity fluctuations.

Partial quote from the conclusions: " … for applications of airframe noise, trailing edges are known to be not a dominant noise source for present aircraft design. Instead, the major noise sources of airframe noise are the leading edge slat, the trailing edge flap, and the landing gear. However, there are at least two reasons that make the study of trailing edge mechanisms useful. One is that the non-linear mechanisms discussed here also apply to edges other than trailing edges. Flow separation also occurs at the slat cusp and at the side edge corners of the trailing edge flap. …trailing edge noise … may set a noise floor that affects noise reduction treatments for future aircraft."

Ref. 28 Mosher, M., Watts, M., Jovic, S., and Jaeger, S.: "Calibration of Microphone Arrays for Phased Array Processing", 3rd AIAA/CEAS Aeroacoustics Conference, Atlanta, Georgia, May, 1997, AIAA-97-1678-CP.

Abstract: An array of microphones was calibrated so that it could be used to make accurate measurements of point sources. This paper describes the analysis and procedures that differ from calibrating a single microphone for accurate measurements. Calibration involves the phase of all microphones and electronic instrumentation and the amplitude and directivity response of the entire

array. Procedures include measuring the phase response of the instrumentation, phase checking with a point source, calibrating a source in an anechoic chamber and using the calibration source to calibrate the array for amplitude and for directivity. Results show good phase fidelity, a frequency dependent amplitude deviation from a simple free-field microphone and fairly smooth directivity characteristics that can be corrected with a non-linear neural net model.

Ref. 29 Sen, R.: "A Study of Unsteady Fields Near Leading-edge Slats," AIAA 97-1696, 3rd AIAA/CEAS Aeroacoustics Conference, Atlanta, Georgia, May, 1997.

Copy of the abstract: This paper outlines an idealized two-dimensional mode/ for studying unsteady near-fields induced in the vicinity of leading-edge slats. The dynamic elements of the model consist of a slat separation bubble, modeled as a free vortex, bound vorticity distributions on the slat and a nearby wing, and wakes shed off each airfoil. The problem is formulated as one of thin-airfoil theory: both wing and slat are modeled as flat vortex sheets, and wakes are modeled as flat surfaces of discontinuity on which vortex elements convect with the mean flow. Dynamics is governed by a system of coupled integral-differential equations. We outline a numerical approach in which the bound vorticity distributions are represented by series of orthogonal polynomials with time-varying coefficients. It is shown that dynamic timescales are dependent on the strength and equilibrium position of the separation bubble. These in turn are highly sensitive to slat camber. The slat trailing -edge wake is found to have a strong effect on the dynamics. We also discuss the possibility of enforcing a leading -edge Kutta condition on the slat, in addition to the usual trailing-edge one. It is shown that this requires a weighted average upwash velocity on the slat to vanish, a condition that is unlikely to hold in the dynamic situation.

This paper attempts to initiate from the analytical side an effort to create a slat noise prediction capability. It creates a model of separation bubble dynamics with hopes to use it in future noise prediction schemes.

Ref. 30 Sen, R., Blackner, A., Yee, P., and Stoker, R., "Airframe Noise Generation and Radiation", NASA Contract NAS1-20090, Task 2 Informal Report, Boeing Commercial Airplane Company, Jan. 1997.

Report on 1995/1996 airframe noise activities at Boeing under NASA contract. Discussion broken down into source imaging, theoretical analysis, and empirical modeling and data analysis. Concentrated review on empirical modeling. Contains a useful summarizing statement on flap side-edge noise: " … a steady vortex nominally in a position of stable equilibrium in a potential edge flow, is perturbed by a small vortex simulating turbulence. The spectrum of the resulting motion is dominated by the natural frequency and harmonics associated with oscillation of the base vortex … incoming turbulence spectra are filtered through local vortex oscillation dynamics, the vortex selectively amplifying portions of incoming spectra and in the process setting up a multi-peaked near field." Using theoretical insight, defines non-dimensional quantities:

$Str = \frac{fh^2}{\Gamma_E}$, $\Pi_1 = \frac{hV_{CROSS}}{\Gamma_E}$, $\Pi_2 = \frac{c_F}{h}$, where f=frequency, Γ_E =edge vortex circulation, h=flap thickness, V_{CROSS} =cross-flow velocity near edge, c_F =flap chord. Attempts to find relationships among these quantities in the measured data were only partially successful.

Divides airframe noise sources into leading edge, trailing edge, flap edge, landing gear, and a residual. Develops a calculator for assessing the overall impact of reducing one particular subcomponent at a time. The calculator exists as a group of curves for each airplane considered. For 757 and 737, flap edge noise is most sensitive, and landing gear noise the least. For 777, leading edge is most sensitive, and flap edge the least.

Develops an empirical prediction method by collapsing LSAF elliptical mirror microphone spectral data. Uses reference spectra for each subcomponent and derives scaling laws for geometries and

conditions different from the reference. Agreement with full-scale flight test data is ±2 dB for 737 and 757, and ±3 dB for 777.

777-airframe data analysis:

- Landing gear is a significant noise source
- Gear noise is a function of flap deflection
- The effect of flap deflection was limited by the leading edge configuration schedule
- A 50 Log velocity correlation is an appropriate airframe sound pressure level correction for the effect of air speed.

Concluding remarks mention that valuable engineering experience was gained in the early 90's regarding practical noise control, but no actual applications are mentioned.

Identifies two needs:

- understand basic near field and scattering processes, and their main parametric dependencies
- convey this understanding through relatively condensed packages that fit design cycle time scales.

Future experimental research will require higher resolution in source localization by phased array. this may result in identification of additional noise sources to be included in prediction schemes.

Landing gear noise should be studied through full-scale testing.

Ref. 31 Anon., "NASA AST Program, Noise Reduction Technology, Proceedings of Airframe Noise Workshop," Long Beach CA, collection of viewgraphs, June 1997.

Paper by Storms, Bruce, et al., "Analysis of Flap-Tip Noise Measurements from the Ames 7x10," April 1996:

Raked flap tips can bring about noise reductions if trailing edge is wider than leading edge

Porous flap tips can be quite effective (~ 6 dB), lower tip fence can have ~3 dB benefit

Ffowcs-Williams & Hall theory predicts correct trends ($p^2 \propto M^5 \cos^3 \beta$)

Paper by Storms, Bruce, et al., "Analysis of Slat Noise Measurements in the Ames 7x10," April 1996:

Slat tip fence is very effective in reducing noise

Slat trailing edge serrations can show moderate noise benefit, but large benefit at mid frequencies where there is a 16 dB hump in the untreated slat case

Very nice benefit also when reducing slat gap (or get rid of it completely), but sealed gap not always practical.

Paper by Horne, Hayes, Ross and Storms, "Unsteady Pressure Measurements in Flap and Slat Noise Source Regions," June 11, 1997

Serrated slat trailing edge results in much lower surface pressure fluctuations

Paper by Brooks, Thomas F., "QFF Flap Edge noise Test Results," June 1997

not enough text to tell a story; seems to indicate several moderately effective noise reduction configurations.

Paper by Radeztsky, Ronald, "Experimental Measurements of the Flap-Edge Flowfield," June 1997

Essential features of the vortex system documented: two-vortex system, they merge and break down

Paper by Yueping Guo, "Properties of Surface Pressure Fluctuations on DC10 Flap"

Distinctive spectral humps at large flap angles,
Source of humps possible in aft chord region,
Flow in aft half chord region highly coherent,
Spectra scale well on Strouhal number,
Reynolds number-dependent frequency scaling law

Paper by Joshi, Mahendra, and Guo, Yueping, “Scaling and Reynolds Number Effects of Airframe Noise,” June 1997

Reynolds number effects are significant for models less than about 10%

Reynolds number-dependent frequency scaling should be used in extrapolation

Frequency-dependent amplitude correction should be applied

Hardin, J.C., “Towards a Comprehensive Analysis of Approach Noise Sources”

Sound intensity scales with D^6V^5 where D is a characteristic dimension and V is the free stream velocity.

Landing configured aircraft should be considered as a total system due to component interaction effects

Areas of high surface pressure [does he mean ‘fluctuations’ here?] are footprints of strong acoustic sources

Separated flows and jet/flap interaction regions are potentially important sources

Paper by Singer, Bart A., and Khorrami, Mehdi, R., “Analysis of Steady Reynolds Averaged Navier-Stokes (RANS) Calculations for Flap Side-Edge Flowfield”

Calculations replicate important flow features

Paper by Khorrami, Singer, and Choudhari, “Vortex and Cylindrical-Vortex-Sheet Instability Models”

Vortex axis is parallel to the flap edge in the chord-wise direction. Not enough text to be a useful printed-paper. Summary says this:

Successfully extracted important mean flow features for modeling purpose

Vortex Model: supports broadband unsteadiness; large growth rates

Cylindrical vortex sheet model: supports unsteadiness; captures important measured trends

Paper by Street, C.L., “DNS of Flap-Edge Flowfield Instabilities,” June 1997

(DNS=direct numerical simulation) No turbulence model – provides better resolution and a more representative flow field. Uses incompressible Navier-Stokes.

Starting from the potential flow around edge, flowfield develops in time with features strikingly similar to actual flap-edge flowfield

At moderate Reynolds number, these simulations spontaneously develop unsteady disturbances that evolve faster than the mean state

Instabilities result in significant fluctuating pressure on surface with concentrations at flap corners

Paper by Takallu, M.A., “Reynolds-Averaged Navier-Stokes Simulations of Two Partial-Span Flapped Wing Experiments”

For risk reduction of Langley QFF experiment investigating flap edge noise. Excellent comparisons with QFF and 7x10 data.

Paper by Christopher Tam, “Numerical Simulation of Flap Side Edge Noise”

Was not completed by the time of the presentation. The results should be useful to the development of a semi-empirical design model of flap edge noise.

Paper by Rahul Sen, "Plans for an Interim Flap-Edge Prediction Tool"

Presents initial ideas, no conclusions.

Paper by Yueping Guo, "A Model for Slat Noise Generation"

"For advanced high lift system, slat is main noise source for mid to high frequencies"

Model uses unsteady panel method and Brown & Michael equation for near field; Ffowcs-Williams & Hall equation or matched asymptotic expansion for far field.

Paper by Rahul Sen, "Slat Near Fields and Related Modeling Issues"

Reviews various options for building a slat noise model. Which phenomena need be included, what can be neglected? Says that simplified models will not do the trick because they simply cannot address important details.

Ref. 32 Revell, J.D., Kuntz, H.L., Balena, F., Horne, W.C., Storms, B.L., and Dougherty, R.: Trailing Edge Flap Noise Reduction by Porous Acoustic Treatment", 3rd AIAA/CEAS Aeroacoustics Conference, Atlanta, Georgia, May, 1997, AIAA-97-1646-CP.

Airframe noise generated by commercial aircraft at landing approach is a barrier to the achievement of desired noise reduction goals for the next generation of aircraft. The trailing-edge flap system is a major contributor. Recent research has identified the side-edge region of trailing-edge flaps as the dominant contributor to flap noise. Noise is generated when the side-edge vortex rolls up around the flap and interacts with the flap. Herein, we describe the results of using a porous acoustic treatment at the flap side-edge. Introduction of the porous treatment significantly reduced the radiated noise. Experiments were performed in the NASA-Ames 7- by 10-Foot wind tunnel. Since this wind tunnel has hard walls, special signal processing techniques were used to analyze the data. The data were acquired with a unique acoustic array mounted in the wind tunnel sidewalls. Acoustic results from these analyses are presented here.

Points out that most previous researchers concentrated on the trailing edge and missed the much stronger side-edge noise source.

Appropriate porous treatments in the vicinity of flap side-edges can significantly reduce the flap side-edge contribution to airframe noise at landing approach. The choice of material is critical in terms of its porosity and flow resistance.

Ref. 33 Sen, R., et al, "Airframe Noise Baseline Scale Effects/Analytical and Empirical Models-Progress Toward a Second Generation Flap-Edge Noise Model," NASA Contract NAS1-90740, Boeing Commercial Airplane Company, December 1997.

3-element approach:

- time-averaged computation of side-edge flow field, or an estimate of time-averaged flow features
- unsteady disturbance calculation based on the time-averaged structure
- acoustic radiation module for computing the unsteady far field

Excellent summary of previous flap side-edge work.

Proposes two prediction methods of different degrees of sophistication and faithfulness:

- Method 1: Simpler – starts from existing panel-type mean-flow computations. Unsteady: use instability theory and vortex oscillation. Acoustic radiation: matched asymptotic expansions, simplified use of Ffowcs-Williams-Hawkings (FWH) equation.
- Method 2: More compute-intensive and incorporating fewer empirical pieces. Unsteady: possibly use direct numerical simulation. Acoustic radiation: sophisticated numerical use of FWH.

The research for Method 1 is pretty much completed; it is a matter of implementing it into tools. Method 2 needs a lot more research work.

Ref. 34 Shivashankara, B., and Blackner, A.: "Installed Jet Noise", AIAA-97-1601, 3rd AIAA/CEAS Aeroacoustics Conference, Atlanta, Georgia, May 1997.

Abstract: An experimental investigation of jet noise changes due to installation on an airplane was conducted. A high bypass ratio jet exhaust model was tested in the Boeing Low Speed Aeroacoustic Facility wind tunnel in combination with the model of a large 4-engine airplane. Most prior jet noise tests in the literature have been either jets by themselves or jets next to airplane models under static conditions. The test reported in this paper more fully simulated both the airplane installation and the ambient flow. The jet was tested by itself and installed in either the inboard engine location or the outboard engine location. Various flap settings were tested. Noise sources were mapped using the elliptic mirror microphone. Far field noise data was acquired at several azimuthal angles. The installed jet noise was significantly higher than that of the isolated jet. Installation effects were seen to depend on ambient flow, flap setting and engine location. Detailed noise source maps and noise levels extrapolated to full scale conditions are presented in this paper.

Conclusions: The presence of the airplane increases jet noise. Noise increases monotonically with increasing flap deflection. Secondary-ambient and mixed-ambient are the dominant jet noise components. Both jet noise components increase due to installation effects. Installation effects are somewhat smaller for the outboard location. Noise is not axi-symmetric for high bypass ratio jets (with pylon and bifurcation) and installed jets.

Ref. 35 Khorrami, M.R., Singer, B.A, Takallu, M.A., "Analysis of Flap Side-Edge Flowfield for Identification and Modeling of Possible Noise Sources," SAE Paper 971917, Traverse City MI, May 1997.

The Reynolds Averaged Navier-Stokes (RANS) equations were solved for a wing with a half-span flap to simulate experiments performed in the NASA Ames 7x10 foot wind tunnel. The steady-state solutions were obtained using the CFL3D flow solver with various turbulence models and grids. Interrogation of the RANS computations revealed pertinent features of the flap side-edge flow field. The extracted flow field features were used to guide the development of two possible noise-source models, namely, 1) a vortex-instability model and 2) a cylindrical vortex-sheet model. Both models predict flow unsteadiness (possible noise sources) in the relevant frequency ranges.

Ref. 36 Street, C.L.: "Numerical Simulation of Fluctuations Leading to Noise in a Flap-Edge Flow field," AIAA 98-0628, 36th Aerospace Sciences Meeting and Exhibit, Reno, Nevada, January, 1998.

In this paper we develop an approximate computational framework for simulation of the fluctuating flow field associated with the complex vortex system seen at the side edge of a flap in a multi-element high-lift airfoil system. The eventual goal of these simulations is to provide an estimate of the spectral content of these fluctuations, in order that the spectrum of the noise generated by such flow fields may be estimated. Results from simulations utilizing this computational framework are shown.

Ref. 37 Radeztsky, R.H., Singer, B.A., and Khorrami, M.R.: "Detailed measurements of a flap side-edge flow field," AIAA Paper 98-0700, 36th Aerospace Sciences Meeting and Exhibit, Reno, Nevada, January, 1998.

Detailed flow measurements were performed with a five-hole probe in the flap side-edge region of a wing with a half-span flap. The experiments were conducted in the NASA-Langley Quiet Flow Facility as a part of an extensive experimental and computational investigation of airframe-related noise sources. Basic flow properties were verified using static pressure taps, pressure-sensitive paint, and oil-flow visualization. Detailed five-hole probe surveys were conducted in a set of planes at ten streamwise stations for flap deflections of 29 and 39 degrees. These measurements show

the development of a two-vortex system at the flap side edge. The vortex path and strength are determined, and the process of vortex merging is documented in detail in the mid-chord region. At the higher flap deflection angle, vortex bursting is observed, which may be a factor in the observed higher noise levels for this condition. Results are compared with Reynolds-averaged Navier-Stokes calculations of a similar configuration (AIAA Paper 98-0768). These measurements and calculations form the basis for instability modeling and unsteady calculations that will ultimately lead to an understanding of flap side-edge noise sources.

Ref. 38 Humphreys, W.M., Brooks, T.F., Hunter, W.W., and Meadows, K.R: "Design and Use of Microphone Directional Arrays for Aeroacoustic Measurements", AIAA Paper 98-0471, 36th Aerospace Sciences Meeting and Exhibit, Reno, Nevada, January, 1998.

An overview of the development of two microphone directional arrays for aeroacoustic testing is presented. These arrays were specifically developed to measure airframe noise in the NASA Langley Quiet Flow Facility. A large aperture directional array using 35 flush-mounted microphones was constructed to obtain high resolution noise localization maps around airframe models. This array possesses a maximum diagonal aperture size of 34 inches. A unique logarithmic spiral layout design was chosen for the targeted frequency range of 2-30 kHz. Complementing the large array is a small aperture directional array, constructed to obtain spectra and directivity information from regions on the model. This array, possessing 33 microphones with a maximum diagonal aperture size of 7.76 inches, is easily moved about the model in elevation and azimuth. Custom microphone shading algorithms have been developed to provide a frequency- and position-invariant sensing area from 10-40 kHz with an overall targeted frequency range for the array of 5-60 kHz. Both arrays are employed in acoustic measurements of a 6 percent of full-scale airframe model consisting of a main element NACA 63_2-215 wing section with a 30 percent chord half-span flap. Representative data obtained from these measurements is presented, along with details of the array calibration and data post-processing procedures.

Ref. 39 Storms, B.L., et al., "An Aerodynamic Study of an Unswept Wing with a Three-Dimensional High-lift System," NASA/TM-1998-112222, February 1998.

Abstract: Experimental and computational results are presented for the aerodynamics and acoustics of an unswept wing with a half-span flap and both a full- and three-quarter span slat. The wing spanned the wind tunnel test section with no exposed wing tip. Concurrent aerodynamic and acoustic measurements were obtained for high-lift riggings representative of landing-approach configurations. Phased microphone array measurements identified two noise sources at the mid-span flap tip that were approximately equal in intensity at 7 kHz. The noise source at the flap forward side edge is dominant at higher frequencies, while the source from the flap aft upper surface is dominant at lower frequencies. The resulting overall spectra generally decay monotonically with a peak frequency less than 2 kHz, since no peak was evident in the measurement range from 2-38 kHz. Both flap lift and flap-tip noise increase with increasing flap deflection. Raking the flap tip relative to the freestream flow yielded significant changes in the flaptip vortex formation and resulting noise level. A flap-tip noise model based on flap-tip velocities and flow angles accurately predicted the change in noise with flap deflection and rake-angle variation. A flap-tip fence and porous flap tip both yielded significant overall noise reduction of 3 dB and 4-8 dB, respectively. Two noise sources were identified for the slat. Slat-gap noise was dominant for a low slat loading while slat-tip noise was significant at a high slat loading. The slat-tip flow field is similar to that of the flap tip, and a slat-tip fence resulted in significant noise reduction of 3-6 dB. Slatgap noise is apparently associated with a feedback mechanism between the recirculating flow in the slat cove and the high-velocity flow through the slat gap. Serration of the slat trailing edge yielded a peak noise reduction of 18 dB while serration of the slat cusp was significantly less effective. Unsteady-pressure and hotwire measurements revealed important details of both the flap and slat flow structures. Component interactions were found to be small (less than 2 dB) between the flap and slat noise sources.

Ref. 40 Khorrami, M.R., and Singer, B.A.: "Stability analysis for noise-source modeling of a part span flap," AIAA Paper 98-2225, June 1998.

Abstract: The relevant and important flow features of the local mean flow field in the vicinity of a flap side edge are extracted from an extensive computational and experimental database. Based on the local flow features, possible mechanisms for flow-induced noise sources that are responsible for sound generation at flap side edges are conjectured. Relatively simple flow models for the dominant noise sources are proposed and developed. The models are based on the most amplified instability modes of the local shear flow. Stability analysis of the modeled flow field provides an estimate of the frequencies associated with the local flow unsteadiness. Computed frequencies show the proper trend and are in good agreement with NASA Langley's acoustic microphone array and unsteady surface-pressure measurements.

Ref. 41 Macaraeg, M.G., "Fundamental Investigation of Airframe Noise," AIAA-98-2224, 4th AIAA/CEAS Aeroacoustics Conf., Toulouse, FR, June 1998.

Abstract: An extensive numerical and experimental study of noise mechanisms associated with a subsonic high-lift system has been performed at NASA Langley Research Center (LaRC). Investigations involving both steady and unsteady computations and experiments on a small scale, part-span flap model are presented. Both surface (steady and unsteady pressure measurements, hot films, oil flows, pressure sensitive paint) and off-surface (5 hole-probe, particle-imaged velocimetry, laser velocimetry, laser light sheet measurements) were taken in. the LaRC Quiet Flow Facility (QFF) and several hard-wall tunnels up to flight Reynolds number. Successful microphone array measurements were also taken providing both acoustic source maps on the model, and quantitative spectra. Critical directivity measurements were obtained in the QFF. NASA Langley unstructured and structured Reynolds Averaged Navier-Stokes codes modeled the flap geometries; excellent comparisons with surface off-surface experimental data were obtained. Subsequently, these mean-flow calculations were utilized in both linear stability and direct numerical simulations of the flap-edge flow field to calculate unsteady surface pressures and far field acoustic spectra. Accurate calculations were critical in obtaining not only noise source characteristics but shear layer correction data as well. Techniques utilized in these investigations as well as brief overviews of results will be given.

Good overview of NASA plans and strategy.

Ref. 42 Streett, C.L.: "Numerical Simulation of a Flap-Edge Flowfield," AIAA 98-2226, 4th AIAA/CEAS Aeroacoustics Conf., Toulouse, FR, June 1998.

Abstract: In this paper we develop an approximate computational framework for simulation of the fluctuating flowfield associated with the complex vortex system seen at the side edge of a flap in a multi-element high lift airfoil system. The eventual goal of these simulations is to provide an estimate of the spectral content of these fluctuations in order that the spectrum of the noise generated by such flowfields may be estimated. Results from simulations utilizing this computational framework are shown.

Uses three aproximations: Lighthill acoustic analogy, incompressible NS equations, series of 2D simulations instead of full 3D.

Conclusions: Demonstrated in this paper is a computational framework to predict the spectral content of fluctuations in the flow field near the side edge of a flap in a multi-element high-lift system. The framework is heuristically justified by comparison with high-resolution steady RANS solutions of the complex multi-vortex system; these RANS solutions are then utilized as mean flow fields within which unsteady disturbances are simulated. Simulations show two basic families of disturbance modes: the first is associated with instability of the cylindrical shear layer, which overlays the side edge separation in upstream stations. The second family of disturbance modes is associated with instabilities of the vortex and its jet-like core flow, and possesses significant oscillatory structure in the streamwise direction. When the results from the simulations are fed into a Lighthill acoustic

analogy prediction of the generated sound, preliminary results indicate surprisingly good agreement with experiment.

Ref. 43 Guo, Y., Hardy, B., Bent, P., Yamamoto, K., Joshi, M., "Noise Characteristics of the DC-10 Aircraft High Lift System," NASA Contractor Report by Boeing, Report No. CRAD-9310-TR-4893, Sept. 1998.

Abstract: This report presents the analysis of data from an airframe noise test conducted in the NASA Ames 40 feet by 80 feet wind tunnel, using a 4.7% DC-10 aircraft model. Discussions are given on both far field free microphone data and measurements from a phased microphone array. Major trends derived from the data are discussed, including far field frequency characteristics, flow Mach number dependence of acoustic radiation, effects of flap and/or slat deployment, far field directivity and correlations between noise and static loading on the wing. Data from the phased microphone array are used to identify locations of major noise sources and to reveal dependencies of various noise sources on flow conditions and high lift system configurations. The effects of flap side edge fences on far field noise are also discussed, which shows a reduction of a few dB in flap-related noise. Scalability of data from small-scale model test to full-scale flight is studied. It is shown that conventional extrapolation procedures, which scale down frequencies and scale up amplitudes of the noise spectra by the ratio of the model dimension to that of full scale aircraft, may cause significant error, especially for models with dimensions less than about 10% of full scale size. For the 4.7% DC-10 model, it is shown that the conventional extrapolation from small-scale data to full scale significantly underestimates the noise levels of full-scale flight tests; the discrepancies are as much as 8 dB in the important mid and high frequency region. These discrepancies are postulated as the manifestation of the flow Reynolds number effects. Improvement for the extrapolation that takes account of the Reynolds number effects are proposed and it is shown that comparisons between the extrapolated small-scale data and full-scale flyover data are greatly improved when the Reynolds number dependent extrapolation is used.

Ref. 44 Guo, Y., Bent, P., Yamamoto, K., Joshi, M., "Surface Pressure Fluctuations on DC-10 High Lift System and Their Correlation with Far Field Noise," NASA Contractor Report by Boeing, Report No. CRAD-9310-TR-4872, September 1998.

Abstract: This report discusses unsteady surface pressures on the high lift system of a 4.7% DC-10 aircraft model, measured in the NASA Ames 40-feet by 80-feet wind tunnel. Results of the data analysis, for various slat/wing/flap configurations and under various flow conditions, are discussed in detail to identify major trends relevant to airframe noise generation. Spectral analysis is used to derive cross correlation/coherence, both among unsteady surface pressures and between far field noise and near field fluctuations, which are then used to reveal the most coherent motions in the near field and to identify potential sources of airframe noise. Dominant flow features in the flap side edge region, such as the formation of a double-vortex structure, are shown to manifest themselves by their imprints in the unsteady surface pressures as a series of spectral humps. The spectral humps are shown to be well correlated to the radiated noise, indicating the existence of a major noise source in the flap side edge region. The peak frequencies of the humps are scalable on the Strouhal number based on the flow velocity and a length scale that depends on the local flow Reynolds number and characterizes the coherence length of the vertical patches. This Reynolds number dependent scaling is shown to have significant implications in the extrapolation of data from small-scale model test to full-scale applications, especially for those with dimensions smaller than about 10 percent of the full-scale model. The effects of flap side edge fences on surface pressures are also discussed. The application of the fences effectively increases the thickness of the flap so that the double-vortex structure has more time to evolve. As a result, the coherence time scale is increased and the dominant frequency is decreased, which is shown to be the case from the data. An immediate consequences of this is a downward shift in the characteristic frequency of the flow features, and hence, a downward shift in the noise spectra. Since airframe noise typically has a spectrum with a negative slope in almost the entire mid to high frequency domain, a downward shift of the spectrum in frequency results in lower levels for fixed frequency bands. For aircraft noise

certification where the noise level is calculated for fixed frequency bands, this clearly appears as a reduction in noise levels.

Ref. 45 Guo, Y., Stoker, R., Hardy, B., Bent, P., Joshi, M., "DC-10/MD-11 Acoustic Test in NASA Ames 12-ft Pressurized Wind Tunnel," NASA Contractor Report by Boeing, Report No. CRAD-9310-TR-4894, September 1998.

Abstract: This report presents the results of an acoustic test in the NASA Ames 12 feet pressurized wind tunnel, using a 4.7% semispan model of the DC-10/MD-11 aircraft. The test is tasked with two main objectives; one is to study the feasibility of using untreated pressure wind tunnels for acoustic testing and the other is to examine the Reynolds number effects on airframe noise sources. This effort is the first, in a series of similar tests under the NASA Advanced Subsonic Technology (AST) Noise Reduction Program, to address these two issues, and has been very successful in meeting both objectives. By using a phased microphone array for acoustic measurements, it is shown that airframe noise sources can be located quite clearly, not only at atmospheric pressures as has previously been demonstrated, but also in pressurized environments with no acoustic treatments. The phased microphone array measurements identify major source locations, as well as provide far field noise spectra through integration of the source strengths in the beam-forming domain. The integrated spectra are compared with free field microphone data, which shows good agreements. Reynolds number effects are discussed by analyzing the array data at different tunnel pressures. It is shown that noise levels increase with flow Reynolds number at high frequencies but do not seem to be significantly affected by it at low frequencies. The variations of the noise levels are found to be most noticeable at small Reynolds numbers, indicating a possible asymptotic behavior, in which case, the effects of flow Reynolds number very quickly become negligible as it increases above a certain value.

Ref. 46 Guo, Y., "A semi-analytical/semi-empirical model for flap side edge noise prediction", NASA Contract NAS1-20103, Task 2, Report CRAD-9310-TR-3765, The Boeing Company, Sept. 1998.

Abstract: This report documents the development of a semi-analytical/semi-empirical model for noise generation by flow separation in the flap side edge region of aircraft high lift systems. The model is based on the concept that complex flow features such as shear layer instabilities that cause flow separation in the flap side edge region generates noise by producing unsteady vorticity fluctuations. These vorticity fluctuations are modeled here by unsteady nonlinear motions of vortex sheets, representing thin shear layers in real flows, and by dynamic vortex shedding from the sharp corners, modeling vorticity production by flow separation. The model calculates the near field flow fluctuations, including unsteady pressures on the flap surfaces, which are then used to compute the far field radiation. Both the unsteady surface pressures on the flap and the far field predictions are compared with available test data, which shows very good agreement not only in the dominant trends, such as frequency characteristics, flow Mach number dependence and far field directivity, but also in the absolute amplitudes of the noise levels. The model is coupled to the aerodynamic properties of the high lift system because the inputs that it requires include aerodynamic parameters such as the static chordwise loading distribution on the flap. This can be readily derived from conventional aerodynamic design computations, which makes the model a potential candidate suitable for engineering applications. For instance, it can be developed into a tool for assessing the acoustic impact of aerodynamic design changes in aircraft high lift system design.

Ref. 47 Sen, R.: "Theoretical Investigation of Slat Noise", NASA Contract NAS1-97040, Task 2, Boeing Commercial Airplane Company, December 1998.

Models the overall dynamics of the local flow near the slat: slat separation bubble interacting with flow around the slat, usually at a negative angle of attack. Slat source appears as a baffled edge-source with the leading edge of the main wing providing the baffle. Flow and acoustic phenomena are decoupled from each other as done in other theoretical work.

Ref. 48 Anon., "NASA AST Program, 3rd Airframe Noise Workshop." collection of view-graphs, Boeing-Seattle November 1998.

Paper by Michele G. Macaraeg, "Achieving Program Milestones: The NASA/Industry Partnership"

Flap Noise Final Engineering Tool:

- Compute relevant aerodynamic parameters using inexpensive method (panel, potential, low-resolution RANS)
- Utilize established parameterization to estimate details of noise-producing local features from aero parameters
- Compute parameters of model spectral features using established correlations / weakly-nonlinear integral stability theory
  - center frequency, bandwidth, relative amplitude
- Apply overall noise level calibration from data

Paper by Thomas F. Brooks, "Coherence over Directivity Field – Array Size Effects"

Re flap edge noise

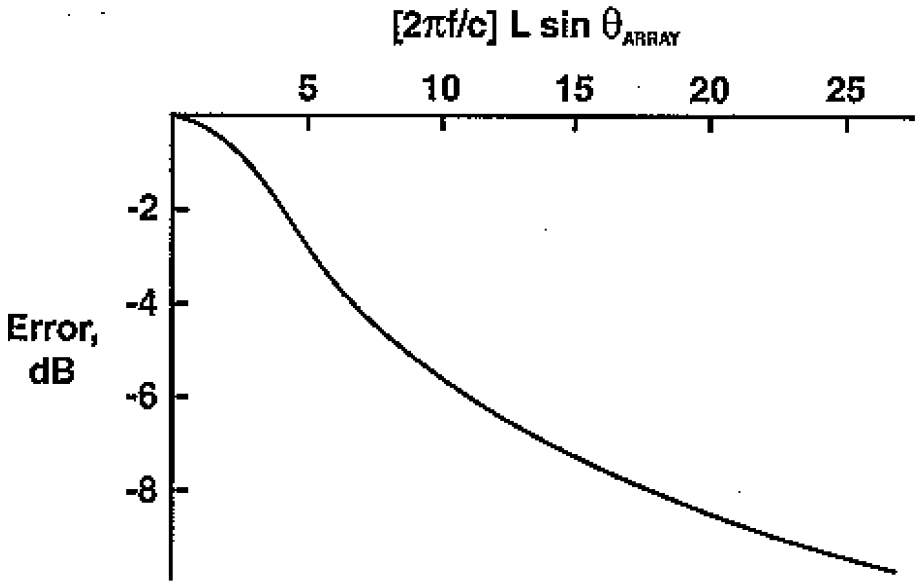

where f=frequency, c=speed of sound, L = size of object to be resolved, θ_{ARRAY}=aperture of phased array as seen from object

Paper by Dale Ashby and Steve Jaeger, "Aeroacoustic Research Model (STAR) Model"

26% scale semispan model of Boeing 777 in Ames 40x80 tunnel. Produced a lot of good data. Shows list of desired enhancements.

Paper by Yueping Guo and David H. Reed, "Flap Noise Modeling"

Condensation of Ref. 46.

Paper by Julie Hayes and Paul Soderman, "Reynolds Number Effects Measured on a 4.7% Scale DC-10/MD-11 Model in the 12' PWT"

Reynolds number effect on acoustics and aerodynamics:

- Higher lift coefficient at higher Re
- Possible asymptotic boundary layer thinning
- Tones and broadband noise are affected

- Tones become tighter and louder
- Broadband noise increases 2 to 4 dB [more details desirable here]
- Strouhal dimension is of order of boundary layer thickness

Flap tip noise related to flap loading:

- Increased flap loading causes increased flap tip noise
- Changes in wing loading alone do not affect flap tip noise amplitude
- Flap tip tones occur at large flap deflections

Paper by Lockard, Streett, and Macaraeg, “Experimentally observed variations in flap-edge noise with configuration and operating condition changes”:

- Most flap noise scales near V^5
- Most features scale with Strouhal number
- Small influence of Reynolds number above 3.6E6
- 3D effect important

Paper by Choudhari, Khorrami, Berkman, Sadowski, “Analysis of Flap-Side-Edge Flow Field for Energy Efficient Transport Model in LTPT”

- Steady RANS CFD in close agreement with measured LTPT data
- Characteristics of FSE vortex system are configuration dependent
- FSE flow field in LTPT more complex than 7x10/QFF model: multiple, non-axisymmetric vortices

Paper by C.L. Street, “Physics of Flap-Edge Noise: Source and Reduction”

Results from swept wing test: Noise from outboard flap side edge increases far faster with flap angle than inboard, most likely due to increase in vortex strength.

Ad hoc noise reduction schemes are all but useless to the industrial designer. Noise reduction schemes must be based on physics insight.

Trailing edge serrations remove tone at 30 deg deflection, Mach 0.2

Telephone conversation between C.L. Streett and Robert Rackl on 2000/9/28 - major comment: Guo’s method glosses over some important details, gives apparently right results for wrong reasons, and looses ‘component 3’ completely which is the tone in the case when the coalesced vortex stays attached to the flap surface. The details of concern here are that computational and experimental work show that component 1 is very strong, being generated from the coalesced vortex whereas Guo’s method works only up to the point where the two vortex systems are about to (but not yet) coalesced. Then Guo applies a frequency scaling with Reynolds number that is not appropriate because it does not reach a reasonable asymptotic limit.

Paper by Tom Dong and Christopher Tam, “Numerical Simulations of Airframe Noise – Flap Side Edge Noise”

Linear Euler computations include compressibility.

Computed results indicate that instability waves exist in shear layers from lower and upper surfaces of the flap as well as in the wake of the main element. These instability waves interact with flap surface and with each other forming feedback mechanisms. Major noise sources are: instability/flap surface interaction, feedback among instabilities, and scattering of boundary layer disturbance at corners of flap side edge. Feedback is dominant noise source for downward noise radiation. High frequency (f~1 KHz) instability waves from the lower surface are the dominant sources in regions near leading edge, while low frequency (f=100~200) instability waves from the upper surface are the dominant ones in regions near mid-chord; this is as observed in experiments. The overall radiated noise is expected to be broadband due to its sources’ strong dependence on the streamwise location.

Paper by Thomas F. Brooks, “Flap Edge Noise Directivity: Flat and Round Edges”

QFF Test. Unfortunately, lack of color in reproduced slides prevents useful examination of data.

Paper by Rob Stoker, “Full-scale Landing Gear Noise Test Results”

777 gear in LSAF.

2-3 dB reduction by removing small pieces

6-wheel truck shows more noise than 2-wheel truck only at frequencies below 1 KHz.

See also Ref. 59.

Paper by Singer, Lockard, Brentner, Atkins, “Computational Acoustic Analysis of Slat Trailing Edge”

Shows very favorable comparison between predicted and measured slat noise spectra. Noise increases with slat deflection angle as one would expect. Reynolds number effect is small. Effort needs to continue.

Paper by Pat Moriarty, “Unsteady Measurements Near a Leading-Edge Slat”

Flow spectra appear to be influenced by whether slat measurement position is upstream of a deflected flap or not: peaks at much lower frequency if no flap downstream.

Pressure transducer spectra show peak that seems to scale with Strouhal number as Mach number is varied.

Serrated slat trailing edge removes spectral peaks in hot wire spectra, and a lot of broadband as well.

Paper by Lockard, Streett, Macaraeg, “Experimentally Observed Variations in Slat Noise with Configuration and Operating Condition Changes”

Noise scales with V^5 only approximately. Weak dependence on Reynolds number. High frequency broad tone is highly deflection dependent. From the summary:

- Most features scale with the Strouhal number
- Small influence of Reynolds number above 3.6E6
- Tonal noise often dominates and is sensitive to the configuration
- Slat tips should be realistic in models
- Flap angle does not affect slat noise
- Need more extensive CFD to understand the underlying flow physics of configurations with sweep and taper
  - Influence of slat loading on tones and broadband noise
  - Ineffectiveness of slat cap

Further work is necessary to understand the flow physics causing the observed changes in slat noise with different configurations.

Paper by Christopher Tam and Nikolai Pastuchenko, “CAA Simulation of Slat noise Using a Simplified Model”

Concludes that acoustic feedback may be an important mechanism for the generation of airframe gap noise. See Ref. 65.

Paper by Storms, Hayes, and Ross, “Aeroacoustic Measurements of Slat Noise on a Three-Dimensional High-Lift System”

- 7x10 slat noise scales to tones in fly-over spectra
- Mach No dependence suggests two sources; peak noise level varies as per trailing edge theory
- Slat deflection reduction → gradual reduction in slat noise
- Slat loading and gap velocity increase with angle of attack, but slat noise peaks then decreases for higher angle of attack

- Slat trailing edge serrations yield significant noise reduction: _" spacing up to 5 dB lower than 1" spacing
- Slat noise is **not** a simple function of slat trailing edge velocity
- Noise levels are a strong function of slat deflection and angle of attack: suggests feedback mechanism between trailing edge and unsteady cove flow and/or cusp separation

Paper by Berkman, Khorrami, Choudhari, Sadowski, "Investigation of Slat Flow Field for Energy Efficient Transport Model in LTPT"

- Excellent agreement of CFD predictions with surface measurements (steady)
  - Flap side edge flow field unaffected by addition of slat
- Relevant slat flow features were captured and investigated
  - Recirculating zone, separated shear layer, slat wake
  - essentially 2D flow field
- Parametric study of slat deflection angle, gap, and overhang
  - slat loading increases at lower slat deflection angle
  - wing suction peak gets stronger as slat gap and overhang increases
- Database for prediction of slat noise was generated
- Flow features giving rise to unsteadiness were identified
  - blunt slat trailing edge shedding
  - 2D time accurate simulation with very fine grid

Paper by Rahul Sen, "Slat noise: inviscid modeling, fundamental source types, and radiation characteristics"

See Ref. 47. Summary:

- Present study models inviscid near-field mechanisms
  - 'large-scale' dynamics of vorticity fields near slat (dynamics of 'base flow')
  - in numerical form (e.g. Guo), should also resolve aspects of inviscid instabilities
  - time scales give frequencies in low- to mid-range of measured slat spectra
  - leads to M^5-type edge-scattered radiation, with *wing LE* playing role of diffracting edge
  - source terms are contributed by
    - fluctuating slat lift forces, on parts of slat that cut across wing-shaped 'streamlines'
    - motion of free-vorticity centroid across wing-shaped 'streamlines'
    - source strength is proportional to overall strength of separation bubble
  - decaying oscillatory dynamics gives a broadly humped spectrum
  - possibility of purely oscillatory regimes will be explored
- Other mechanisms proposed in AST are viable in high-freq range
  - edge noise due to slat TE
  - fluctuating gap flow

Paper by Khorrami, Berkman, Choudhari, "Unsteady RANS Computations of LTPT Slat with a Blunt Trailing Edge"

Summary:

- Identified an important source mechanism for slat noise [does not say what that is, but looks like trailing edge vortex shedding]
- Successfully duplicated the relevant experimental trends with regard to effects of Re, δ_s, T.E. thickness
- Demonstrated the ability of unsteady RANS to provide necessary input for farfield acoustics

Paper by Thomas Brooks, "Slat Noise – Effect of Operation Configuration and Modifications (Preliminary Measurements)"

No summary chart. Addition of serrations at slat trailing edge increases noise (opposite to what another paper reported).

Paper by Hardy, Fields, Guo, Sen, Stoker, "Airframe Noise Subcomponent Model"

Describes start of project. To be completed April 1999.

Paper by Don Garber, “Flyover Noise Metrics”

Review of EPNL.

Because of the non-linear, discontinuous, and extremely counter-intuitive translation from source noises to received noise metrics, it is necessary to play out the effect of any aircraft source noise or operational change through a complete system prediction to determine the real benefit of that change.

Paper by John Rawls, “ANOPP – Results / Status / Plans”

Among other improvements, there is this one: Acoustic Data (ACD) module added to permit 1/3 octave band SPL databases to be incorporated into the ANOPP system.

At the time of that writing there were plans to incorporate into ANOPP modules for airframe noise subcomponent prediction.

Compares ANOPP and Boeing methods of airframe noise prediction:

ANOPP	**Boeing**
Fink Method	
Semi-empirical model developed from a wide range of airframe types, flight speeds, flap and landing gear positions and wing platforms. Data from 16 aircraft including Prue-2 Sail Plane, Boeing 747, Lockheed C5A, Lockheed Jetstar, Convair F106B	Empirical correlation of data from 737, 737X, 757, NLA scale models. Full scale comparison with 737-300, 757-200, and 777-200.
Airframe Noise components:	
Wing	High Speed Aileron
Flaps	Flap Edge
	High Frequency
	Low Frequency
Horizontal Tail	
Vertical Tail	
Leading Edge Slat	Leading Edge Slat
Landing Gear	Landing Gear
Main	
Nose	
	Predicts only for one direction: 90° from nose directly under aircraft. Rawls adds formulas to make it predict in all directions.

Generally, Fink seems to predict a little lower level than Boeing.

Then shows how much airframe needs to be suppressed given a certain amount of engine noise suppression.

Ref. 49 Khorrami, M.R., Singer, B.A., and Radeztsky, R.H.: "Reynolds Averaged Navier-Stokes computations of a flap side-edge flow field," AIAA J., Vol.37, No.1, pp. 14-22, January 1999.

Abstract: An extensive computational investigation of a generic high-lift configuration comprising a wing and a half-span flap reveals details of the mean flowfield for flap deflections of 29 and 39 deg. The computational effort involves solutions of the thin-layer form of the Reynolds-averaged Navier-Stokes equations. For both flap deflections, the steady results show the presence of a dual-vortex system: a strong vortex forming on the lower portion of the flap side edge and a weaker one forming near the edge on the flap top surface. Downstream, the vortex on the flap side edge grows and eventually merges with the vortex on the flap top surface. Comparison of on- and off-surface flow quantities with our previous experimental measurements shows remarkable agreement. For the 39-deg flap deflection, the calculation also reveals the occurrence of a vortex breakdown, which is corroborated by five-hole probe velocity measurements performed in the Quiet Flow Facility at NASA Langley Research Center. The presence of the vortex breakdown significantly alters the flowfield near the side edge.

Conclusions: Steady RANS calculations of a high lift airfoil with a half-span flap were performed for 29 and 39 degree flap deflections. The computer results are in excellent agreement with the companion experimental measurements revealing the complex nature of the vortex system at the side edge. At the higher deflection, the computations accurately capture the occurrence and location of vortex breakdown near the side edge. – The present computations clearly show that, given the proper care (grid distribution, post processing, etc.), the CFD analysis can be used as a routine diagnostic tool on a fairly complex three-dimensional flow field. In fact, during the course of the present study, on several occasions, the computer results directed subsequent experimental measurements to be focused on a particular region of interest. The usefulness of the volumetric CFD database goes far beyond the comparison attempted in this paper and a mere corroboration of the experimental measurements. The wealth of information provided by the CFD database has given us insight into the nature of the flow physics at the flap side edge and has allowed us to design tip modifications to alter the flow field for noise reduction purposes. In addition, the computed result currently is being utilized to construct ideal flow models and to develop appropriate noise prediction tools.

Ref. 50 Singer, B.A., Brentner, K.S., Lockard, D.P. and Lilley, G.M., "Simulation of Acoustic Scattering from a Trailing Edge," AIAA-99-0231. – Also: Singer, B.A., Brentner, K.S., Lockard, D.P. and Lilley, G.M., "Simulation of Acoustic Scattering from a Trailing Edge," J. Sound & Vibration (2000) 230(3), 541-560.

Abstract: Three model problems were examined to assess the difficulties involved in using a hybrid scheme coupling flow computation with the Ffowcs Williams and Hawkings equation to predict noise generated by vortices passing over a sharp edge. The results indicate that the Ffowcs Williams and Hawkings equation correctly propagates the acoustic signals when provided with accurate flow information on the integration surface. The most difficult of the model problems investigated inviscid flow over a two-dimensional thin NACA airfoil with a bluff-body vortex generator positioned at 98 percent chord. Vortices rolled up downstream of the bluff body. The shed vortices possessed similarities to large coherent eddy in boundary layers. They interacted and occasionally paired as they convected past the sharp trailing edge of the airfoil. The calculations showed acoustic waves emanating from the airfoil trailing edge. Acoustic directivity and Mach number scaling are shown.

Ref. 51 Berkman, M.E., Khorrami, M.R., Choudhari, M., and Sadowski, S.S.:"Investigation of high-lift flow field of an energy efficient transport wing," AIAA Paper 99-0926, January 1999.

Abstract: The high-lift flow field around a multi-element Energy Efficient Transport wing is investigated both experimentally and numerically. Special emphasis is placed on resolving aeroacoustically relevant local features of the mean flow field, viz., separated flow regions including recircula-

tion bubbles, free shear layers/wakes/jets, and vortices. Such features are typically present in slat and flap cove areas, flap side-edge regions, and slat-main wing confluent boundary layer. The flow fluctuations sustained in these regions can generate significant noise, especially via interaction with nearby geometric inhomogeneities. The experimental measurements and computed results presented here show excellent agreement for mean aerodynamic quantities and provide valuable physical insight into the potential sources of flow unsteadiness. While the generic features of the computed flow field are similar to other published studies, the specific details of the acoustically relevant flow features are found to depend on the geometry of the high-lift configuration.

Ref. 52 Brooks, T.F., Humphreys, W.M., "Effect of Directional Array Size on the Measurement of Airframe Noise Components", AIAA paper 99-1958, presented at 5th AIAA/CEAS Aeroacoustics Conference in Seattle, May 1999.

A study was conducted to examine the effects of overall size of directional (or phased) arrays on the measurement of aeroacoustic components. An airframe model was mounted in the potential core of an open-jet windtunnel, with the directional arrays located outside the flow in an anechoic environment. Two array systems were used; one with a solid measurement angle that encompasses 31.6° of source directivity and a smaller one that encompasses 7.2°. The arrays, and subarrays of various sizes, measured noise from a calibrator source and flap edge model setups. In these cases, noise was emitted from relatively small, but finite size source regions, with intense levels compared to other sources. Although the larger arrays revealed much more source region detail, the measured source levels were substantially reduced due to finer resolution compared to that of the smaller arrays. To better understand the measurements quantitatively, an analytical model was used to define the basic relationships between array to source region sizes and measured output level. Also, the effect of noise scattering by shear layer turbulence was examined using the present data and those of previous studies. Taken together, the two effects were sufficient to explain spectral level differences between arrays of different sizes. An important result of this study is that total (integrated) noise source levels are retrievable and the levels are independent of the array size as long as certain experimental and processing criteria are met. The criteria for both open and closed tunnels are discussed. The success of special purpose diagonal–removal processing in obtaining integrated results is apparently dependent in part on source distribution. Also discussed is the fact that extended sources are subject to substantial measurement error, especially for large arrays.

Ref. 53 Dong, T.Z., Tam, C.K.W., and Reddy, N.N.: "Direct Numerical Simulation of Flap Side Edge Noise", AIAA-99-1803, presented at 5th AIAA/CEAS Aeroacoustics Conference in Seattle, May 1999.

Abstract: Direct numerical simulations of noise generation and radiation from aircraft flap side edges are performed in the presented paper. The objective of this work is to identify the generating mechanism of flap side edge noise. A CFD/CAA approach is taken in which the mean flow field around a three element high-lift system is provided by RANS/CFD calculations and the unsteady flow field involving shear layer instability waves and acoustic waves is calculated by a linearized Euler/CAA method. The high accuracy DRP finite difference scheme with PML boundary conditions is used to guarantee the accuracy of the unsteady calculations. A multi-domain, multiple time step technique is used to enhance the efficiency of the calculations. The computed results indicate that the feedback/interaction among side edge shear layer instability waves is the dominant noise generating mechanism.

Major noise sources are: instability/flap surface interactions, feedback/interactions among instability waves, and scattering of boundary layer disturbance at corners of side edge.

Ref. 54 Singer, B.A., Lockard, D.P., Brentner, K.S., Khorrami, M.R., Berkman, M.E., and Choudhari, M.: "Computational Acoustics Analysis of Slat Trailing-Edge Flow" AIAA Paper No. 99-1802, presented at AIAA Aeroacoustic Conference, Seattle, May 1999.

Abstract: An acoustic analysis based on the Ffowcs Williams and Hawkings equation was performed for a high-lift system. As input, the acoustic analysis used unsteady flow data obtained from a highly resolved, time-dependent, Reynolds-averaged Navier-Stokes calculation. The analysis strongly suggests that vortex shedding from the trailing edge of the slat results in a high-amplitude, high frequency acoustic signal, similar to that which was observed in a corresponding experimental study of the high-lift system.

Vortex shedding from the trailing edge of the slat is responsible for a loud high frequency noise observed in experiments.

Ref. 55 Khorrami, M.R., Berkman, M.E., Choudhari, M., Singer, B.A., Lockard, D.P., and Brentner, K.S.: "Unsteady flow computations of a slat with blunt trailing edge," AIAA Paper 99-1805, presented at 5th AIAA/CEAS Aeroacoustics Conference in Seattle, May 1999.

Abstract: A detailed computational study of a high-lift configuration was conducted. The unsteady Reynolds Averaged Navier-Stokes (RANS) computations focused on the accurate simulation of the local flow field of a slat having a blunt trailing edge. At a slat deflection angle of 30 degrees relative to the main element, the simulations reveal the presence of strong vortex shedding at the slat trailing edge. The resulting flow unsteadiness produces large amplitude propagating waves. The local spatial resolution of the computed solution is sufficiently fine to capture the nearfield structure and propagation direction of the generated sound. The calculated shedding frequency is in good agreement with the measured acoustic frequencies obtained at NASA Langley's Low Turbulence Pressure Tunnel. At a lower slat deflection angle of 20 degrees, the computation suggests that the shedding process is severely damped and that no waves propagate, in agreement with the acoustic measurements.

Ref. 56 Guo Y., "Prediction of flap side edge noise", AIAA Paper 99-1804, presented at 5th AIAA/CEAS Aeroacoustics Conference in Seattle, May 1999.

Abstract: This paper presents a model for noise generation by flow separation in the flap side edge regions of aircraft high lift systems. The model is based on the concept that complex flow features such as shear layer instabilities that cause flow separations generate noise by producing unsteady vorticity fluctuations. These vorticity fluctuations are modeled here by unsteady nonlinear motions of discrete vortices, representing shear layers in real flows, and by dynamic vortex shedding from the sharp corners of the flap side edges, modeling vorticity production by flow separation. The model calculates the near field flow fluctuations, including unsteady pressures on the flap surfaces, which are then used to compute the far field radiation. Both unsteady surface pressures and far field predictions are compared with available test data, which shows very good agreement in the trends, such as frequency characteristics and flow Mach number dependence.

Is sensitive to the need for engineering models that need only trivial amounts of computer time.

Ref. 57 Guo Y., "Application of Ffowcs Williams/Hawkings equation to two-dimensional problems", report by The Boeing Co. to NASA LaRC, contract NAS1-20268, Task 20, June 1999. – Also: Guo, Y.P., "Application of the Ffowcs Williams/Hawkings equation to two-dimensional problems," J. Fluid Mech. (2000), vol. 403, pp.201-221.

Abstract: This report discusses the application of the Ffowcs Williams/Hawkings equation to two-dimensional problems. A two-dimensional version of this equation is derived which not only provides a very efficient way for numerical implementation, but also reveals explicitly the features of the source mechanisms and the characteristics of the far field noise associated with two-dimensional problems. It is shown that the sources can be interpreted, similarly to those in three-dimensional spaces, as quadrupoles from turbulent flows, dipoles due to surface pressure fluctuations on the bodies in the flow, and monopoles from non-vanishing normal accelerations of the body surfaces. The cylindrical spreading of the two-dimensional waves and their far field directivity become apparent in this new version. It also explicitly brings out the functional dependencies of the radiated sound on parameters such as the flow Mach number and the Doppler factor due to source

motions. These dependencies are shown to be quite different from those in three-dimensional problems. The two-dimensional version is numerically very efficient because the domains of the integration are reduced by one from the three-dimensional version. The quadrupole integrals are now in a planar domain and the dipole and monopole integrals are along the contours of the two dimensional bodies. The calculations of the retarded time interpolation of the integrands, a time-consuming but necessary step in the three-dimensional version, are completely avoided by making use of Fast Fourier Transform. To demonstrate the application of this, a vortex/airfoil interaction problem is discussed, which has many practical applications and involves important issues such as vortex shedding from the trailing edge.

Ref. 58 Guo, Yueping, "Modeling of Noise Reduction by Flap Side Edge Fences," report by The Boeing Co. to NASA LaRC, contract NAS1-20268, Task 20, June 1999.

This report presents a study on the effects of flap side edge fences on the noise generation mechanisms associated with flap side edge flows. The noise sources in these flows are postulated to be flow separation at the sharp corners of the flap side surface and shear layer instabilities in the cross flow around the flap side edge. These mechanisms are modeled by unsteady vortex shedding from the sharp comers and the subsequent nonlinear motions of the shed vortices in the flow. The relevance of this model is justified because in high Reynolds number flows, local flow separation at sharp corners is acoustically equivalent to vorticity injection at the corners into the essentially potential flow outside of the very small separation region. Furthermore, viscous shear layers in these flows are usually very thin so that their evolutions due to instabilities can be well modeled by nonlinear motions of concentrated vortices. In this model, noise is generated by unsteady vorticity fluctuations, as described by the theory of vortex sound. The use of side edge fences changes the local geometry of the flap side edge, which in turn causes changes in both the steady mean flow and the unsteady vortex motions. It is shown that fences both reduce the amplitudes of the far field radiation and lower the characteristic frequencies of the radiated sound. The former can be attributed to the reduced velocity of the local cross flow, due to the blockage effects of the fences, and the latter to the increased dimension of the flap side surface. The increase in the side surface dimension makes the evolution of the shear layers, which basically occurs along the side surface, more gradual, effectively increasing its characteristic time scale, and thus, lowering its dominant frequency. All these predictions are shown to agree very well with experimental data.

Ref. 59 Stoker, R.W., "Landing Gear Noise Test Report", report by Boeing Co. to NASA LaRC under Contract NAS1-97040, Task 8, February 1999.

A full scale 737-400 landing gear was tested in LSAF. Small tubes, hoses and hollow pins create high frequency noise and contribute to the overall radiated landing gear noise spectrum. Removing hoses and taping over all open-ended pins reduced noise radiated from the landing gear by 2-3 dB. When adding 4 wheels (to obtain a 6 wheel truck) low frequency noise below 1 KHz was increased by around 5 dB. Gear noise scales quite well with V^6 in amplitude, and with linear Strouhal number in frequency.

Ref. 60 Storms, B.L., Ross, J.C., Hayes, J., and Moriarty, P.: "Acoustic Measurements of Slat Noise on a Three-Dimensional High-Lift System", AIAA-99-1957, presented at 5th AIAA/CEAS Aeroacoustics Conference in Seattle, May 1999.

Abstract: Experimental results are presented for the aerodynamics and acoustics of an unswept wing with a half-span flap and a full-span slat. Concurrent aerodynamic and acoustic measurements were obtained for high-lift riggings representative of landing-approach configurations. Phased microphone array measurements indicate that slat gap noise is most significant for high slat deflections where the slat is lightly loaded. More specifically, the peak noise level for the 25-deg slat deflection was 20 dB higher than that of the 9-deg slat deflection. Measurements of intermediate angles indicate a gradual decrease in slat noise as slat deflection is decreased. Strouhal frequency scaling of the 25-deg slat configuration suggests that vortex shedding from the slat trailing edge may be an important noise mechanism. However, a non-linear relationship between slat

noise level and angle of attack suggests a more complex phenomenon. Computational results detail the strength of the shear layers in the slat-cove flow field. Variations in the slat-cove shear layers with slat deflection and angle of attack are presented. From correlations between the computed results and the measured acoustics, it is hypothesized that a Kelvin-Helmholtz instability develops in the slat cove and a feedback mechanism forms between the slat-cove and slat trailing-edge flow fields.

Conclusions: A simple three-dimensional high-lift system with a half-span flap and a full-span slat was studied experimentally. Coincident acoustic and aerodynamic measurements identified the slat trailing-edge flow field as the dominant noise source. Slat noise was most significant for the highest slat deflection (25 deg) where the slat was lightly loaded. The slat noise was characterized by a broad spectral peak with noise source contributions that moved spanwise with frequency. The peak noise level decreased gradually with slat deflection yielding a 20 dB difference between the 25-deg and 9-deg slat deflections. Noise spectra for the 25-deg slat deflection at different free stream velocities collapsed well using a velocity-to-the-fifth-power relation and a Strouhal number based on trailing edge thickness and slat gap velocity. This result suggests that slat noise is associated with vortex shedding from the slat trailing edge. However, unexplained variations in Strouhal number with slat deflection and slat gap velocity indicate that a more complex phenomenon may be present. Slat loading and slat gap velocity were found to increase continuously with angle of attack for a constant slat deflection. Slat noise, however, decreased with increasing angle of attack and slat-gap velocity under certain conditions. A laminar separation bubble with turbulent reattachment on the slat upper surface was observed experimentally for the 5-deg slat deflection and predicted for slat deflections less than 19 deg. Evidence suggests that the state of the slat upper-surface boundary layer may affect the vortex shedding from the slat trailing edge, but this conjecture warrants further investigation considering the limited experimental data.

Reynolds-averaged Navier-Stokes computations revealed that the flow reattachment location in the slat cove is relatively insensitive to slat deflection. This result was confirmed experimentally with flow tufts. The width of the recirculation region, however, is reduced at lower slat deflections and higher angles of attack. Computational surveys of the flow field in the slat gap region suggest significant shear between the low-speed recirculation region and high-speed slat gap flow. The shear was found to decrease with decreasing slat deflection and increasing angle of attack. Because this trend correlates well with the trend in the measured acoustics, it is hypothesized that a Kelvin-Helmholtz instability develops in the slat cove region and grows as the flow is accelerated through the slat gap. This disturbance may be amplified by feedback from the slat trailing edge under certain conditions. These observations highlight the complex dependencies of slat noise on the associated aerodynamics.

Ref. 61 Hayes, J.A., Horne, W.C., Jaeger, S.M., Soderman, P.T., "Measurement of Reynolds Number Effect on Airframe Noise in the 12-foot Pressure Wind Tunnel," AIAA-99-1959, 5th AIAA/CEAS Aeroacoustics Conference, Seattle, May 1999.

Abstract: Flap-tip noise sources on a 4.7% DC-10/MD-11 model respond to increasing Reynolds number (Re) with increases in high frequency sound generation. Sound level increases of 3 dB in frequencies greater than 15 kHz (700 Hz full-scale) are observed with increasing Re between 1.7×10^6 and 5×10^6 (based on the model mean aerodynamic chord). The effect is most apparent with the doubling of Re from approximately 2×10^6 to 4×10^6; above 5×10^6 no further increase in sound level is observed. Noise measurements were made up to a Re of 6.7×10^6 (22% of full-scale Re). Corresponding aerodynamic measurements show that lift on the model increases over the same Re range. A case is made to relate the sound generation to the model lift through flap loading alone. The cornerstone of this case is the comparison of data from the DC-10 and the MD-11 configurations. The conversion of the DC-10 model to the MD-11 configuration by adding a winglet provides a significant improvement in total lift with no increase in flap-tip noise. Relating the source strength uniquely to flap loading explains this finding. Re variation was accomplished by wind tunnel pressurization using the NASA Ames Research Center 12-Foot Pressure Wind Tunnel. A wall-

mounted phased microphone array provided the acoustic data. Re effects on both broadband and tonal features in the data are described, and the implications for prediction of full-scale airframe noise from scale models are discussed.

Ref. 62 Sen, Rahul, and Stoker, Robert W., "Airframe Noise Test of a 0.063-scale 777 Model: Test Report," report by The Boeing Co. to NASA LaRC, contract NAS1-97040, Task 2, December 1999.

Abstract: A 6.3% scale 777-200 semi-span model was tested in the Low Speed Aeroacoustic Facility (LSAF) at Boeing. Data were acquired using a microphone phased array, freefield microphones, and Kulite pressure transducers. Additionally, a wake survey system was used to map the wake of the landing gear and high-lift system. Results were obtained for several Mach numbers, angles of attack, and for several directivity angles. Two landing gear configurations were examined during this test. The first configuration was a low-fidelity landing gear. The second configuration was a high-fidelity gear built from stereo lithography, which included many of the pieces present on the full-scale model. Results from acoustic testing show increased noise from the high-fidelity gear. The phased array results show noise emanating from both the landing gear and from the flap trailing edge behind the landing gear.

Ref. 64 Sen, R,, Hardy, B, Yamamoto, K., Guo, Y., Miller, G., "Airframe Noise Subcomponent Definition and Model," NASA Contractor Informal Report, Contract NAS1-97040, Task 9, January 2000.

Main objectives:

- greater number of fluid dynamic parameters
- greater detail in source models
- more detailed source classification scheme
- detailed landing gear source model that incorporates full-scale spectral features
- larger database of airplanes
- inclusion of high-resolution phased array data
- inclusion of data-based (where available) source directivity models

While progress has been good in all of those areas, it has also been somewhat uneven. This is mainly due to the large effort expended on aerodynamic calculations. Consequently, acoustic modeling of high lift sources has not been able to take full advantage of the available aerodynamic database. A related consequence is that the trailing edge noise source has not been updated at this point; for this source, Fink's model stands for the time being. On the other hand, an extensive aerodynamic database is now in place, providing a solid foundation for subsequent source model refinements.

Source directivity modeling is another area in which progress was somewhat hampered, in this case due to a scarcity of experimental data.

The greatest changes at this stage are in the landing gear model, despite the currently limited availability of full-scale gear-noise data. The model presented here establishes a totally new paradigm for landing gear source components, much as Ref. 30 did for sources associated with the high lift system.

Presents a comprehensive list of high lift system subcomponents for noise (i.e., sans landing gear):

- leading edge slat
- outboard flap edge
- inboard flap edge
- trailing edge
- high speed aileron
- residue noise floor

Formulas for each component are given as a function of aerodynamic and geometry parameters. Similarly, a list of landing gear noise subcomponents is given, but those components are not necessarily associated with landing gear parts, except tires:

- Low frequency
- High frequency
- Mid frequency
- Tire

Again, prediction formulas for the landing gear subcomponents are provided.

Ref. 65 Tam, C.K.W., Pastouchenko, N., "Gap Tones: A Component of Airframe Noise," AIAA 2000-0606, 38th Aerospace Sciences Meeting and Exhibit, January 2000, Reno NV.

CAA simulations find feedback process gap regions (slat, main wing/flap) capable of emitting strong tones. Predicted tone frequencies agree well with experimental measurements. [NOTE: Ref. 64 does not mention tones at all].

Ref. 66 Storms, Bruce L., Hayes, Julie A., Jaeger, Stephen M., Soderman, Paul T., "Aeroacoustic Study of Flap-Tip Noise Reduction Using Continuous Moldline Technology," AIAA 2000-1976, 6th AIAA/CEAS Aeroacoustics Conference, June 12-14, 2000, Lahaina HI.

Dramatic reduction of flap-tip airframe noise was accomplished with continuous moldline technology (CMT). The most common application of CMT involves a flexible panel that deforms to provide a continuous surface between two movable parts. In this study, CMT was applied at the flap-tip junction of a wind tunnel model comprised of a simplified wing with a half-span hinged flap. With an exposed flap tip (no CMT), a compact noise source at the flap tip was the dominant airframe source. With CMT applied, the flaptip source was reduced below measurable levels. A phased array of microphones provided source location and sound level determination. The low model noise levels and high ambient noise of the wind tunnel made it a challenge to quantify the sound levels. Initial implementation of a 100-element phased array provided inadequate noise rejection for accurate source level measurement. Replacing the initial array with an array recessed behind Kevlar cloth reduced the boundary layer noise level on the individual sensors. With the recessed array, an adequate signal-to-noise ratio (SNR) was attained to provide accurate sound level measurement of the flap-tip source. With the elimination of the flap tip using CMT, no other airframe noise source was detected louder than 6-8 dB below the hinged flap-tip noise level. Sources below this level were undetectable due to background noise and sidelobe energy from other noise sources.

Ref. 67 Guo, Y.P., "Ffowcs Williams/Hawkings Equation for Two-Dimensional Problems," AIAA 00-2066, 6th AIAA/CEAS Aeroacoustics Conference, Lahaina HI, June 2000.

Abstract: This paper presents the derivation of the Ffowcs Williams/Hawkings equation in two-dimensional space. The results not only provide a very efficient way for numerical implementation, but also reveal explicitly the features of the source mechanisms and the characteristics of the far field noise associated with two-dimensional problems. It is shown that the sources can be interpreted similarly to those in three-dimensional spaces, as quadrupoles from turbulent flows, dipoles due to surface pressure fluctuations on the bodies in the flow, and monopoles from non-vanishing normal accelerations of the body surfaces. The cylindrical spreading of the two-dimensional waves and their far field directivity become apparent in this new version. It also explicitly brings out the functional dependencies of the radiated sound on parameters such as the flow Mach number and the Doppler factor due to source motions. These dependencies are shown to be quite different from those in three-dimensional problems. The two-dimensional version is numerically very efficient because the domains of the integration are reduced by one from the three dimensional version. The quadrupole integrals we now in a planar domain and the dipole and monopole integrals are along the contours of the two dimensional bodies. The calculations of the retarded time interpolation of the integrands, a time-consuming but necessary step in the three-dimensional version, are completely avoided by making use of Fast Fourier Transform. To demonstrate the application

of this, two examples are given, one for flap side edge noise and the other for noise from trailing edge vortex shedding of aircraft high lift components.

Ref. 68 Guo, Y.P., Joshi, M.C., Bent, P.H., Yamamoto, K.J., "Surface pressure fluctuations on aircraft flaps and their correlation with far-field noise," J. Fluid Mech (2000), vol. 415, pp. 175-202.

Abstract: This paper discusses unsteady surface pressures on aircraft flaps and their correlation with far-field noise. Analyses are made of data from a 4.7% DC-10 aircraft model test, conducted in the 40 x 80 feet wind tunnel at NASA Ames Research Center. Results for various slat/wing/flap configurations and various flow conditions are discussed in detail to reveal major trends in surface pressure fluctuations. Spectral analysis, including cross-correlation/coherence, both among unsteady surface pressures and between far-field noise and near-field fluctuations, is used to reveal the most coherent motions in the near field and identify potential sources of noise related to flap flows. Dependencies of surface pressure fluctuations on mean flow Mach numbers, flap settings and slat angles are discussed. Dominant flow features in flap side edge regions, such as the formation of double-vortex structures, are shown to manifest themselves in the unsteady surface pressures as a series of spectral humps. The spectral humps are shown to correlate well with the radiated noise, indicating the existence of major noise sources in flap side edge regions. Strouhal number scaling is used to collapse the data with satisfactory results. The effects of flap side edge fences on surface pressures are also discussed. It is shown that the application of fences effectively increases the thickness of the flaps so that the double-vortex structures have more time to evolve. As a result, the characteristic timescale of the unsteady sources increases, which in turn leads to a decrease in the dominant frequency of the source process. Based on this, an explanation is proposed for the noise reduction mechanism of flap side edge fences.

Ref. 69 Guo, Y.P., Modeling of Noise Reduction by Flap Side Edge Fences," AIAA 00-2065, 6th AIAA/CEAS Aeroacoustics Conference, Lahaina HI, June 2000.

Abstract: This paper discusses the effects of fences on side edge cross flows. Experimental data are reviewed to show that fences can modify the cross flow in the side edge region of aircraft flaps in such a way that noise reduction can be achieved. Near field pressure data reveal that fences reduce the characteristic frequency of the flow fluctuations. This leads us to postulate that the fences make the far field noise spectra shift downward. Because airframe noise spectra typically have a negative slope in the most important mid to high frequency domain, this downward shift leads to an equivalent reduction of total noise, when measured by conventional metric such as the Effective Perceived Noise Level (EPNL) in aircraft certification. To explain the decrease of the characteristic frequency of the flow fluctuations due to the fences, an analytical model is developed, based on vortex dynamics. The predictions from the model are shown to be in very good agreement with measured data, both for the dominant frequency in the baseline case without the fences and for the trends of decreasing frequency with increasing fence height.

Ref. 70 Guo, Yueping, "A Discrete Vortex Model for Slat Noise Prediction", report CRAD-9402-TR-5170 by The Boeing Company to NASA Langley Research Center, September 2000.

Abstract: This report documents a discrete vortex model for predicting slat noise due to vortical flow fluctuations in the slat cove region and the interactions between the vortical flow and the slat trailing edge. The model simulates flow separation at the slat cusp and trailing edges by vortex shedding in the form of discrete, multiple point vortices. The near field flow is solved by implementing the vortex shedding model in an unsteady panel method, in which the effects of the high lift system are accounted for by time-dependent source panels on the body surfaces. Time domain solutions for the near field flow are derived by the fourth order Runge-Kutta method, which shows the development of the slat cove vortical flow from the vorticity shed at the slat cusp. The flow reaches an oscillatory equilibrium at which flow fluctuations are induced by the balance between the vorticity convected away by the mean flow and that shed by flow separation. The convected vorticity passes through the gap between the slat trailing edge and the main wing, causing vortex/edge interaction. Thus, the

model captures the noise generation mechanisms of both the unsteady fluctuations of the highly vortical flow in the slat cove and the scattering of vortical energy into acoustic energy by the slat trailing edge. The noise prediction is done by the Ffowcs Williams/Hawkings equation. It is shown that the noise from these two mechanisms has broadband spectral characteristics, covering about two decades in frequency. The noise spectrum has a negative slope, with the fall-off approximately following the inverse square of frequency. Because the sources are high frequency in nature and are non-compact, the overall sound pressure level is shown to scale on the flow Mach number according to a power law with the power index approximately equal to 2.5. This is in sharp contrast to the fifth or sixth power law for low Mach number, low frequency noise. It is shown that the cove flow fluctuations mainly cause pressure fluctuations on the surface of the forward portion of the main wing, which radiates to the fly-over direction normal to the wing chord. The vortex/trailing edge interaction is shown to mostly induce fluctuations on the slat, causing radiation in the direction normal to the slat chord. Predictions from the model are validated by experimental data in terms of the spectral characteristics, the far field directivity and the Mach number scaling, which all show good agreements. Functional dependencies on the angle of attack, the slat deployment angle and the slat gap are also derived and validated by experimental data. It is shown that the most promising noise reduction comes from decreasing the slat gap. By reducing the slat gap by one percent of the stowed wing chord, it is shown that 5 dB noise reduction can be achieved in the peak radiation angle, consistent with test data. Noise variation with the angle of attack and/or the slat deployment angle is shown to depend on how well the incoming steady flow aligns with the tangent of the slat surface near the cusp where vortex shedding occurs.

Ref. 71 Brooks, T.F., Humphreys, W.M.Jr., "Flap Edge Aeroacoustic Measurements and Predictions," AIAA 2000-1975, 6th AIAA/CEAS Aeroacoustics Conference, Lahaina HI, June 2000.

Abstract: An aeroacoustic model test has been conducted to investigate the mechanisms of sound generation on high-lift wing configurations. This paper presents an analysis of flap side-edge noise, which is often the most dominant source. A model of a main element wing section with a half-span flap was tested at low speeds of up to a Mach number of 0.17, corresponding to a wing chord Reynolds number of approximately 1.7 million. Results are presented for flat (or blunt), flanged, and round flap-edge geometries, with and without boundary-layer tripping, deployed at both moderate and high flap angles. The acoustic database is obtained from a Small Aperture Directional Array (SADA) of microphones, which was constructed to electronically steer to different regions of the model and to obtain farfield noise spectra and directivity from these regions. The basic flap-edge aerodynamics is established by static surface pressure data, as well as by Computational Fluid Dynamics (CFD) calculations and simplified edge flow analyses. Distributions of unsteady pressure sensors over the flap allow the noise source regions to be defined and quantified via cross-spectral diagnostics using the SADA output. It is found that shear layer instability and related pressure scatter is the primary noise mechanism. For the flat edge flap, two noise prediction methods based on unsteady surface pressure measurements are evaluated and compared to measured noise. One is a new causality spectral approach developed here. The other is a new application of an edge-noise scatter prediction method. The good comparisons for both approaches suggest that the prediction models capture much of the physics. Areas of disagreement appear to reveal when the assumed edge noise mechanism does not fully define the noise production. For the different edge conditions, extensive spectra and directivity are presented. Significantly, for each edge configuration, the spectra for different flow speeds, utilizing aerodynamic performance and boundary layer scaling methods developed herein successfully scaled flap angles, and surface roughness.

Ref. 72 Choudhari, M.M., Lockard, D.P., Macaraeg, M.G., Singer, B.A., Streett, C.L., Neubert, G., Stoker, R.W., Underbrink, J., Berkman, M.E., Khorrami, M.R., Sadowski, S.S., "Aeroacoustic Experiments in the NASA Langley Low-Turbulence Pressure Tunnel," NASA TM-2002-211432, February 2002.

Abstract: A phased microphone array was used in the Langley Low-Turbulence Pressure Tunnel to obtain acoustic data radiating from high lift wing configurations. The data included noise localization

plots and acoustic spectra. The tests were performed at Reynolds numbers based on the cruise-wing chord, ranging from 3.6×10^6 to 19.2×10^6. The effects of Reynolds number were small and monotonic for Reynolds numbers above 7.2×10^6.

This report contains data on the effects of several noise reduction concepts: modifying the shape of the flap side edge, μ-tabs on flap side edges, 'noise weeder' at flap side trailing edge, filling the slat cove, seriating the slat trailing edge, and varying the slat deflection angle.

10 Appendix: Description of Compact Disk with Deliverable Data

The following are the file naming conventions:

- Files ending with `.inp` are ANOPP input files.
- Files ending with `.tbi` are files to be included (embedded into) ANOPP input files.
- Files ending with `.dat` are ANOPP output files.
- Files ending with `.dta` contain noise 'deltas' (difference between baseline and baseline with noise reduction concept).
- Files ending with `.sup` contain the same data as .dta files but in fractional form as opposed to decibels, for use in ANOPP's General Suppression module.
- Files ending with `.lay` are TekPlot layout files which produce graphs calling on files ending with .plt (TekPlot ASCII data files).
- Files ending with `.pl` are Perl scripts.
- Occasional `readme.txt` files in various directories contain further explanations of peculiarities in a directory.

Outside of the 0_Documentation directory, all files are flat ASCII text files.

The format of these tables and the computer files is such that they can be directly incorporated into an input file for running ANOPP, using the Acoustic Data Module (ACD). The user of these data is presumed to be familiar with preparing ANOPP input data streams.

The following table shows the compact disk's directory structure and file names:

Table 7 Compact Disk Directory Structure and File Names

0_Documentation
AirframeNoiseStudies.pdf
1_SmallTwin
1_Baseline
STAF2K_makelib.inp
1_FlapsDetent_1
1_Flaps
Inboard.tbi
Outboard.tbi
Aileron.tbi
2_Leading Edge Devices
Slat.tbi
4_Total
Total.tbi
readme.txt

2_FlapsDetent_30
1_Flaps
Inboard.tbi
Outboard.tbi
Aileron.tbi
2_LeadingEdgeDevices
Slat.tbi
4_Total
Total.tbi
readme.txt
3_LandingGear
Nose.tbi
Main.tbi
5_NoiseReductionConcepts
STAS2K_makelib.inp
1_Flaps
Fences
ibFence1Delta.dta, .lay, .plt, .sup
ibFence2Delta.dta, .lay, .plt, .sup
ibFence3Delta.dta, .lay, .plt, .sup
obFence1Delta.sup
obFence2Delta.sup
obFence3Delta.sup
readme.txt
mTabs
mTabs_Flap.dta
mTabsInboardFlap.sup
mTabsOutboardFlap.sup
readme.txt
Porous Tips
PorousDelta.dta
PorousDelta_IB.sup
PorousDelta_OB.sup

readme.txt
Side Egde Shaping
IpDelta_Flap.dta
IpDelta_InboardFlap.sup
IpDelta_OutboardFlap.sup
readme.txt
2_LeadingEdgeDevices
CoveFiller
SlatCoveFillDelta.dta, .plt, .sup
SlatGap
SlatGapDelta.dta, .plt, .sup
3_Landing Gear
SuppressHighFreq
MainGearHiF.dta, .plt, .sup
SuppressHighMediumFreq
MainGearHiMedF.dta, .plt, .sup
2_MediumTwin
1_Baseline
MTAF2K_makelib.inp
1_FlapsDetent_5
1_Flaps
Inboard.tbi
Outboard.tbi
Aileron.tbi
2_Leading Edge Devices
Slat.tbi
4_Total
Total.tbi
readme.txt
2_FlapsDetent_30
1_Flaps
Inboard.tbi

Outboard.tbi
Aileron.tbi
2_LeadingEdgeDevices
Slat.tbi
4_Total
Total.tbi
readme.txt
3_LandingGear
Nose.tbi
Main.tbi
5_NoiseReductionConcepts
MTAS2K_makelib.inp
1_Flaps
Fences
ibFence1Delta.dta, .lay, .plt, .sup
ibFence2Delta.dta, .lay, .plt, .sup
ibFence3Delta.dta, .lay, .plt, .sup
obFence1Delta.sup
obFence2Delta.sup
obFence3Delta.sup
readme.txt
mTabs
mTabs_Flap.dta
mTabsInboardFlap.sup
mTabsOutboardFlap.sup, .plt
readme.txt
Porous Tips
PorousDelta.dta
PorousDelta_IB.sup
PorousDelta_OB.sup
readme.txt
Side Egde Shaping
IpDelta_Flap.dta

IpDelta_InboardFlap.sup
IpDelta_OutboardFlap.sup
readme.txt
2_LeadingEdgeDevices
Cove-Filler
SlatCoveFillDelta.dta, .plt, .sup
SlatGap
SlatGapDelta.dta, .plt, .sup
3_Landing Gear
SuppressHighFreq
MainGearHiF.dta, .plt, .sup
SuppressHighMediumFreq
MainGearHiMedF.dta, .plt, .sup
3_LargeQuad
1_Baseline
LQAF2K_makelib.inp
1_FlapsDetent_10
1_Flaps
Inboard.tbi
Outboard.tbi
Aileron.tbi
2_Leading Edge Devices
Slat.tbi
4_Total
Total.tbi
readme.txt
2_FlapsDetent_30
1_Flaps
Inboard.tbi
Outboard.tbi
Aileron.tbi

2_LeadingEdgeDevices
Slat.tbi
4_Total
Total.tbi
readme.txt
3_LandingGear
Nose.tbi
Main.tbi
5_NoiseReductionConcepts
LQAS2K_makelib.inp
1_Flaps
Fences
ibFence1Delta.dta, .lay, .plt, .sup
ibFence2Delta.dta, .lay, .plt, .sup
ibFence3Delta.dta, .lay, .plt, .sup
obFence1Delta.sup
obFence2Delta.sup
obFence3Delta.sup
readme.txt
mTabs
mTabsDelta.lay
mTabsInboardDelta.dta, .plt, .sup
mTabsOutboardDelta.dta, .plt, .sup
readme.txt
Porous Tips
PorousDelta.dta
PorousDelta_IB.dta, .plt., .sup
PorousDelta_OB.dta, .sup
Side Egde Shaping
IpDelta_InboardFlap.dta, .plt, .sup
IpDelta_InboardFlap_azi0.lay
IpDelta_OutboardFlap.dta, .plt, .sup
IpDelta_OutboardFlap_azi0.lay

readme.txt
2_LeadingEdgeDevices
CoveFiller
SlatCoveFillDelta.dta, .lay, .plt, .sup
SlatGap
SlatGapDelta.dta, .lay, .plt, .sup
3_Landing Gear
SuppressHighFreq
LandingGDelta_Mach259_2.dta, .lay, .plt, .sup
SuppressHighMediumFreq
LandingGDelta_Mach259_1.dta, .lay, .plt, .sup
4_OverFlightSim
1_Baseline
1_SmallTwin
1_Takeoff
st_Kum.plt
sttko.inp
sttko.dat
sttko.plt
sttko.lay
2_Approach
st_Kum.plt
stapp.inp
stapp.dat
stapp.plt
stapp.lay
2_MediumTwin
1_Takeoff
mtcutb_Kum.dat
mtsidl_Kum.dat
mttko.inp
mttko.dat
mttko.plt

mttko.lay
2_Approach
mtapp_Kum.plt
mtapp.inp
mtapp.dat
mtapp.plt
mtapp.lay
3_LargeQuad
1_Takeoff
lqtko_kum.plt
lqsid_kum.plt
lqtko.inp
lqtko.dat
lqtko.plt
lqtko.lay
2_Approach
lqapp_kum.plt
lqapp.inp
lqapp.dat
lqapp.plt
lqapp.lay
5_NoiseReductionConcepts
1_SmallTwin
1_Takeoff
sled
sttko_sled.inp
sttko_sled.dat
sttko_sled.plt
sttko_sled.lay
2_Approach
allnear
stapp_allnear.inp
stapp_allnear.dat

stapp_allnear.plt
stapp_allnear.lay
allreds
stapp_allreds.inp
stapp_allreds.dat
stapp_allreds.plt
stapp_allreds.lay
Fences
stapp_fences.inp
stapp_fences.dat
stapp_fences.plt
stapp_fences.lay
mtabs
stapp_mtabs.inp
stapp_mtabs.dat
stapp_mtabs.plt
stapp_mtabs.lay
noflaps
stapp_noflapnoise.inp
stapp_noflapnoise.dat
stapp_noflapnoise.plt
stapp_noflapnoise.lay
Porous
stapp_porous.inp
stapp_porous.dat
stapp_porous.plt
stapp_porous.lay
seshap
stapp_seshap.inp
stapp_seshap.dat
stapp_seshap.plt
stapp_seshap.lay

sled
stapp_sled.inp
stapp_sled.dat
stapp_sled.plt
stapp_sled.lay
smaing
stapp_smaing.inp
stapp_smaing.dat
stapp_smaing.plt
stapp_smaing.lay
2_MediumTwin
1_Takeoff
sled
mttko_sled.inp
mttko_sled.dat
mttko_sled.plt
mttko_sled.lay
2_Approach
allnear
mtapp_allnear.inp
mtapp_allnear.dat
mtapp_allnear.plt
mtapp_allnear.lay
allreds
mtapp_allreds.inp
mtapp_allreds.dat
mtapp_allreds.plt
mtapp_allreds.lay
Fences
mtapp_fences.inp
mtapp_fences.dat
mtapp_fences.plt
mtapp_fences.lay

mtabs
mtapp_mtabs.inp
mtapp_mtabs.dat
mtapp_mtabs.plt
mtapp_mtabs.lay
noflaps
mtapp_noflapnoise.inp
mtapp_noflapnoise.dat
mtapp_noflapnoise.plt
mtapp_noflapnoise.lay
Porous
mtapp_porous.inp
mtapp_porous.dat
mtapp_porous.plt
mtapp_porous.lay
seshap
mtapp_seshap.inp
mtapp_seshap.dat
mtapp_seshap.plt
mtapp_seshap.lay
sled
mtapp_sled.inp
mtapp_sled.dat
mtapp_sled.plt
mtapp_sled.lay
smaing
mtapp_smaing.inp
mtapp_smaing.dat
mtapp_smaing.plt
mtapp_smaing.lay
3_LargeQuad
1_Takeoff
sled

lqtko_sled.inp
lqtko_sled.dat
lqtko_sled.plt
lqtko_sled.lay
2_Approach
allnear
lqapp_allnear.inp
lqapp_allnear.dat
lqapp_allnear.plt
lqapp_allnear.lay
allreds
lqapp_allreds.inp
lqapp_allreds.dat
lqapp_allreds.plt
lqapp_allreds.lay
Fences
lqapp_fences.inp
lqapp_fences.dat
lqapp_fences.plt
lqapp_fences.lay
mtabs
lqapp_mtabs.inp
lqapp_mtabs.dat
lqapp_mtabs.plt
lqapp_mtabs.lay
noflaps
lqapp_noflapnoise.inp
lqapp_noflapnoise.dat
lqapp_noflapnoise.plt
lqapp_noflapnoise.lay
Porous
lqapp_porous.inp
lqapp_porous.dat

lqapp_porous.plt
lqapp_porous.lay
seshap
lqapp_seshap.inp
lqapp_seshap.dat
lqapp_seshap.plt
lqapp_seshap.lay
sled
lqapp_sled.inp
lqapp_sled.dat
lqapp_sled.plt
lqapp_sled.lay
smaing
lqapp_smaing.inp
lqapp_smaing.dat
lqapp_smaing.plt
lqapp_smaing.lay
5_ProjectTools
an2tp.pl
concat.pl
cvACDtbl1.pl
cvKingo.pl
supplt.pl

REPORT DOCUMENTATION PAGE

Form Approved
OMB No. 0704-0188

1. REPORT DATE *(DD-MM-YYYY)*	2. REPORT TYPE	3. DATES COVERED *(From - To)*
01- 06 - 2005	Contractor Report	

4. TITLE AND SUBTITLE
Airframe Noise Studies – Review and Future Direction

5a. CONTRACT NUMBER
NAS1-97040

5b. GRANT NUMBER

5c. PROGRAM ELEMENT NUMBER

6. AUTHOR(S)
Rackl, Robert G.; Miller, Gregory; Guo, Yueping; and Yamamoto, Kingo

5d. PROJECT NUMBER

5e. TASK NUMBER
Task Number 12

5f. WORK UNIT NUMBER
23-781-20-12

7. PERFORMING ORGANIZATION NAME(S) AND ADDRESS(ES)
NASA Langley Research Center
Hampton, VA 23681-2199

Boeing Commercial Airplanes
Seattle, WA 98124

8. PERFORMING ORGANIZATION REPORT NUMBER

9. SPONSORING/MONITORING AGENCY NAME(S) AND ADDRESS(ES)
National Aeronautics and Space Administration
Washington, DC 20546-0001

10. SPONSOR/MONITOR'S ACRONYM(S)
NASA

11. SPONSOR/MONITOR'S REPORT NUMBER(S)
NASA/CR-2005-213767

12. DISTRIBUTION/AVAILABILITY STATEMENT
Unclassified - Unlimited
Subject Category 71
Availability: NASA CASI (301) 621-0390

13. SUPPLEMENTARY NOTES
Langley Technical Monitor: Robert A. Golub
An electronic version can be found at http://ntrs.nasa.gov
A CD-ROM supplement for CR-2005-213767 is available upon request from NASA CASI.

14. ABSTRACT

This report contains the following information: 1) a review of airframe noise research performed under NASA's Advanced Subsonic Transport (AST) program up to the year 2000, 2) a comparison of the year 1992 airframe noise predictions with those using a year 2000 baseline, 3) an assessment of various airframe noise reduction concepts as applied to the year 2000 baseline predictions, and 4) prioritized recommendations for future airframe noise reduction work. NASA's Aircraft Noise Prediction Program was the software used for all noise predictions and assessments. For future work, the recommendations for the immediate future focus on the development of design tools sensitive to airframe noise treatment effects and on improving the basic understanding of noise generation by the landing gear as well as on its reduction.

15. SUBJECT TERMS
Airframe noise; Flap edge noise

16. SECURITY CLASSIFICATION OF:			17. LIMITATION OF ABSTRACT	18. NUMBER OF PAGES	19a. NAME OF RESPONSIBLE PERSON
a. REPORT	b. ABSTRACT	c. THIS PAGE			STI Help Desk (email: help@sti.nasa.gov)
					19b. TELEPHONE NUMBER *(Include area code)*
U	U	U	UU	141	(301) 621-0390